

1-1-2012

Evaluating the Performance of Two Solar Domestic Hot Water Systems of the Archetype Sustainable Houses

Kamyar Tanha
Ryerson University

Follow this and additional works at: <http://digitalcommons.ryerson.ca/dissertations>

 Part of the [Computer-Aided Engineering and Design Commons](#), and the [Environmental Engineering Commons](#)

Recommended Citation

Tanha, Kamyar, "Evaluating the Performance of Two Solar Domestic Hot Water Systems of the Archetype Sustainable Houses" (2012). *Theses and dissertations*. Paper 793.

EVALUATING THE PERFORMANCE OF TWO SOLAR DOMESTIC HOT WATER
SYSTEMS OF THE ARCHETYPE SUSTAINABLE HOUSES

By

Kamyar Tanha

B.Sc. (Mechanical Engineering)

University of Tehran, Iran, 2001

A thesis

presented to Ryerson University

In partial fulfillment of the
requirements for the degree of

MASTER OF APPLIED SCIENCE

In the program of
Mechanical Engineering

Toronto, Ontario, Canada, 2012

© Kamyar Tanha, 2012

Author's Declaration

I hereby declare that I am the sole author of this thesis. This is a true copy of the thesis, including any required final revisions, as accepted by my examiners.

I authorize Ryerson University to lend this thesis to other institutions or individuals for the purpose of scholarly research.

I further authorize Ryerson University to reproduce this thesis by photocopying or by other means, in total or in part, at the request of other institutions or individuals for the purpose of scholarly research.

I understand that my thesis may be made electronically available to the public.

EVALUATING THE PERFORMANCE OF TWO SOLAR DOMESTIC HOT WATER SYSTEMS OF THE ARCHETYPE SUSTAINABLE HOUSES

Kamyar Tanha

Master of Applied Science

Program of Mechanical Engineering

Ryerson University, Toronto, Ontario, Canada, 2012

Abstract

This thesis is focused on the performance of the two SDHW systems of the sustainable Archetype houses in Vaughan, Ontario with daily hot water consumption of 225 litres. The first system consists of a flat plate solar thermal collector in conjunction with a gas boiler and a DWHR. The second SDHW system consists of an evacuated tube collector, an electric tank and a DWHR. The experimental results showed that the DWHRs were capable of an annual heat recovery of 789 kWh. The flat plate and evacuated tube collectors had an annual thermal energy output of 2038 kWh and 1383 kWh. The systems were also modeled in TRNSYS and validated with the experimental results. The simulated results showed that Edmonton has the highest annual energy consumption of 3763.4 kWh and 2852.9 kWh by gas boiler and electric tank and that the solar thermal collectors and DWHRs are most beneficial in Edmonton.

Acknowledgements

This thesis would not have been come to the light without extended cooperation of author's supervisor Dr. Alan S. Fung. His guidance helped to finish this stupendous task. The author conveys from the bottom of his heart, his total indebtedness to his supervisor. The author is ever grateful to Dahai Zhang, a Ph.D. candidate for his generous help. He also expresses gratitude to his colleagues for their continuous support. He is very grateful to the Regional Municipality of Peel, Regional Municipality of York, City of Toronto, Building Industry and Land Development (BILD) Association, Toronto Region and Conservation Authority (TRCA), MITACS Accelerate, Reliance Home Comfort and Union Gas Ltd for their financial support to implement the monitoring project. The author would also express special thanks to Mr. David Nixon, Warren Yates, Derrik Ashby and Gil Amdursky for their concerted effort on implementing the instrumentation of monitoring system and Professor Leo Salemi of George Brown College for system networking support.

This work is dedicated to my respected parents, and my lovely wife.

All of whom tried me in various ways to guide me and help forward the cause espoused by me.

Table of Contents

Author's Declaration.....	ii
Abstract.....	iii
Acknowledgements.....	iv
List of Tables.....	ix
List of Figures.....	xii
Abbreviations.....	xviii
Nomenclature.....	xx
Chapter 1 : Literature Review.....	1
1.1. Objectives.....	4
Chapter 2 : Literature Review.....	5
2.1. Drain Water Heat Recovery.....	5
2.2. Solar Thermal Collectors.....	8
2.3. DHW Draw Profiles.....	11
2.4. Renewable Technologies in DHW production.....	13
Chapter 3 : Domestic Water Heating.....	17
3.1. Domestic Water Heater Types.....	18
3.1.1. Conventional Storage Tanks.....	18
3.1.2. Tankless Water Heaters.....	19
3.1.3. Integrated Space/Water Heaters.....	19
3.1.4. Heat Pump Water Heaters.....	20
3.1.5. Solar Water Heaters.....	21
3.2. Efficiency of Domestic Water Heaters.....	22
3.3. Domestic Water Heater Standards.....	24
Chapter 4 : Archetype House Description.....	27

4.1. DWH System of House-A.....	29
4.2. DWH System of House-B	31
Chapter 5 : Methodology	34
5.1. Monitoring System.....	34
5.2. Data Acquisition (DAQ) System.....	34
5.2.1. LabVIEW Software	35
5.2.2. SQL Server Management Studio.....	35
5.3. Sensors	36
5.3.1. Temperature Sensors	37
5.3.2. Liquid Flow Meters	37
5.4. Calibration of Sensors	37
5.6. Energy Consumption, Generation and Efficiency Calculation Equations	40
5.6.1. Water	40
5.6.2. Propylene Glycol (PG) Solution.....	41
5.6.3. Energy Consumption, Generation and Efficiency Equations for Equipment in House- A	42
Thermal power supplied to the DHWT by the boiler is obtained by using:.....	44
Thermal power supplied to the house load by the DHWT is also achieved from Equation (5- 7).....	44
5.6.4. Energy Consumption, Generation and Efficiency Equations for Equipments in House- B.....	47
Thermal power supplied by the solar preheat tank is calculated by using Equation (5-7)....	47
Thermal power supplied by the electric tank is calculated by using Equation (5-7).....	48
Chapter 6 : Data analysis	51
6.1. Drain Water Heat Recovery System	51
6.1.1. Performance of DWHR Systems	52

6.1.2. DWHR Systems in the Twin Archetype Houses	54
6.1.3. Daily Water Draw Profiles	55
6.1.4. Operational Performance of DWHR Systems	57
6.1.5. Extrapolated Data	68
6.2. Solar Thermal Collectors	71
6.2.1. Flat Plate Solar Thermal Collector	74
6.2.2. Evacuated Tube Solar Thermal Collector	79
6.2.3. Solar Thermal Collectors' Performance Comparison	86
6.2.4. Extrapolated Data	89
6.3. Overall Performance of the Archetype Houses' SDWH Systems	91
Chapter 7 : TRNSYS Simulations	94
7.1. Twin Houses SDWH Systems Modeling	95
7.2. House-A SDWH System	98
7.3. House-B SDWH System	100
7.4. SDWH Systems Performance in Major Canadian Cities	102
Chapter 8 : Author's Contribution and Conclusion	107
8.1. Conclusions	107
8.2. Recommendations	110
Appendix A: Sensor address, list, type and location	112
Appendix B: Experimental Uncertainty Analysis	125
B1. Uncertainty of Sensors and Calibrators	125
B2. Propagation of Errors	126
B3. Uncertainty analysis of mechanical system/equipment	126
References	128

List of Tables

Table 3-1: Water Heating Secondary Energy Use and Intensity by Energy Source (NRCan, 2009)	17
Table 3-2: Energy Efficiency Regulations for Canadian Water Storage Tank Heaters (Canada Gazette, 2004).....	25
Table 3-3: U.S Standards for Federally Regulated Water Heaters (California Energy Commission, 2006).....	26
Table 4-1: Comparison of HVAC systems among housing standards (Zhang, et al. 2011)....	28
Table 4-2: Basic design features of House-A and House-B (Zhang et al., 2011).....	28
Table 4-3: Structural features of the twin houses (Zhang et al., 2011).....	28
Table 4-4: Mechanical features of the twin houses (Zhang et al., 2011).....	29
Table 4-5: Detail specifications and technical data of the DHW system components in House-A	31
Table 4-6: Detail specifications and technical data of the DHW system components in House-A	33
Table 5-1: Sensor name and its output signal	34
Table 5-2: List of DWH systems' components with their related sensors and input parameters	36
Table 5-3: List of sensors for DHW systems and calibrators (Barua, 2010).....	38
Table 5-4: List of events and different flow rates used for the water draw Schedule in winter	39
Table 5-5: List of events and different flow rates used for the water draw Schedule in summer	39
Table 6-1: General specifications of Power-pipe R3-36 DWHR	54

Table 6-2: Averaged flow rates and temperatures during a shower event in February (DWHR is cooled down).....	58
Table 6-3: Averaged flow rates and temperatures during a sink usage (DWHR is not cooled down)	60
Table 6-4: Averaged flow rates and temperatures during a shower event in August (DWHR is cooled down).....	62
Table 6-5: Monthly heat recovery by DWHR systems.....	69
Table 6-6: Viessmann solar collectors' specifications in TRCA Archetype Houses (Viessmann Ltd., 2010).....	71
Table 6-7: Efficiency equation variables of the two Solar Collectors in TRCA houses (Viessmann Ltd., 2010).....	73
Table 6-8: Total and average deliverable energy by the flat plate collector during winter and summer periods.....	79
Table 6-9: Total and average deliverable energy by the EVT collector during winter and summer periods.....	85
Table 6-10: Annual energy consumption, generation and recovery by SDWH system's components of House-A	93
Table 6-11: Annual energy consumption, generation and recovery by SDWH system's components of House-B.....	93
Table 7-1: Comparison of the annual performance of the SDWH system's components of House-A.....	100
Table 7-2: Comparison of the annual performance of the SDWH system's components of House-B.....	101

Table 7-3: Annual performance of the House-A, SDWH system's components in different Canadian cities	103
Table 7-4: Annual performance of the House-B, SDWH system's components in different Canadian cities	103
Table 7-5: Annual cost / savings by House-A SDWH system's components in different Canadian cities	104
Table 7-6: Annual cost / savings by House-B SDWH system's components in different Canadian cities	104
Table 7-7: Annual GHG emission by House-A SDWH system's components in different Canadian cities	105
Table 7-8: Annual GHG emission by House-B SDWH system's components in different Canadian cities	105

List of Figures

Figure 1-1: Distribution of Canadian residential energy consumption in 2007 (NRCan, 2009)	1
Figure 3-1: Residential Gas-fired Storage Water Heater (DOE, 2011b)	18
Figure 3-2: Electric Demand Water Heater (DOE, 2011b)	19
Figure 3-3: Indirect Water Heater (DOE, 2011b)	20
Figure 3-4: Solar Domestic Hot Water System (ES Renewables Ltd, 2011)	22
Figure 4-1: South View of the Archetype Sustainable Twin Houses	27
Figure 4-2: DHW Heating System of House-A with the Related Monitoring Points	30
Figure 4-3: DHW Heating System of House-B with the Related Monitoring Points	32
Figure 5-1: Snapshot of LabVIEW front panel showing the operating information of the DWHR in House-B	36
Figure 5-2: Comparison of water density variations with temperature from Equation (5-1) using TRCA data and Tanaka et al. data	41
Figure 5-3: Comparison of PG density with temperature by CHEM Group data and equation result	42
Figure 5-4: Schematic view of gas boiler with related sensors of House-A	42
Figure 5-5: Schematic view of DHWT with related sensors of House-A	43
Figure 5-6: Schematic view of flat plate solar collector with related sensors of House-A	44
Figure 5-7: Schematic view of House-A DWHR system with related sensors	46
Figure 5-8: Schematic view of solar preheat tank with related sensors of House-B	47
Figure 5-9: Schematic view of electric backup tank of House-B with related sensors	48

Figure 5-10: Schematic view of evacuated tube solar collector with related sensors in House-B	49
Figure 5-11: Schematic view of House-B DWHR system with related sensors.....	50
Figure 6-1: General View of a Drain Water Heat Recovery System (Zaloum et al., 2007)....	52
Figure 6-2: Overview of PowerPipe R3-36 unit in House-B and the wrapped tubes view	54
Figure 6-3: Average daily hot water draw profile	56
Figure 6-4: High Resolution Daily Hot Water Draw Pattern	56
Figure 6-5: Average measured water mains temperatures to the Archetype Houses	57
Figure 6-6: DWHR cold side and hot side temperatures variations for a typical shower in February	59
Figure 6-7: DWHR's instantaneous effectiveness and inlet drain water temperature changes for a shower in February	59
Figure 6-8: DWHR heat recovery rate curve for a typical shower in February	60
Figure 6-9: DWHR's effectiveness and inlet drain water temperature changes for a sink usage with the completely warmed up unit in February	61
Figure 6-10: DWHR heat recovery rate curve for a sink usage with the completely warmed up unit in February.....	61
Figure 6-11: DWHR cold side and hot side temperatures variations for a typical shower in August.....	62
Figure 6-12: DWHR heat recovery rate curve for a typical shower in August	63
Figure 6-13: Effectiveness as a function of inlet water temperature for similar drain water flow rates	64

Figure 6-14: Effectiveness as a function of drain flow rate for different coil/drain flow rate ratio	65
Figure 6-15: Effectiveness as a function of drain flow rate from TRCA experimental results and the study by Zaloum et al. (2007)	65
Figure 6-16: NTU vs. drain flow rate for different coil/drain flow rate ratio	66
Figure 6-17: Effectiveness as a function of drain water temperature for different drain flow rates with coil/drain ratio of 0.8	67
Figure 6-18: Comparison of the predicted effectiveness of the DWHR with the experimental results	68
Figure 6-19: DWHR systems inlet and outlet temperatures profile	70
Figure 6-20: Main components of a flat plate Solar Collector (Viessmann Ltd., 2010b)	74
Figure 6-21: Flat plate solar collector efficiency curve changes with solar radiation (Mar/14/2011)	75
Figure 6-22: Figure 3: Solar loop inlet and outlet temperature and thermal energy output of flat plate collector	75
Figure 6-23: Flat plate solar collector efficiency changes with solar radiation on tilted surface in winter	76
Figure 6-24: Flat plate solar collector efficiency changes with solar radiation on tilted surface in summer	76
Figure 6-25: Flat plate solar collector thermal energy output and solar pump energy consumption variations with solar radiation in winter	77
Figure 6-26: Flat plate collector thermal energy output and solar pump energy consumption variations with solar radiation in summer	77

Figure 6-27: Flat plate collector instantaneous efficiency curve vs. reduced temperature difference for winter and summer testing periods	78
Figure 6-28: Main components of an evacuated tube solar collector (Viessmann Ltd., 2010b)	80
Figure 6-29: Heat absorption mechanism from the solar energy in a Evacuated Tube Solar Collector (http://www.echomaterico.net/blog/?p=497)	80
Figure 6-30: Evacuated tube solar collector efficiency curve changes with solar radiation (Mar/14/2011)	81
Figure 6-31: Evacuated tube solar collector efficiency changes with solar radiation on tilted surface in winter	82
Figure 6-32: Evacuated tube solar collector efficiency changes with solar radiation on tilted surface in summer	82
Figure 6-33: EVT collector thermal energy output and solar pump's energy consumption variations with solar radiation in winter	83
Figure 6-34: EVT collector thermal energy output and solar pump's energy consumption variations with solar radiation in summer	83
Figure 6-35: EVT collector instantaneous efficiency curve vs. reduced temperature difference for winter period	84
Figure 6-36: EVT collector instantaneous efficiency curve vs. reduced temperature difference for summer period	84
Figure 6-37: Solar collectors' daily thermal energy output variations with solar radiation in winter	86
Figure 6-38: Solar collectors' daily thermal energy output variations with solar radiation in summer	86

Figure 6-39: Daily thermal energy output from solar thermal collectors in winter testing period	87
Figure 6-40: Daily thermal energy output from solar thermal collectors in summer testing period	87
Figure 6-41: Cumulative thermal energy output by the two solar thermal collectors in winter	88
Figure 6-42: Cumulative thermal energy output by the two solar thermal collectors in summer	89
Figure 6-43: Annual cumulative thermal energy output by the two solar thermal collectors	90
Figure 6-44: Monthly thermal energy output by the two solar thermal collectors	91
Figure 6-45: Comparison of thermal energy output of flat plate collector and energy consumption of gas boiler	92
Figure 6-46: Comparison of thermal energy output of evacuated tube collector and energy consumption of electric tank	92
Figure 7-1: TRNSYS model overview of SDWH system of House-B	95
Figure 7-2: Comparison of experimental and TRNSYS model thermal energy output of flat plate solar thermal collector	98
Figure 7-3: Monthly thermal energy output of flat plate collector from experimental data and TRNSYS model	99
Figure 7-4: Monthly heat recovery by DWHR from experimental data and TRNSYS model	99
Figure 7-5: Comparison of experimental and TRNSYS model thermal energy output of evacuated tube solar thermal collector	100
Figure 7-6: Monthly thermal energy output of evacuated tube collector from experimental data and TRNSYS model	101

Figure 7-7: Monthly water mains temperatures for six Canadian major cities..... 102

Abbreviations

ACH	Air Change Per Hour
ASME	American Society of Mechanical Engineers
ASHRAE	American Society of Heating, Refrigerating and Air-Conditioning Engineers
BILD	Building Industry and Land Development Association
BTU	British Thermal Unit
CCHT	Canadian Centre for Housing Technology
CFP	Compact Field Point
CHP	Combined Heat and Power
COP	Coefficient of Performance
CPUC	The California Public Utilities Commission
CSA	Canadian Standard Association
DAQ	Data Acquisition System
DOE	US Department of Energy
DHWT	Domestic Hot Water Tank
DHW	Domestic Hot Water
DWH	Domestic Water Heating
DWHR	Drain Water Heat Recovery
EU	European Union
FSEC	Florida Solar Energy Centre
GAL	U.S. Gallon (3.78 LITERS)
GHG	Greenhouse Gas
GJ	Giga Joules

GPM	Gallon Per Minute
GSHP	Ground Source Heat Pump
HHV	Higher Heating Value (for natural gas 37.8 MJ/m ³)
HPWH	Heat Pump Water Heater
HVAC	Heating, Ventilating and Air Conditioning
IEA	International Energy Agency
kWh	Kilowatt Hour
LEED	Leadership in Energy and Environmental Design
MB	Megabyte
MBH	Mega BTU per Hour
MCHP	Micro Combined Heat and Power
NIST	National Institute of Standards and Technology
NI	National Instrument
NRCan	Natural Resources Canada
NTU	Number of Heat Transfer Units
OBC	Ontario Building Code
PG	Propylene Glycol
PV	Photovoltaic
Pa	Pascal (Pressure Unit N/m ²)
RTD	Resistance Temperature Detector
SDHW	Solar Domestic Hot Water
SQL	Structured Query Language
SRCC	Solar Rating and Certification Corporation
SSMS	SQL Server Management Studio

TOU	Time-of-use
TRCA	Toronto and Region Conservation Authority
USG	US Gallon
ZNEH	Zero Net Energy Home

Nomenclature

A	gross area of the solar collector, (m ²)
C	capacity rate for the water = $q \rho c_{\text{water}}$ (kJ/K.sec)
C _{min}	minimum capacity rate, (kJ/K.sec)
C _{max}	maximum capacity rate, (kJ/K.sec)
c _{PG}	specific heat of PG, (kJ/kg.K)
c _{pwater}	specific heat of water = 4.1813 (kJ/kg.K)
C _r	heat capacity rate ratio
	minimum liquid flow rate, (GPM)
Q	thermal power, (kW)
Q _{Electrical}	electrical power, (kW)
q	flow rate, (m ³ /sec)
T	temperature, (°C)
T _{cold}	cold water temperature, (°C)
T _{hot}	hot water temperature, (°C)
T _{mean}	mean temperature of solar collector's inlet and outlet, (°C)
T _a	ambient temperature, (°C)
UA	overall heat transfer coefficient (kW/°C)

Greek symbols

	density of PG, (kg/m ³)
ρ _{water}	density of water, (kg/m ³)
I _T	solar irradiance, (W/m ²)
η	efficiency, (%)
ε	effectiveness, (%)

Chapter 1 : Literature Review

Decreasing energy requirements and conserving energy, alongside with exploring renewable and environmentally friendly sources of energy is becoming more important as the concerns for limited energy resources in the near future continue to grow, especially in a cold climate country like Canada. The residential sector consumes about 16% of the total energy consumption in Canada and the total greenhouse gas (GHG) emissions of this sector is 15% of all GHGs emitted in Canada (NRCan, 2009). Domestic water heating (DWH) is estimated to be the second largest energy end-use for Canadian households, exceeded only by space heating, and as shown in Figure 1-1, accounts for about 18% of total household energy consumption (NRCan, 2009). Although there has been an approximate decrease of 20% in per household energy used to heat water since 1990, the overall energy required for this purpose has increased. This has been due to the fact that the total number of households has grown more quickly compared to the energy efficiency improvements of more advanced water heaters. This has led to an overall increase of 6% in the annual energy needed for Canadian residential water heating, from 243.0 PJ to 257.9 PJ (NRCan, 2009).

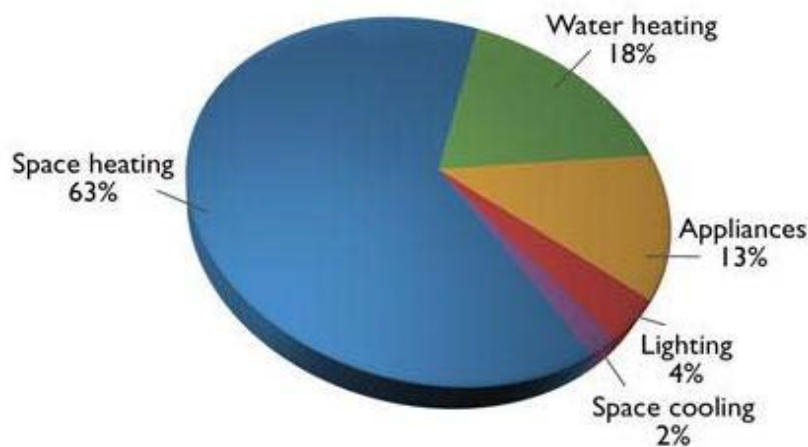


Figure 1-1: Distribution of Canadian residential energy consumption in 2007 (NRCan, 2009)

Several studies have been performed in order to investigate different methods in reducing the amount of energy required for residential DWH, from using more energy efficient water heaters to using devices and methods for heat recovery and systems that use renewable energy sources to provide heating like solar thermal collectors.

Drain Water Heat Recovery (DWHR) systems are fairly simple in design and are used to recuperate part of the energy contained in drain water that would otherwise be lost. DWHR systems usually consist of a main pipe around which a spiral coil is wrapped. Both main pipe and coil are made of copper to enhance heat transfer. These systems are usually inserted vertically into the regular plumbing system as a replacement of a section of drain pipes. It should be noted that there have been also case studies of DWHR units being installed horizontally into the plumbing system of high rise buildings (Wong, Mui, & Guan, 2010). The drain water flows inside the main pipe and adheres to the inner wall and the inlet cold water from the city mains circulates in the spiral coil in a close, indirect contact with the water in the main pipe. The nature of this system implies that there must be simultaneous water flow in the drain pipe and in the coil in order to maximize heat recovery and this occurs mostly when showers are used (Bernier et al., 2004).

Solar collectors are being increasingly used for the purpose of producing domestic hot water (DHW). Aside from cost and greenhouse gas emissions savings, solar collectors are known for their relative simplicity and durability. Usually, there are two types of collectors used for producing hot water: flat plate and evacuated tube collectors.

There are several advantages for the flat plate collectors; these collectors use both beam and diffuse solar radiation, do not require tracking of the sun and are low-maintenance, inexpensive and mechanically simple (Weiss & Rommel, 2008). In such a collector, solar radiation enters through the transparent cover and reaches the absorber sheet. The collected heat should then be transferred to the absorber pipes via a good thermal conductivity media where the heat is finally transferred to the fluid which is usually a mixture of water and glycol with anticorrosion additives. The fluid would also act as a protection to the collector from frost damage. The main losses of the flat-plate collectors can be classified as optical and thermal losses. The thermal losses rapidly increase with higher operating temperatures, while the optical losses are almost constant, and grow with increase in sunlight incident angle (Weiss & Rommel, 2008). The other negative point with these types of solar collectors is that their efficiency is reduced in cold climate conditions.

Evacuated tube solar collectors can be classified into two main groups: direct flow tubes and heat pipe tubes. All evacuated tube solar collectors have similar technical specifications: 1- they consist of a row of parallel evacuated glass tubes to reduce conduction losses and eliminate

convection losses, and 2- the upper end of the tubes are connected to a header pipe. The main difference between the two types of evacuated tube collectors is that the heat carrier fluid inside of the copper heat pipe is not connected to the solar loop (supply and return piping system in which, a heat transferring liquid is being circulated between the collector and the hot water tank) and the connection can be either “dry” or “wet”. In “dry” connection, the heat has to be transferred from the condenser through the material of the header tube, whereas in the case of a “wet” connection, the fluid of the solar loop flows directly around the condenser of the heat pipes. A heat pipe is hollow with very low pressure inside and has a small quantity of water and some other additives. When the pipe is heated above a certain temperature, the liquid vaporizes to the top of the heat pipe or condenser and transfers the heat. As a result, the vapor condenses back to liquid and returns to the bottom of the heat pipe to once again repeat the process. To ensure circulation, heat pipe collectors should be tilted to a minimum angle of 20° (Weiss & Rommel, 2008).

The government of Ontario has a great interest in sustainable energy design and is playing an important role in this regard by providing encouraging initiatives, rules and regulations like the newly passed Ontario Green Energy and Economy Act. The introduction of the new Ontario Building Code (OBC) format, including the *Energuide 80* alternative compliance option has caused a great interest in more efficient mechanical systems. This study highlights the DWH systems of the two semi-detached “Sustainable Archetype Houses” at the Living City Campus located at Kortright Center in Vaughan, Ontario. The two houses are named House A and House B and this project has been implemented by the *Toronto and Region Conservation Authority* (TRCA) along with the *Building Industry and Land Development* (BILD) Association. A comprehensive energy monitoring system has been implemented in this project to monitor the thermal performance of the twin houses and to investigate the effectiveness and efficiency of the mechanical systems used (Zhang, Barua, & Fung, 2011). The aim of this project has been to demonstrate different sustainable housing technologies in the near and medium term future. The DWH system of House A consists of a flat plate solar collector in conjunction with a back-up mini gas boiler and a DWHR unit. The DWH system of House B consists of an evacuated tube solar collector in conjunction with an electric water heater and DWHR unit. This is a dual tank system, the second of which is a solar pre-heat tank which can also be connected to the

desuperheater of the ground source heat pump and/or the Sterling engine based co-generation system.

1.1. Objectives

The main objective of this thesis is to compare the two solar domestic water heating (SDWH) systems and assess the annual energy savings, fuel cost and GHG emissions from the two systems.

The specific objectives of the thesis are listed below:

- Collecting data from all of the related sensors of the two SDWH systems, including the two DWHR systems, the two solar thermal collectors, mini gas boiler and electric water heater.
- Analyzing the data obtained, evaluating the effectiveness and performance of the components, and cross checking them with the manufacturers' data and their contributions to energy, fuel cost and GHG emissions savings.
- Creating a detailed model of the entire DHW system, including DWHR system, of the two houses, using TRNSYS 16 with a typical daily hot water draw profile implemented that simulates the hot water consumption patterns of a typical Canadian household of four occupants. The two models must first be validated with the experimental data. The TRNSYS models can then be used to simulate the annual performance of each system and to compare the benefits of each system, with regards to lowering annual energy demand, fuel cost and GHG emissions.
- Assessing the performance and benefits of using these SDWH systems in similar Canadian residential households in five major cities, namely Toronto, Montreal, Halifax, Vancouver and Edmonton, based on the validated TRNSYS models.

Chapter 2 : Literature Review

The literature review for the DWH systems is divided into four sections: the first part discusses the research done on drain water heat recovery, the second part is about the work done on the solar thermal collectors which can be used for DWH, the third part discusses the work on the modeling and simulation of DWH systems and the last part focuses on residential DHW draw profile researches.

2.1. Drain Water Heat Recovery

In a study prepared for the Virginia Power Company, the performances of some major water heaters were characterized and combinations of water heating equipment which would maximize energy savings and minimize the impact on peak conditions of the power system were investigated (Taylor & Crossman, 1996). In this study, three different resistance water heaters with the same capacity but different energy factors were tested, with and without a specific DWHR unit manufactured by a Vaughn company, known as GFX. For this purpose, three different water draw profiles were used for a 24 hour testing duration and the energy factor, energy consumption and hourly standby losses were measured. A total of 130.5 litres of water in test 1 and 206 litres in tests 2 and 3 were drawn. The draw patterns used were developed to reflect the patterns typically seen by Virginia Power field monitoring. The tanks set point temperatures were set to 49°C (120 °F) and the drain water temperature was kept at 37.8°C (100 °F). The results showed that the upper elements of the water heaters did not energize when the DWHR unit was added to the water heating systems. It was shown that the DWHR increases the amount of available water at set-point temperature in the heaters and that it could also increase the energy factors of the water heaters from 57% to 73%. It was also concluded that the addition of DWHR could reduce the energy consumed by the heaters by 47% to 64%. The DWHR unit effectiveness was evaluated to be in the range of 55% to 60%.

Another study performed a comprehensive research for Natural Resources Canada (NRCan) and the Manitoba Hydro Electrical Board on residential drain water heat recovery systems (Proskiw, 1998). This report provides descriptions of the activities done in the field of drain water heat recovery, various types of residential DWHR systems with their benefits, and list of commercially available DWHR systems. According to this report, DWHR systems can be

classified into four categories of 1) combined storage tank/heat exchanger which uses thermal conduction and convection to transfer heat between the wastewater and potable water, 2) combined storage tank/heat exchanger with heat pump for facilitating the heat transfer process, 3) non-storage type heat exchanger which is connected directly to the drain line and 4) point-of-use type which is incorporated directly into an end-use device, such as a shower with no thermal storage. The report has also performed a comprehensive review of the commercially available DWHR units including the already mentioned GFX. It was mentioned that the GFX works best with simultaneous flow conditions and the main advantages of it were listed as relatively low cost and easy installation, and not requiring maintenance. The only disadvantage was that this type of DWHR did not include thermal storage. This report also stated that various DWHR systems could provide a heat recovery of about 30% to 55% of the total DHW load.

Another research funded by the U.S. Department of Energy (DOE) investigated the performance of the DWHR unit, GFX, through collected data (DOE, 2001). The unit had a 3 in. diameter for the main copper pipe with ½ in. copper coils wrapped around it. The unit was 60 in. in length and was installed in a single family home in Tennessee and was intended to recuperate the heat from the shower drain water only. The performance of the unit was evaluated for different piping configurations and shower temperatures. It was shown that the shower temperature had a significant effect on the performance of the unit; with cooler shower temperatures, more of the unit contribution would go to preheating the cold water, whereas for warmer shower temperatures, most of the captured energy by the unit would go to preheating the hot water. The unit was also tested for three different flow configurations: I) balanced flow where all water is preheated; II) unbalance flow where the cold water was preheated only and III) unbalanced flow where the hot water was preheated only. The results obtained from the analysis showed that with the water heater set-point temperature of 57°C (135°F) and incoming water temperature of 14.5°C (58°F), the energy savings by the unit were in the range of 30% to 50% with the highest amount of heat recovery for the balanced flow configuration.

In an investigation to assess the performance of a specific DWHR model, GFX, a test facility of the unit and the piping connections were constructed (Hewitt & Henderson, 2001). The testing procedure was performed under controlled conditions for both the temperatures and flow rates of the drain and the cold-side city main water. With the fixed inlet cold water temperature of 11°C ± 1°C, it was concluded that the unit required a settling time of 1-1.5 minutes before reaching its

steady state. The experimental results showed that the unit can recycle as much as 60-75% of waste water heat depending on the amount of drain water flow rate and temperature. It was also concluded that in real applications, the external conditions and the indoor air temperature of the system will affect the amount of heat transfer by the unit and that insulating the unit will improve its performance.

In a study performed at the Canadian Centre for Housing Technology (CCHT) on the performance of DWHR units, the performances of eight different DWHR units were examined and a standard test for future performance testing was developed (Zaloum, Lafrance, & Gusdorf, 2007). This was a continued study on the performance of DWHR units in which it was concluded that these units were only capable of recovering energy during simultaneous water draws and that the units tested had a minimum of 46% for the in situ thermal effectiveness for different flow configurations. The tested units consisted of 3 inch copper drain pipe wrapped with either 1/2 or 3/8 inch soft copper tubing with different unit lengths from different manufacturers. The experiments on the units were performed for two different flow configurations, 1- preheating the cold water to the hot water tank and 2- preheating the cold water to the tank and shower, three different flow rates and three different shower temperatures were used to assess the performance and heat transfer rate of each unit. All tests were performed under the same operating conditions. The performance of the units was measured in terms of Number of Thermal Units (NTU) and effectiveness with the NTU versus flow rates showing a better correlation. It was concluded that the NTU-curves were independent of the two flow configurations and an energy saving calculator, which could show the performance and benefits of different units was also developed. It was also concluded that the shape of the wrapping tubes and the size of the gap between the tubing and the main pipe have significant effect on the performance of the units. It was also found that there was an optimal balance between the performance and size of the units; that was the shorter units perform best on a per foot basis.

In a set of experiments performed at the University of Waterloo on a variety of DWHR units from Renewability company named PowerPipe™, the effectiveness of the units was investigated (Collins, 2009). The tests were performed under similar conditions for the cold inlet water temperature, shower temperature and flow rate. The DWHR units tested were of three different nominal diameters of 2 in., 3 in. and 4 in. and with different pipe lengths. The wrapping tubes for all the units were 3/8 in. type L with four parallel wraps. The results from the experiments

showed a clear trend for the effectiveness, pressure loss and the heat recovery of the units with changes of length; that was for the same pipe diameter, the increase in length of the main pipe will lead to increase in effectiveness, pressure loss and amount of heat recovery. The results also indicated that for the units with the same length for the main pipe, the increase in the pipe diameter will also increase the effectiveness, pressure loss and heat recovery.

One other study has investigated the potential for shower water heat recovery from bathrooms equipped with instantaneous water heaters in high-rise residential buildings of Hong Kong (Wong et al., 2010). This was done through experiments on the performance of a single-pass counter-flow heat exchanger which was installed horizontally beneath the shower drain for preheating the cold water going to a heater. The thermal energy exchange was evaluated using the effectiveness-number of transfer units (ϵ -NTU) approach. Shower usage patterns including shower duration and water flow rate obtained from a sample field survey, and water temperatures at shower head, shower drain and main supply water were measured and used to obtain the potential energy savings. It was concluded that 4-15% shower water heat recovery could be achieved through the use of the specified heat recovery unit of 1.5 m in length and drainage pipe diameter of 50 mm.

2.2. Solar Thermal Collectors

A research performed by the National Renewable Energy Laboratory for the U.S. Department of Energy, described the design, simulation and performance of a solar water heating system installed at the top of the hot water recirculation loop of a federal building in Philadelphia (Walker, Mahjouri, & Stiteler, 2004). The main aim of this research was to offer a means of facilitating implementation of solar water heating in commercial buildings. The solar heating system consisted of 360 evacuated heat-pipe collector tubes with gross area of 54 m² and net absorbing area of 36 m². The system reheated the water rather than preheating cold water, and water would go through the headers of the heat pipe collector solar array if a 4°C temperature difference existed between the solar collector outlet and the recirculation loop. Each tube contained a sealed copper pipe, and the pipe was continuously bounded to a coated copper fin as the absorber plate. The coating had an absorptivity of 92% throughout the solar spectrum and an emissivity of less than 6% through the infrared spectrum. Hourly simulations showed that for the 50°C hot water daily consumption of 3562 liters, the annual energy delivery of the solar heating

system would be 111 GJ of solar heat, based on the 34% efficiency of the system including all heat losses from all sources like freeze protection. It was also mentioned that the annual average collector efficiency based on the net and gross area of the collector was 61.5% and 41% respectively. Initial monitoring results showed that the system was able to return water to the boiler about 5°C hotter than the supplied to the solar heating system.

In a series of comparison tests on different solar thermal collectors, the performance for DHW production and space heating were investigated (Druck et al., 2004). Twelve systems were equipped with flat plate collectors and four with evacuated tube collectors. The systems were tested for their thermal performance, durability and reliability, environmental and safety aspects. The effective collector areas varied from 3.2 m² to 5.7 m² for all solar collectors. The effective usable storage volume of the domestic hot water was in the range of 268 liters up to 419 liters. For all sixteen systems, the solar energy was transferred to the domestic hot water using a tube heat exchanger. The systems were simulated for a single-family house located at Wurzburg, Germany using TRNSYS simulation software. The house had a south facing inclined roof of 45°. The daily hot water load was 200 liters at 45°C. The Solar Domestic Hot Water (SDHW) systems were tested according to EN 12976-2 for solar thermal collectors. With regards to the assessment of the thermal performance of the systems, a total of four SDHW systems obtained rankings of “very good”, two of which were flat plate solar collectors. Their results also showed that the system with the evacuated tube collector of 3.2 m² in area had the shortest energy payback period of 1.3 years. A shortcoming of this study was that they ranked their systems on the basis of very good, good or fair without discussing the criteria used for this ranking. Their study also stated the environment benefits of these systems without giving any comparison data to support their results.

A study performed at Centre of Excellence for Solar Engineering at Ingolstadt University has investigated the performance of the vacuum tube and flat plate solar collectors of the solar assisted heating systems of a two-family house (Trinkl et al., 2005). The heating system of one of the houses consisted of a flat plate solar collector, oil furnace and in-floor heating while the other house was equipped with evacuated tube solar collectors and a stratification tank. The two sets of solar collectors had the same south facing orientation with almost similar shadow effects. The behavior of the components within each of the two systems and the delivered energy of the two types of solar collectors were monitored by the installed measurement equipment. The

results obtained from the monitoring system for the winter testing period indicated that the flat plate collectors can generate higher energy per gross area despite their lower nominal efficiency. The results also showed that although the energy yield per aperture area of the vacuum solar collector was higher during the periods with higher ambient temperatures, it was almost equal to the energy yield by the flat plate collector when the ambient temperature was low. It was also shown that with moderate solar irradiance and low ambient temperatures during the winter testing period, flat plate collectors were the only operating collectors. During days with high solar irradiance and low ambient temperatures which were generally assumed to be perfect operating conditions for the vacuum tube solar collectors, the results showed that the vacuum tube collectors were only operating for short periods in the afternoon while the flat plate collectors were operating the whole day with sufficient amount of heat production. This was due to the fact that the vacuum tube collectors were covered with frost or snow, which was caused by their slow defrosting due to their efficient vacuum insulation. It was also concluded that although both collector types were suitable for the central European climate solar heating systems, the vacuum tube collector could not provide the additional energy expected and in winter offered conceptual weaknesses.

Another study has investigated the thermal performance of a glass evacuated tube solar collector with different absorber tube shapes through numerical and experimental analysis (Kim & Seo, 2007). The studied solar collector consisted of two-layered glass tube and a copper absorber tube. A total of four different models according to the shape of the absorber were used: model 1 had strip-type finned tubes, model 2 had a U-tube welded inside a circular fin, model 3 had a U-tube welded on a copper plate and model 4 had a U-tube welded inside a rectangular duct. Six different cases were also studied which depended on the size of the absorber tubes: cases 1 to 3 for diameters of 12.7, 19.05 and 25.4 mm used for the absorber tube of model 1, and cases 4 to 6 for models 2 to 4 with fixed absorber tube diameter of 12.7 mm. At first, the performance and efficiency of single tubes for the various cases were investigated with only beam irradiation of 1000 W/m^2 to be considered. The obtained results showed that as the incidence angle for different cases increased, the efficiency was decreased with case 4 being the only exception. The efficiency of case 4 (model 2) remained constant at 63.2% with the increase of the incidence angle from 0° to 60° . When the performances of the solar collectors consisting of three tubes were studied, the diffuse irradiation and the shadow effects from the neighboring tubes were also

considered to achieve more realistic performance estimation. The simulation results from both numerical and experimental analysis showed that model 3 had the best performance for different incidence angles. It was also concluded as the center distance of the tubes becomes shorter, the performance of the solar collector increases even though there was an increase in the shadow effect.

Another study conducted on the solar collectors has presented comparative tests on flat-plate and evacuated-tube solar collectors (Zambolin & Del Col, 2010). The flat-plate one was a standard glazed flat-plate collector and the evacuated-tube was a direct flow through type with external compound parabolic concentrator reflectors; the two were installed in parallel and tested under the same operating conditions. The study tried to find the efficiency of the two collectors in steady-state and quasi-dynamic conditions according to the EN 12975-2 standard. The other objective was to characterize and compare the daily energy performance of the collectors by plotting the collected solar energy against the daily incident solar radiation. The tests were performed for several inlet temperatures and flow rates at a tilt angle of 30° for reproducing different conventional uses like hot water and solar cooling. It was concluded that with a constant operating temperature difference, the daily energy collected showed a linear relationship with the daily solar radiation energy and the flat-plate collector was more sensitive to this temperature difference. It was also shown that the daily efficiency could be estimated by using the parameters of the quasi-dynamic model. From the daily tests, it was concluded that the evacuated-tube collector displayed a higher efficiency for a larger range of operating conditions in comparison to the flat-plate collector due to its geometry which made the most of the absorbing area be exposed to the quasi-normal incident radiation for a longer period of the day. The daily efficiency curves could also be used for quick evaluation of solar collectors in a wide range of operating conditions.

2.3. DHW Draw Profiles

One study has tried to investigate residential hot water use patterns in Canadian households using a market research approach (Stevenson, 1983). The field survey was performed in over 600 single family households across Canada with different water heaters for a two-week period. The overall hourly hot water draw patterns showed a daily peak usage for the early mornings and evenings. From the obtained data, three user groups were identified: low use, high morning use and high evening use. It was also found that showers were the largest source of hot water usage

with close to 41% of the daily hot water usage. A “typical” household was defined with the following characteristics: the presence of children, family size 3 or more and presence of dishwasher. The average daily demand for this group was concluded to be 310 liters. It was also found that in households with gas water heaters, hot water consumption was about 25% more compared to the ones equipped with electric heaters.

Another study has investigated the daily hot water profile patterns by monitoring the data from Canadian residences (Perlman & Mills, 1985). The study has provided two sets of data: one for “all families” and one for “typical” families; the typical family was defined as those with two adults and two children where clothes washer and dishwasher were present. The typical hot water draw profile was assumed to be the most representative one. This profile was an hourly water draw which also showed two sets of peaks, one for the mornings and one for the evenings. The total daily hot water consumption was also concluded to be 240 liters.

Another study has developed different sets of load profiles for the DHW demand for a period of one year in different time scales (Jordan & Vajen, 2001). The load profiles were prepared within the scope of the Solar Heating and Cooling Program of the International Energy Agency (IEA SHC). The load profiles were developed in three time steps of 1, 6 and 60 minutes. The DHW profiles were generated for different daily demands, depending on the size of the family. Four categories of loads with specified mean flow rates were defined and the profile for each of them were generated separately and superposed afterwards. The actual flow rate values were then spread around the mean value using the Gaussian distribution. The times of occurrence of different categories during the year were derived from a probability function specified by the writers.

Another study has performed a comprehensive monitoring of over 200 residences in Florida, collecting data on water heater energy use and demand on a 15-minute basis (Parker, 2003). The monitored residences were equipped with different water heaters with the majority of the homes being equipped with electrical heaters. The daily histogram of hot water energy use was derived from the sample houses for a one year period. The resulting graph showed only one peak occurring in the early morning. The various parameters having impact on daily DHW energy use were also investigated. It was shown that the most important parameters were the number of household occupants, the average daily ambient temperature and mains water temperature.

2.4. Renewable Technologies in DHW production

In a research project by Florida Solar Energy Centre (FSEC), the water heating electrical energy consumption, efficiency and time of day demand of eighty single family residences in Florida with four different heating systems were investigated through monitoring systems for two years (Merrigan & Parker, 1990). The four systems were conventional electric heaters, heat pumps, desuperheaters and solar hot water systems, which were equally divided among the residences. The results from the collected data showed that daily electricity consumption of electric resistance water heaters was 8.3 kWh on average. The annual average electrical consumption of deuperheaters, heat pump water heaters and solar hot water systems was determined to be 7.4 kWh, 6.1 kWh and 2.7 kWh per day respectively. Electrical demand taken at 15-minute intervals showed that the electric heaters contributed approximately 1.1 kW and 0.2 kW per customer to the utility winter peak and summer peak respectively which accounted for about 25% of the utility winter peak demand and 5% of the summer peak demand in Florida. The electric water heaters had an average efficiency of 82% with a load factor of 50%. Load factor is defined as the ratio of average demand over the peak demand. It was concluded that the solar hot water systems had the highest peak demand reduction of 0.7 kW and 0.2 kW per customer in the winter and summer, respectively. The average coefficient of performance (COP) for the solar hot water systems was shown to be 2.35 with an annual load factor of 41%. The desuperheater units could help reduce the peak demands for summer and winter by a minimum of 0.2 kW per customer and were shown to have an average COP of 1.1 and an annual load factor of 54%. The heat pump water heaters were concluded to have about twice the efficiency of an electric heater with a load factor of 52%. The peak demand reduction for heat pump water heaters were shown to be about 0.6 kW per customer for winters and almost negligible for summers.

Another study has investigated two methods for reducing the amount of energy required for producing the domestic hot water (DHW) in residences through TRNSYS simulations (Bernier et al., 2004). The first method was a DWHR at different piping configurations and the second one was a classic solar domestic hot water heating system. All TRNSYS components used for the simulations were the standard ones except for the DWHR unit for which a new model was created. This model was empirically based and used steady-state effectiveness data for a range of flow rates obtained from the manufacturer data. The steady-state effectiveness was then multiplied by a damping factor to illustrate the transient behavior of the DWHR unit and its

transient effectiveness. TRNSYS simulations were performed using a typical Canadian residence hot water consumption profile calculated by DHW-Calc software tool and the actual annual temperatures of water mains of the city of Montreal. From the simulation results, it was concluded that the DWHR unit could recover 36% to 49% of the energy needed to heat water for showers, depending on its location in the plumbing system. This was equivalent to 12% to 17% of savings in the total energy needed for producing DHW. The solar DHW system was shown to be able to provide about 56% of the energy needed for the DHW heating. It was concluded that with the addition of the DWHR unit to the solar system, the amount of energy delivered by the solar heating system and the solar thermal collector efficiency decreases; however, the total renewable fraction could be 69% for the DWHR configuration with the highest energy recovery. Another research study has examined four different means of DHW production in zero net energy homes (ZNEH) by performing energy simulations using TRNSYS (Biaou & Bernier, 2005). The methods were a regular electric hot water tank, a desuperheater of a ground source heat pump (GSHP) combined with a regular electric hot water tank, a flat plate solar collector with an electric tank as the backup and a heat pump water heater (HPWH) which was indirectly coupled with the GSHP. The modeled house was a two-storey 156 m² residence in northern Montreal. The space cooling and heating were provided by a closed-loop water to air GSHP. The electricity required for space conditioning, DHW production and the appliances was provided by a PV array whose size depended on the DHW producing method. The PV model was a 1.22 m² mono-crystalline silicon panel with a peak power of 175 Watts at standard testing conditions. The domestic hot water profile used was based on the study by Perlman and Mills (1985) with water mains' monthly average temperature for Montreal. The simulation results showed that the annual electricity requirements for domestic hot water heating would be 4605 kWh. The comparison of the four alternatives for DHW heating showed that the solar thermal heating is the best option with the annual contribution of 73%. With the solar thermal system, the annual electricity required for producing hot water would only be 1410 kWh. HPWH and desuperheater were the next best options which would help reducing the electricity required for DHW heating to 2116 kWh and 2895 kWh respectively. It was also concluded that with the utilization of thermal solar collectors with the total area of 6 m² for two solar panels, 46 PV panels with a peak capacity of 8.05 kW would be needed to provide the house's annual electricity requirements of 10864 kWh.

Another study has tried to assess and optimize a system of domestic hot water production in a net zero energy triplex using TRNSYS simulations (Picard, Bernier, & Charneau, 2007). The triplex was a three unit residence with two occupants in each unit. The DHW producing system included a standard solar domestic hot water system, a grey water heat recovery device and desuperheaters from the three GSHPs. The heat recovery unit configuration was set up in a way to allow preheating the inlet water going to the showers. The total daily DHW consumption was assumed to be 287 liters per day for the three units with the hot water set point temperature of 55°C. The monthly water mains temperatures of Montreal were used for the simulation. The solar collector area was oversized to increase the winter solar fraction and minimize the use of PV electricity. As a result, a secondary solar tank was added to the whole system to avoid the losses of solar DHW production in the summers. The extra DHW in the secondary tank could then be sold to the neighboring residences. Through simulations for different configurations and system parameters, it was shown that the addition of the secondary solar tank to the DHW production system consisting of a 10 m² evacuated tube solar collector surface, desuperheater, DWHR device and a 600 liters solar storage tank, the annual solar production could reach 7120 kWh from the original 5130 kWh. With the secondary solar tank, the annual renewable fraction could be increased to 1.085 from the original 0.732 with the maximum renewable fraction of 2.1 for July which has the highest amount of solar radiations.

Another study investigated the impacts of DWHR units on the peak electrical demands of electric hot water tanks using TRNSYS simulations (Eslami-nejad & Bernier, 2009). The DHW tank model used in TRNSYS was a standard model and the DWHR model was the one developed by Picard et al. (2004) and for the simulation purposes, ten different yearly water draw profiles at one minute intervals were generated and used. The tank used was a 175 liters tank with two 3-kW heating elements. The study also used the annual daily water mains' temperature of Montreal. As the first part of the simulation, the effects of water mains' temperature on the amount of energy consumption of the electric tank were examined. The impact of the DWHR unit on the peak electrical demands was also examined and it was shown that the peak demand would have 10.4% and 21.5% reductions at the two daily peaks reported by Hydro Quebec. On an annual basis, it was concluded the use of DWHR can lead to the DHW heating energy demand of 4501 kWh from the original value of 5299 kWh without the unit. It was also concluded that with a total number of 1.2 million electrical DHW tanks being equipped

with heat recovery units, there would be a minimum 280 MW reduction to the two electrical peaks combined.

Another research has tried to simulate different DHW systems using TRNSYS to study their fuel consumptions, GHG emissions and 30-year lifecycle costs (Gill & Fung, 2011). This case study had two parts. The first part was based on an energy efficient house with R2000 Standard in Whitby, Ontario. Seventeen DHW systems, including two panel SDHW systems with electric and gas heating backup tanks, modulating gas combo boiler, on demand gas water heater and conventional electric and gas hot water tanks with the option of DWHR were simulated. Yearly simulations were performed for daily hot water demands of 225 litres. Simulation results showed that SDHW system with electric hot water tank backup with TOU option was the best in energy consumption and GHG emissions reduction with 1220 kWh of electricity consumption and 266 kg of GHG emissions, compared to the conventional electric hot water tank with 4783 kWh of electricity consumption and 1136 kg of GHG emissions. In the second part, 96 different scenarios for the SDHW system of Net Zero Energy Healthy Housing project in Toronto, which consisted of two flat plate solar collectors, were simulated in TRNSYS. The obtained results concluded that the SDHW system with DWHR and 225 L daily hot water demand of 60°C could achieve up to 80% reductions in electricity cost and GHG emissions, when compared with conventional electrical tank without DWHR.

Chapter 3 : Domestic Water Heating

As mentioned earlier, DWH accounts for approximately 18% of total household energy consumption in Canada. Over the years, there has been a shift from using oil-fired water heaters to those that use natural gas, which on average are more energy efficient. In addition, current minimum energy performance standards mean that new water heaters use less energy than older models. These changes have resulted in a 19% decrease in the annual energy used per household for heating water, from 24.5 GJ in 1990 to 19.4 GJ in 2008 (See Table 3-1). DWH energy consumption for Canadian households in 2008 was estimated to be 256 PJ (NRCan, 2009). Electricity and natural gas are the major sources of energy reported in use for water heating; in 2008, 53.8 PJ of electricity and 187.5 PJ of natural gas were used for this purpose, with electricity having about 21% and natural gas about 73.2% share of the required energy for DWH in Canada. The energy source selection firstly depends on the availability of the energy source and the related costs, usage and maintenance.

Table 3-1: Water Heating Secondary Energy Use and Intensity by Energy Source (NRCan, 2009)

	1990	2005	2006	2007	2008
Total Water Heating Energy Use (PJ)	242.8	253.3	251.7	258.0	255.9
Energy Use by Energy Source (PJ)					
Electricity	60.1	53.9	54.3	53.0	53.8
Natural Gas	154.3	181.8	180.5	188.2	187.5
Heating Oil	23.3	13.3	12.5	12.3	10.2
Other	4.3	1.1	1.2	1.3	1.3
Wood	0.8	3.1	3.1	3.2	3.1
Shares (%)					
Electricity	24.7	21.3	21.6	20.5	21.0
Natural Gas	63.5	71.8	71.7	72.9	73.2
Heating Oil	9.6	5.3	5.0	4.8	4.0
Other	1.8	0.4	0.5	0.5	0.5
Wood	0.3	1.2	1.2	1.3	1.2
Energy Intensity (GJ/household)	24.5	20.1	19.7	19.9	19.4

3.1. Domestic Water Heater Types

Domestic water heaters are available in five distinct types. These types are:

3.1.1. Conventional Storage Tanks

Conventional storage tanks are the most common type used in Canada (See Figure 3-1). The heating source for these heaters can be electricity, natural gas or heating oil. These systems heat and store water in a tank and water enters and leaves the tank simultaneously. As water heating is constantly maintained, regardless of any hot water demand, these water heaters are subject to standby as well as distribution heat losses. These losses are even higher for residences with low hot water use patterns (Wiehagen & Sikora, 2003). The more recent models have a much better efficiency compared to the conventional models and can perform as much as 40% better (NRCan, 2009). The higher performance is due either to having better tank insulation for better heat retention and less standby heat loss or to having a better heat exchanger, which enhances the heat transferred to the water. There are positive and negative points for each energy source. Electric water heaters are easy to install and can be located in various areas of the household and there is no need for venting. The negative point of using such heaters is that it usually takes longer time to heat water, compared to other energy sources, and to compensate for this, electric water heaters tend to have larger storage volumes. As a result, electric fueled storage tanks have usually one of the highest annual operating costs (Aguilar, White, & Ryan, 2005).

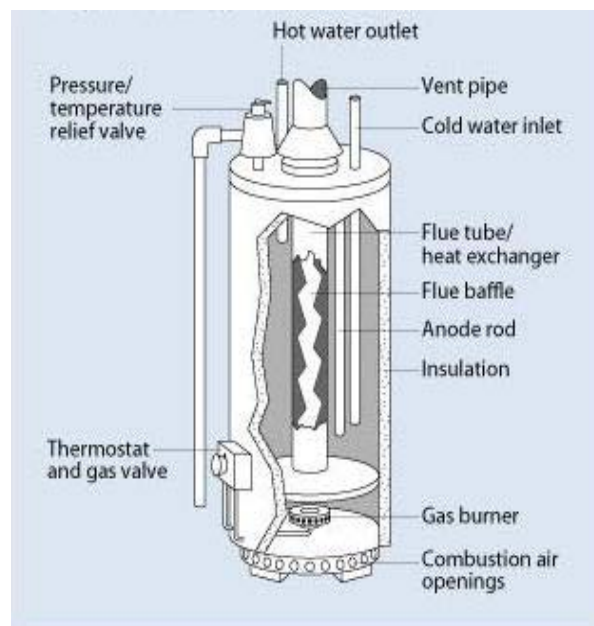


Figure 3-1: Residential Gas-fired Storage Water Heater (DOE, 2011b)

Natural gas water heaters can quickly produce hot water and should be vented through a chimney or wall. Other than having access to natural gas, the location of such heaters in a house may be restricted by access to the gas line or chimney. Heating oil water heaters are the fastest in producing hot water, which allows the option for smaller tanks. The downsides to these heaters are that there are fewer models to choose from, and there is also need for storage tanks and regular fuel delivery.

3.1.2. Tankless Water Heaters

On demand or instantaneous water heaters, as shown in Figure 3-2, do not have a storage tank. The water is heated only when it is needed and thus, standby heat losses through tank walls and water pipes are avoided (NRCan, 2009). These heaters usually have a gas burner or an electric element surrounded by flowing water. The burner or element ignites when hot water is delivered on demand. Tankless water heaters are usually installed to serve a specific need near the point of use and are best suited for households with low simultaneous demands. The operating costs for the gas demand models are usually, not always, lower (Aguilar et al., 2005).

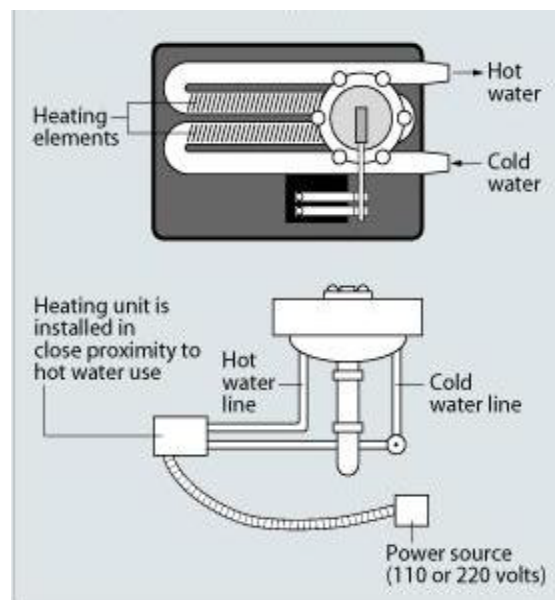


Figure 3-2: Electric Demand Water Heater (DOE, 2011b)

3.1.3. Integrated Space/Water Heaters

Integrated space/water heating systems combine the household heating requirement with the household hot water needs, thus saving costs on total system installation. This type of heaters can be divided into two separate types: 1- Tankless coil water heaters and 2- Indirect water heaters.

A tankless coil water heater uses a heating coil or heat exchanger installed in a main furnace or boiler used for space heating to heat water almost instantaneously (DOE, 2011). These water heaters provide hot water on demand, like the on-demand water heaters, but because they rely on the furnace or boiler to heat the water directly, tankless coil water heaters work most efficiently during cold months when the space heating system is used frequently and is less efficient in warmer climates. While this system avoids the need to have a separate water heating system, this means that the space heating system must be operated in the non-heating seasons just to heat water.

Indirect water heaters offer a more efficient choice for households, even though they require a storage tank (DOE, 2011b). Indirect systems can be fired by gas, oil, electricity, solar energy or a combination of these. An indirect water heater uses the main furnace or boiler to heat the fluid that circulates through the heat exchanger in the storage tank. Because the energy stored by the water tank allows the furnace to turn off and on less often, these systems are more efficient than the tankless coils.

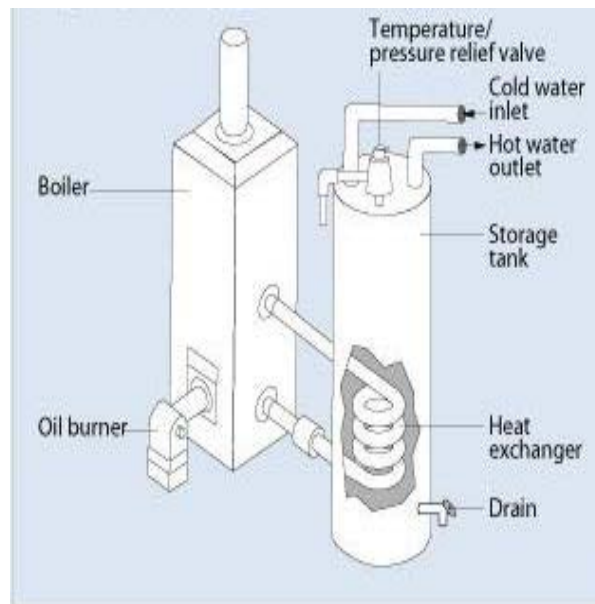


Figure 3-3: Indirect Water Heater (DOE, 2011b)

3.1.4. Heat Pump Water Heaters

Heat pumps use electric power to transfer heat from a low-temperature heat source to a high temperature heat sink which in this case, is the water stored in the hot water tank. Air source heat pumps (ASHP) heat water by removing heat from ambient air. These water heaters are in use in

the United States, but lack popularity in Canada due to the warm temperatures required for proper function. Most of these heaters have back-up heating elements to heat water during cold periods.

Ground source heat pumps (GSHP) draw heat from the ground through the buried loops close to the household for space heating during winter months and from the indoor air during the summer for space cooling. A desuperheater needs to be added to the GSHP system, if the system is to be used for water heating purposes. According to the U.S. Department of Energy (DOE), heat pump water heaters require installation in locations that remain in the 4.4°C to 32.2°C range year-round and provide at least 28.3 cubic meters of air space around the water heater (DOE, 2011b).

3.1.5. Solar Water Heaters

Solar water heating systems, as shown in Figure 3-4, use the sun's energy for water heating. The main components in these systems are a solar collector, a water storage tank of solar heat, a means of circulation such as pumps, a heat exchanger (in most systems), pipes containing water or other fluids, a control system for safety and efficiency, a water supply and a back-up heating system. There are generally four system layouts available for these systems which describe the relationship of the key components in a solar water heating system (Laughton, 2010). The key distinguishing features of the mainstream categories of system layout are:

- Passive or active;
- Direct or indirect;
- Fully filled or drainback;
- External or internal solar storage tank.

Active systems use pumps to circulate the fluid within the solar loop, which in return, allows more choices on component locations and enables better solar heat management. Passive systems, on the other hand, have very few moving parts, use no pumps or electronic controls and circulate the heat by natural means such as thermosyphoning.

Direct systems use the water entering the building as the heat transfer fluid. Indirect systems, on the other hand, use heat exchangers and a separate heat transfer fluid.

In fully filled systems, heat transfer fluid is present in collectors all the time and all air is removed from the collector and pipes. In drainback systems, the fluid is drained from the

collector once the pump is switched off and some air is always retained. In drainback systems, the collector should be higher than the pipes and tank(s).

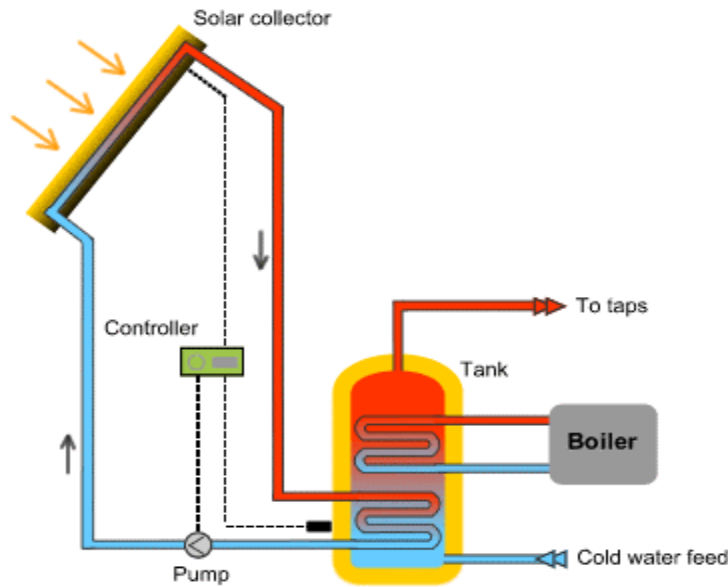


Figure 3-4: Solar Domestic Hot Water System (ES Renewables Ltd, 2011)

3.2. Efficiency of Domestic Water Heaters

The energy factor (EF) is the measure used to rate the overall efficiency of a DHW unit. It is the ratio of the energy output (that is, heat delivered as hot water) of the water heater to the total amount of energy consumed by the water heater. More specifically, EF is the added energy content of the water drawn from the water heater divided by the energy required to heat and maintain the water at the water heater's set point temperature as shown in Equation (3.1) (The U.S. Department of Energy (DOE), 2000).

where:

EF = energy factor

M = mass of water drawn (kg)

C_p = specific heat of water (kWh/kg.°C)

T_{tank} = water heater thermostat set-point temperature (°C)

T_{inlet} = inlet water temperature (°C)

Q_{dm} = water heater's daily energy consumption (kWh)

EF also takes into account standby losses that are estimated as the percentage of heat loss per hour from the stored water compared to the heat content of the water. While higher EF ratings are equated with higher efficiency, they do not include operating costs. Higher EF values may not always mean lower operating costs, especially when fuel sources are compared. However, in general, the lower the EF rating, the higher the operating costs (Aguilar et al., 2005).

An alternative measure of electric DWH unit's efficiency has also been provided through the use of outlet monitoring (Wiehagen & Sikora, 2003). The heater energy rate was determined at the outlet of the water heater, Q_{hw} , and at each location (outlet) where the hot water is delivered, $Q_{out,i}$, where the total outlet energy rate delivered, Q_{out} , is the sum across outlets of the energy delivered at each outlet. Specifically:

where:

T_{hw} = the water temperature at the outlet of the water heater ($^{\circ}\text{C}$)

T_{cw} = cold water inlet temperature ($^{\circ}\text{C}$)

\dot{m}_T = the total system mass flow rate (kg/hr)

C_p = specific heat of the water (kJ/kg.K)

and the total outlet energy (Q_{out}) is defined as:

where:

$T_{out,i}$ = outlet temperature at outlet i ($^{\circ}\text{C}$)

= assigned flow rate at outlet i (kg/hr)

n = number of outlets

The difference between Q_{hw} and Q_{out} indicates energy losses through piping.

The efficiency of the heater unit, Eff_{hw} , is calculated as:

—

where:

Q_{elec} = Total electric input energy (kWh)

The overall system efficiency, Eff_{sys} , can be calculated as follows:

—

In general, the efficiency of a tank water heater decreases as the tank gets larger; in other words, smaller tanks consume less energy per total amount of water heated. The larger standby losses of a larger tank reduce the EF more than is the case with a smaller tank (Aguilar et al., 2005).

Load factor is another measure of the performance of hot water heating systems (Merrigan & Parker, 1990). The load factor is defined as the ratio of the average kilowatt demand over a specified period of time to the maximum demand over the same period:

This is a measure of how well the electric demand of the water heater unit is utilized over a period of time. Since a higher load factor reflects a more even demand for electricity, this can be viewed as an indication of a more efficient water heater; however, it was concluded that this factor did not vary greatly across different types of water heaters.

3.3. Domestic Water Heater Standards

Canada's previous standards for domestic hot water heaters came into effect in February 1995. Amendments to these regulations were made in September 2004. These requirements are in the form of maximum allowable standby losses (the percentage of heat loss per hour from the stored water compared to the heat content of the water) for electric water heaters and minimum Energy Factor, EF , for oil and gas fired storage tanks and are dependent on the size of the storage water tank (Canada Gazette, 2004). Table 3-2 outlines the energy efficiency standards for the hot water storage tank heaters.

Table 3-2: Energy Efficiency Regulations for Canadian Water Storage Tank Heaters (Canada Gazette, 2004)

Energy-using Product	Standard/ Legislative Provision	Energy Efficiency Standard
Electric water heaters	CSA C191-00	Maximum standby loss in W = (a) for tanks with bottom inlet: (i) $40 + 0.2V$ for tanks with $V \geq 50$ L and ≤ 270 L (ii) $0.472V - 33.5$ for tanks with $V > 270$ L and ≤ 454 L (b) for tanks with top inlet: (i) $35 + 0.2V$ for tanks with $V \geq 50$ L and ≤ 270 L (ii) $0.472V - 38.5$ for tanks with $V > 270$ L and ≤ 454 L
Gas water heaters	CSA P.3-04	Minimum energy factor (EF) = $0.67 - 0.0005V$
Gas boilers intended for hot water systems	CGA P.2	Annual fuel utilization efficiency $\geq 80\%$
Oil-fired water heaters	CSA B211-00	Minimum energy factor (EF) = $0.59 - 0.0005V$

Where: V = Volume of storage tank in liters

In the United States, energy standards for water heaters are controlled by the National Appliance Energy Conservation Act (NAECA). Effective January 2004, these energy conservation standards were revised (DOE, 2001). According to these standards, a minimum energy factor is specified to which water heaters must adhere. This factor is dependent on the size and type of water heater. U.S. manufacturers are required by law to meet these minimum energy factor values and to label these values on their products. These values are displayed in Table 3-3.

The energy factor of all small water heaters that are federally regulated consumer products, (other than booster water heaters, hot water dispensers, and mini-tank electric water heaters) shall be not less than the applicable values given in Table 3-3 (DOE, 2001).

Table 3-3: U.S Standards for Federally Regulated Water Heaters (California Energy Commission, 2006)

Appliance	Minimum Energy Factor	
	Effective April 15, 1991	Effective January 20, 2004
Gas-fired storage-type water heaters	$0.62 - (.0019 \times V)$	$0.67 - (.0019 \times V)$
Oil-fired water heaters (storage and instantaneous)	$0.59 - (.0019 \times V)$	$0.59 - (.0019 \times V)$
Electric storage water heaters (Excluding tabletop water heaters)	$0.93 - (.00132 \times V)$	$0.97 - (.00132 \times V)$
Electric tabletop water heaters	$0.93 - (.00132 \times V)$	$0.93 - (.00132 \times V)$
Gas-fired instantaneous water heaters	$0.62 - (.0019 \times V)$	$0.62 - (.0019 \times V)$
Electric instantaneous water heaters (excluding tabletop water heaters)	$0.93 - (.00132 \times V)$	$0.93 - (.00132 \times V)$
Heat pump water heaters	$0.93 - (.00132 \times V)$	$0.97 - (.00132 \times V)$

V = rated volume in gallons.

Chapter 4 : Archetype House Description

The Archetype House is composed of two (almost) identical semi-detached twin houses, named House A and House B. Figure 4-1 shows the south view of the two houses with House A on the left hand side. This site is believed to be the most comprehensive demonstration centre of energy efficiency, renewable energy, conservation and sustainable technologies and materials in North America. The two houses are also equipped with different mechanical equipment and a comprehensive monitoring system for evaluating their performance. House A demonstrates energy efficiency technologies and practices that are current and practical today, while the purpose of House B is to showcase advanced technologies that can be used in residential housing in the near future. Both houses are R2000 and LEED Platinum certified (Dembo et al., 2010).



Figure 4-1: South View of the Archetype Sustainable Twin Houses

Although both houses are built based on the R-2000 standard, there are a few differences in the insulation, windows and mechanical systems. A comparison of the HVAC system among different housing standards is given in Table 4-1.

Blower door tests have been conducted in both houses. The air tightness in House A was found to be 1.317 ACH at 50 Pa and 1.214 ACH at 50 Pa in House B (Dembo et al., 2010).

Table 4-1: Comparison of HVAC systems among housing standards (Zhang et al., 2011)

Equipment	Traditional house	R-2000 standard	TRCA sustainable House
Solar collector for hot water generation	No	No	Yes
Cogeneration systems for power and hot water generation	No	No	Yes
Solar wall for supply of hot air to the zone	No	No	Yes
PV cells for power generation	No	No	Yes
Wind turbine for power generation	No	No	Yes
GSHP for space heating/cooling	No	Yes	Yes
Desuperheater of GSHP for hot water generation	No	No	Yes
HRV/ERV for recovery of heat from exhaust air	No	Yes	Yes
Drain Water Heat Recovery	No	No	Yes
Radiant floor heating	No	Yes	Yes

The basic design features of the two houses are as listed in Table 4-2.

Table 4-2: Basic design features of House-A and House-B (Zhang et al., 2011)

Features	House-A	House-B
Orientation	South facing	South facing
Stories	3	3
Floor	232 m ² /25'×40' (2500 ft ²)	232 m ² /25'×40' (2500 ft ²)
Natural Infiltration	0.06 ACH	0.06 ACH
Winter design conditions	Outdoor temp.: -22°C /-7.6°F Indoor temp.: 22°C/71.6°F	Outdoor temp.: -22°C /-7.6°F Indoor temp.: 22°C /71.6°F
Summer design conditions	Outdoor DB: 31°C /87.8°F Outdoor WB: 24°C/75.2°F Indoor temp.: 24°C/75.2°F	Outdoor DB: 31°C/87.8°F Outdoor WB: 24°C/75.2°F Indoor temp.: 26°C/78.8°F
Heating load	7.91 kW/27 MBH	7.94 kW/27.1 MBH
Cooling load	4.92 kW/16.8MBH	6.18 kW/21.1 MBH
Ventilation	85.42 Liters/sec (181 CFM)	70.79 Liters/sec (150 CFM)

Detail structural features of House-A and House-B are as described in Table 4-3. Both houses have similar structural features except for wall insulations and windows.

Table 4-3: Structural features of the twin houses (Zhang et al., 2011)

Features	House-A	House-B
Basement walls	RSI 3.54 (R20) with Durisol blocks	RSI 3.54 (R20) with Durisol blocks
Walls	RSI 5.31 (R30)	RSI 5.31 (R30)
Wall insulation	Roxul Batt Fibre (R21) + 3" Styrofoam	Heat-Lock Soya Polyurethane Foam and Lcynene spray foam
Windows	2.19 W/m ² .K (0.39 Btu/ft ² .°F) and double paned, low "E", fiberglass framed	1.59 W/m ² .K (0.28 Btu/ft ² .°F) and all triple glazed, low "E" , with argon filled
Roof	RSI 7 (R40) Structurally Insulated Panels (SIPs), which are insulated Styrofoam panels	RSI 7 (R40) Structurally Insulated Panels (SIPs), which are insulated Styrofoam panels

The mechanical features of House-A, House-B are listed in Table 4-4. The only component using renewable energy sources in House-A is a solar thermal collector, whereas photovoltaic system, wind turbine, solar thermal collector and GSHP are used as renewable energy sources in House-B.

Table 4-4: Mechanical features of the twin houses (Zhang et al., 2011)

Features	House-A	House-B
Solar collector	Flat plate collectors	Evacuated tube collectors
PV system	No	Yes
Wind turbine	No	Yes
Heating and cooling	Two-stage air source heat pump packaged with AHU	Ground source heat pump with horizontal loops
	Wall mounted mini gas boiler	Stirling engine micro-cogeneration unit
Ventilation system	HRV	ERV
Auxiliary water heating	Mini gas boiler	Desuperheater & Electric (TOU)
Infloor heating	Basement only	All three floors & basement
Heat recovery from drain water	Yes	Yes

4.1. DWH System of House-A

The DWH system of House-A consists of a hybrid solar system in conjunction with an auxiliary heating system with natural gas and a DWHR unit. The piping setup of the house is in a way that the cold water to the hot water taps is passed through the DWHR unit to get preheated. It should be mentioned that this is not the most efficient setup to use DWHR units. The most efficient way is to route all cold water to the house through DWHR unit. The solar combi-system utilizes a flat plate solar thermal collector and a hot water solar tank for DHW heating. A wall-mounted gas boiler is also used for auxiliary heating when the heating provided by the solar collector alone is not sufficient. The hot water system of the house is a one tank system which serves as a heat exchanger and also DHW tank. The tank is utilized for domestic hot water usage and has a dual mode facility for DHW heating from the solar panel in conjunction with the gas boiler. A mixture of water and USP grade Propylene Glycol (60:40) is used as the heat transfer media between the solar collector and the storage tank. The schematic view of the DWH system of House-A with all of its components and the related sensors for the monitoring system is displayed in Figure 4-2.

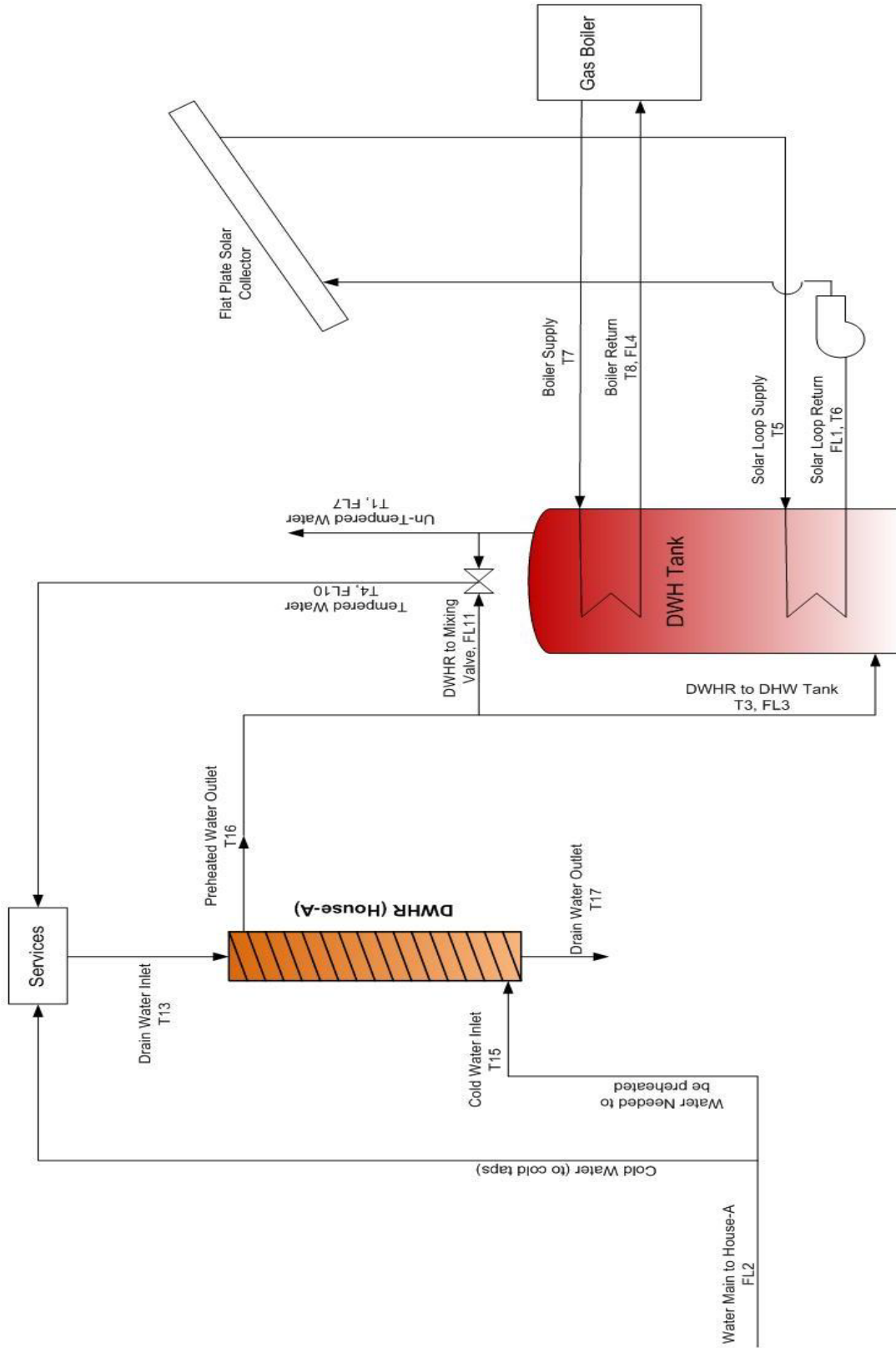


Figure 4-2: DHW Heating System of House-A with the Related Monitoring Points

Detailed specifications of the DHW system components with their specifications, manufacturers and models are shown in Table 4-5.

Table 4-5: Detail specifications and technical data of the DHW system components in House-A

Component	Manufacturer	Model	Technical Data
Flat plate solar collector	Viessmann Manufacturing Co.	VITOSOL 100 SV1	Gross Area: 2.51 m ² (27 ft ²) Absorber Area: 2.32 m ² (25ft ²) Aperture Area: 2.33 m ² (25.1 ft ²)
Wall type mini boiler	Viessmann Manufacturing Co.	VITODENS 100- W24	Max Input Rate: 23.45 kW (80 kBH) Min Input Rate: 8.5 kW (29 kBH)
Domestic hot water tank	Viessmann Manufacturing Co.	VITOCCELL B100	Capacity: 300 lit (79 USG)
Drain water heat recovery	Renewability Energy Inc.	R3-36	Length: 91.44 cm (36") Diameter: 7.62 cm (3") Tube Size: 0.95 cm (3/8")

4.2. DWH System of House-B

As in House-A, the DHW system of House-B also consists of a DWHR unit and a solar hybrid system in conjunction with an auxiliary heating electric tank. Same as the setup in House-A, the cold water mains to the hot water taps of the house is first preheated when passed through the DWHR system. This system utilizes an evacuated tube solar collector and a solar preheat tank for DHW heating. A mixture of water and USP grade Propylene Glycol (60:40) is used as the heat transfer media between the solar collector and the storage tank. The solar storage tank can also supplied with hot water from the desuperheater of the ground source heat pump (GSHP) or the Sterling co-gen system, whichever might be used for space heating of the house. The desuperheater of the GSHP is used for hot water production using the superheated refrigerant from the compressor of the heat pump. The co-gen system is also used as a substitute of the GSHP and is utilized for simultaneous producing of electricity and hot water for the DHW heating or space heating systems. The DHW heating system of the house is a two-tank system. Other than the solar preheat tank, the DHW heating system has an electric backup tank as the auxiliary water heating source. The DHW tank has two sets of electric elements to supply hot water, if the solar heating system is not sufficient.

Figure 4-3 displays the schematic view of the DHW heating system of the house with all of its components and the related sensors for the monitoring system. The specifications of the DHW system components with their specifications, manufacturers and models are shown in Table 4-6.

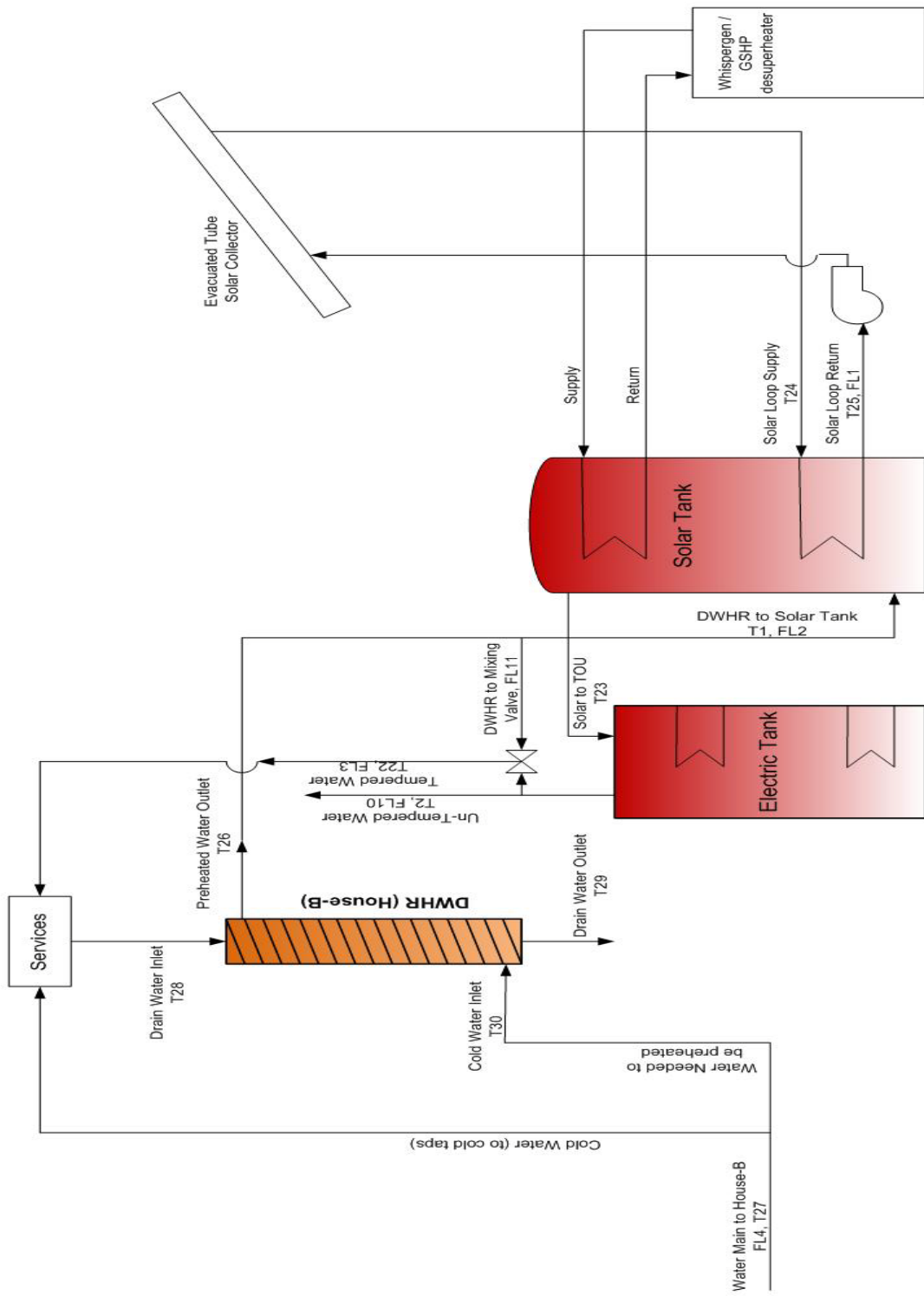


Figure 4-3: DHW Heating System of House-B with the Related Monitoring Points

Table 4-6: Detail specifications and technical data of the DHW system components in House-B

Component	Manufacturer	Model	Technical Data
Evacuated tube solar collector	Viessmann Manufacturing Co.	VITOSOL 300 SP3	Gross Area: 2.88 m ² (31 ft ²) Absorber Area: 2.05 m ² (22ft ²) Aperture Area: 2.11 m ² (22.7 ft ²)
Solar hot water tank	Viessmann Manufacturing Co.	VITOCCELL B100	Capacity: 300 lit (79 USG)
Auxiliary hot water tank	GSW Water Heating	6G50SDE1 (Series 6)	Capacity: 184 lit (48.6 USG) Two elements with 3kW each
Drain water heat recovery	Renewability Energy Inc.	R3-36	Length: 91.44 cm (36") Diameter: 7.62 cm (3") Tube Size: 0.95 cm (3/8")

Chapter 5 : Methodology

In this chapter, the monitoring system used to monitor the performance of the DHW systems of the two Archetype houses, and also the different types of sensors (temperature, flow rate, etc.) for the different equipments of the DHW systems will be described. The equations used for energy consumption, generation and efficiency calculations are also stated.

5.1. Monitoring System

Monitoring systems range from broad research studies to very specific savings verification. The TRCA Archetype House monitoring project has been developed for broad research studies by a group of students from Ryerson University (Zhang et al., 2011). For this project, monitoring priority has been given to performance evaluation of different mechanical equipment, whole house energy consumption and on-site renewable energy production rather than envelope retrofit performance. For development of this monitoring project ASHRAE Standards and Codes for energy monitoring in buildings have been followed (ASHRAE, 1999).

5.2. Data Acquisition (DAQ) System

The DAQ system used for this project is very flexible in layout so as to have distributed sub central DAQ. This has helped reducing the wiring of the sensors which has minimized the associated signal interference.

The DAQ system consists of backplane, controller, module, connector block, power supplier, LabVIEW software platform and a central computer. The selection of modules depends on the output signal of sensors. This output signal is converted into corresponding engineering units by the LabVIEW software (Zhang et al., 2011). Table 5-1 displays the sensors used for the two DHW systems and their related output signals.

Table 5-1: Sensor name and its output signal

Sensors	Nomenclature	Output signal	Conversion unit
Flow rate sensor (liquid flow rate)	FL	Pulse (Hz) or V	GPM (USG)
Direct immersed RTD probe	T	ohm	°C
Surface mounted RTD sensor	T	ohm	°C
Gas meter	NG	mA or V	lpm
Wattnode	W	Pulse	W
Pyranometer (solar radiation)	I _T	mA	W/m ²

Since the houses are extensively wired from various locations, a flexible and expandable distributed DAQ system is essential for obtaining good quality and with minimal noise data. The NI Compact Fieldpoint (CFP) system is an ideal system which provides an easy-to-use, highly expandable programmable automation controller (PAC) composed of rigid I/O modules and intelligent communication interfaces. The Compact Fieldpoint I/O modules filter, calibrate, and scale raw sensor signals as well as performing self-diagnostics.

All CFPs have been connected to the central computer through a network hub. As such, sensor data is captured by the LabVIEW software platform and sensors are addressed in this software according to the nomenclature (Appendix-A). The sensors' outputs mentioned in Table 5-1 are then converted into corresponding engineering units, mentioned in the same table, by the software. With the LabVIEW program, all equipment performance can be evaluated as well. Collected data sampling frequency will be adjusted in this program according to the actual requirement of data acquisition.

5.2.1. LabVIEW Software

Figure 5-1 is a snapshot of the front panel of the LabVIEW program. Both low level (temperature, flowrate, RH, etc.) information and high level information (efficiency, effectiveness, heat generation, heat recovery, etc.) can be displayed on the front panel. Raw signals are converted and post-processed at the background of the front panel. All signals, except for power consumption signals, are acquired at a constant sampling time of 5 seconds, whereas a 0.5 second sampling time applies to the electrical power signal. For the flowrate and power consumption, both the rate and total value are calculated within the sampling period.

5.2.2. SQL Server Management Studio

SQL Server Management Studio is a relational database management system. The user can easily store, retrieve, and manipulate data in this software. Although storage capacity depends on the hard drive, this software has the database capacity of 524272 TB (Terabytes) (SQL Server, 2008). In this monitoring system, all data from the LabVIEW program are stored into the SQL server database directly. The database structure has three vertical columns which consist of Datestamps, Reading, and Channel. Hence, each row has three horizontal values. At 5 second

intervals, each sensor captures 17280 rows/day data, equivalent to 356 kB (kilobytes). Each day 300 sensors accumulate 107 MB (megabytes) records. To deal with the large amount of data, this software has been selected.

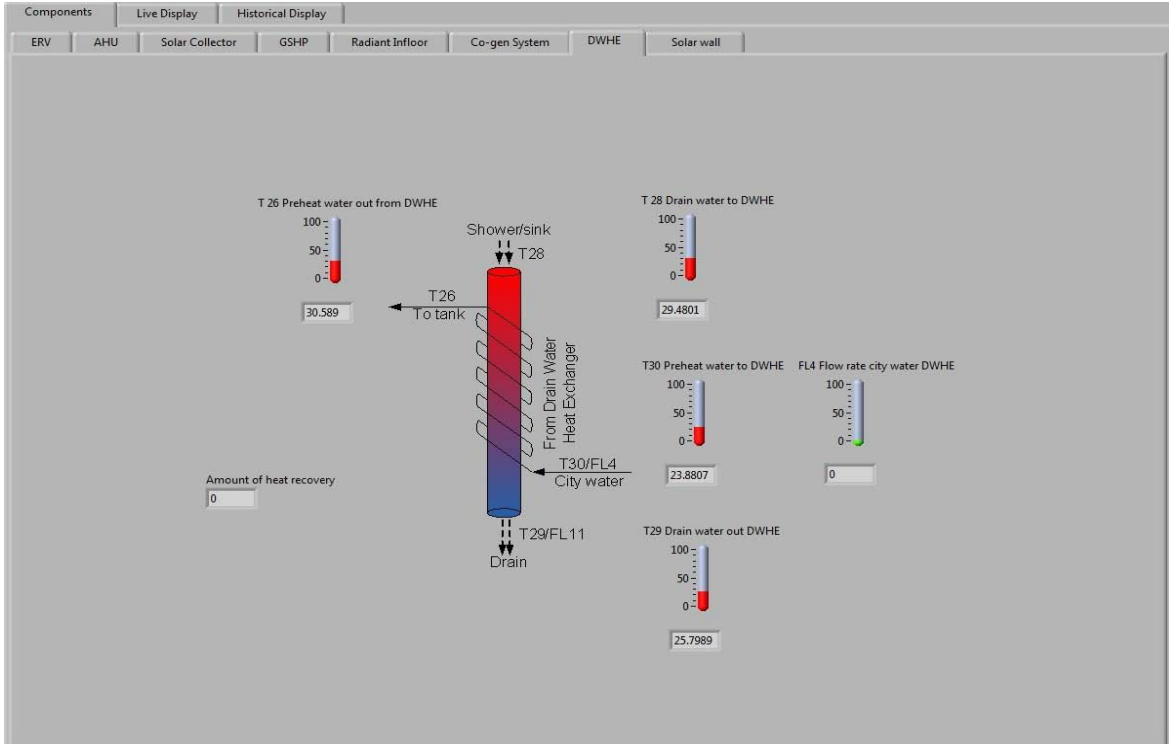


Figure 5-1: Snapshot of LabVIEW front panel showing the operating information of the DWHR in House-B

5.3. Sensors

In both houses, over 300 sensors of various types covering sufficient energy monitoring details have been installed (Zhang et al., 2011). Sensor installation strictly follows the manufacturer’s instruction to avoid any electrical damage and inaccurate readings of the signal. Table 5-2 shows the list of sensors for the DWH systems’ components with their required inputs.

Table 5-2: List of DWH systems’ components with their related sensors and input parameters

Component	Input Parameters	Sensors
Solar Collectors (Evacuated tube or flat plate)	Water & USP grade Propylene Glycol Mix. temperature (inlet and outlet) and flow rate, solar radiation	RTD probe, flow rate sensor, pyranometer and wattnode sensor
Gas Boiler	Mass of natural gas, exhaust gas temperature, supply and return water temperature and flow rate (on return), power consumption	RTD, air flow rate sensor, natural gas meter, matched delta T probe and wattnode sensor

Electric backup Tank	Water temperature (supply and return), flow rate (on return) and power consumption	Matched delta T probe, flow rate sensor and wattnode sensor
Drain Water Heat Recovery (DWHR)	Water temperature (supply and return) of both city and drain water and flow rate (on supply)	Matched delta T probe, surface mounted RTD and flow rate sensor

The connection between the sensors and the connector block of the DAQ system has been installed according to the National Instruments (NI) supplied circuit diagram (Zhang et al., 2011). The sensors types used for the DHW systems are as follows.

5.3.1. Temperature Sensors

Three types of RTD temperature sensors have been used for the measurement of liquid temperature: i) Pt-500 series immersed ΔT RTD sensors, ii) Pt-100 series direct immersed RTD sensors and iii) Pt-100 series surface mounted temperature sensors. For calibration purposes, two sources of reference temperature were used, i.e. a) ice water and b) handheld dry-wells (Barua, 2010).

5.3.2. Liquid Flow Meters

Two types of liquid flow meters have been used for the measurement of liquid flow rate: i) turbine type water flow rate sensors and ii) PROTEUS series water flow rate sensors. All DHW system pipe lines, except for the mini gas boiler primary loop and DHW tank supply loop, use the turbine type flow rate meters. The turbine type meters are manufactured by GEMS and these sensors are capable of reading a wide range of flow rates from as low as 0.5 lit/min to 30 lit/min. The selection of a specific type of sensor depends on the flow rate range on each desired pipe line. The PROTEUS sensors are used for the water lines with high liquid temperatures like the gas boiler loops.

5.4. Calibration of Sensors

As introduced by Feng et al. (2003), “Calibration is the process of mapping raw sensor readings into corrected values by identifying and correcting systematic bias. Sensor calibration is an inevitable requirement due to the natural process of decadence and imperfection”.

In the calibration process of this monitoring system, the off-line calibration technique is applied for temperature sensors (Barua, 2010). In the context of off-line calibration, the collected data

has two components: raw sensor readings and data captured by high quality and high-cost light weight calibrators measuring the same set of readings. The second set of data serves as the standards of what the sensors should measure. The goal of the off-line calibration is to determine a compacting function that provides the mapping from the raw sensor reading to correct values (Feng et al., 2003). All the sensors were calibrated before the start of data collection testings. All sensors have also been cross checked frequently for calibration purposes. The list of calibrators used in this project for calibrating the DHW systems sensors are tabulated in Table 5-3.

Table 5-3: List of sensors for DHW systems and calibrators (Barua, 2010)

Sensors	Calibrator
RTD Temperature Sensors	<ul style="list-style-type: none"> • HART Scientific series 9102S Handheld Dry-wells • MICROCAL 20DPC • Omega series CL3515R
Turbine type water flow rate sensors	<ul style="list-style-type: none"> • Volume bucket and stop watch
PROTEUS series water flow rate sensors	<ul style="list-style-type: none"> • Factory calibrated but cross checked
Pyranometers	<ul style="list-style-type: none"> • Factory calibrated, but randomly checked with the Kortright Conservation Centre weather station data
Wattnodes	<ul style="list-style-type: none"> • Factory calibrated, but cross checked by power meter

5.5. Daily Water Draw Schedule

It is widely accepted that the performance of DWHR units is dependent on the amount of hot water consumption. In a study on the energy savings by the DWHR units, it was noted that unlike other energy saving measures, the total savings of these units are highly dependent on the total number of house occupants (Van Decker, 2008). This study points out that DWHR systems are highly cost effective when implemented in homes with three or more occupants and not so with single occupant homes.

In this project, the daily water schedule used for the two houses is a typical hot water draw for a family of four, which is equal to 225 l/day. This is in accordance with the IEA Schedule Task 26 model (Jordan & Vajen, 2001) which predicts a 225 l/day profile data for a typical Canadian DHW consumption when the delivered water temperature to the end user is 48°C. It should be mentioned that the water used for the hot water draw profile of the two houses is tempered water with an average temperature of 48°C to prevent any risks of burning from hot water. A

tempering valve in each of the houses is used for this purpose. In House A, the tempering valve is used to temper the hot water outlet of the solar tank (which acts as the main DHW tank) and in House B, this valve is used to temper the hot water output of the TOU electric tank. To determine the water draw schedule for the houses, the temperature of the inlet cold water is needed. As mentioned earlier, the water to the houses is supplied from local wells and, therefore, the temperature of the supply water is close to that of the local ground temperature. The temperature of the supply water for the winter and summer testing periods was determined to be around 5°C and 16°C respectively. With the cold water inlet known, the amount of tempered water needed to obtain a hot water temperature of 41°C to 44°C for different events can be easily determined. The specified flow rates for different events for the winter and summer testing periods are listed in Table 5-4 and Table 5-5.

Table 5-4: List of events and different flow rates used for the water draw Schedule in winter

Events	Cold & Hot Water Flow Rate-Mixed (GPM)	Hot Water Flow Rate (GPM)	Cold Water Flow Rate (GPM)
Shower	1.9	1.6	0.3
Bathroom Sink	1.2	1	0.2
Kitchen Sink	1.2	1	0.2
Clothes Washer	3	1.6	1.4
Dishwasher	1.3	1.3	0

Table 5-5: List of events and different flow rates used for the water draw Schedule in summer

Events	Cold & Hot Water Flow Rate-Mixed (GPM)	Hot Water Flow Rate (GPM)	Cold Water Flow Rate (GPM)
Shower	1.9	1.5	0.4
Bathroom Sink	1.2	1	0.2
Kitchen Sink	1.2	1	0.2
Clothes Washer	3	1.5	1.5
Dishwasher	1.3	1.3	0

Six sets of control valves have been devised in each of the houses; three for the cold water flow rates and three for the hot water flow rates and each adjusted manually to provide the required flow rates. These control valves have been adjusted in a way to obtain different flow rates for different household flow rates for different tasks, showers, kitchen tap, restroom taps and etc. The valves are controlled by LabView, which forces the specified valve(s) to be opened according to the imported DHW draw schedule profile. The schedule used does not include the events which use cold water only, but includes the events with both hot and cold water (showers or bathroom sinks) and hot water only (dishwashers). Two events cannot happen at the same

time due to the controlling issues with LabView. The DHW schedule has events of simultaneous hot water draw and drain water flows (showers or sinks) and events where the two water flows cannot happen simultaneously (dishwashers or clothes washers).

5.6. Energy Consumption, Generation and Efficiency Calculation Equations

The basic equations used for power, energy and efficiency calculations of the different equipment used for the two DHW systems will be briefly described in this section. The sources of these basic equations are the ASHRAE Handbooks, TRNSYS manual, and various books and articles. In addition, some equations of density and specific heat of liquids have also been incorporated.

5.6.1. Water

Density of water is a function of temperature. Kravchenko (1966) derived Equation (5-1) for pure water density. From his studies, it was shown that by increasing the pure water temperature from 0°C to 100°C, its density varies from 999.82 kg/m³ to 950.05 kg/m³. Another study has also determined the experimental results of water density within the temperature range of 0°C to 40°C (Tanaka et al., 2001). By comparing the results from this study with Equation (5-1) and by referring to Figure 5-2, it can clearly be seen that there is a good agreement between the equation and experimental results. Hence, Equation (5-1) has been adopted for density of water in thermal energy equations in this project. Specific heat of water does not change greatly with the temperature range of 0°C to 100°C and the constant value of 4.18 — has been considered.

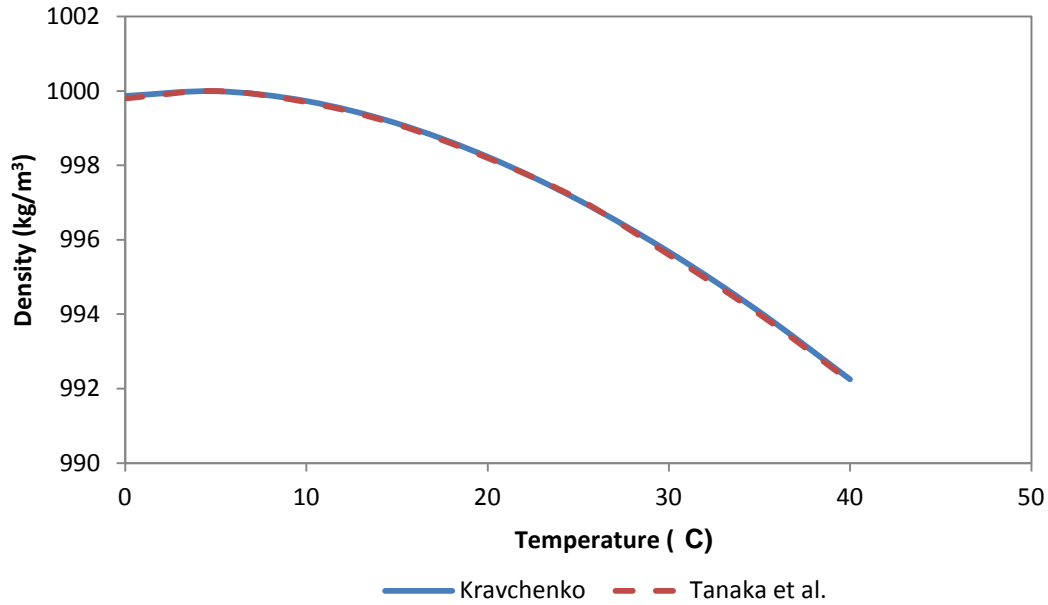


Figure 5-2: Comparison of water density variations with temperature from Equation (5-1) using TRCA data and Tanaka et al. data

The maximum percentage error in temperature difference from the two approaches was less than 0.05%.

5.6.2. Propylene Glycol (PG) Solution

A Propylene glycol and water solution (40:60) is the liquid used for solar collector loops as the heat transfer medium. The density of this solution varies from 1060.46 kg/m³ to 968.20 kg/m³ as the temperature changes from -12°C to 104°C. Specific heat of the solution also changes with temperature. The CHEM Group Inc has supplied the data for density and specific heat of this PG solution. From this data, Equations (5-2) and (5-3) have been derived:

$$\rho = 1060.46 - 0.0011T$$

$$c_p = 4.18 + 0.0001T$$

T values are in °C. The evaluated density values from Equation (5-2) are then compared with CHEM Group data. Figure 5-3 shows that there is a good agreement between CHEM Group data and the results from Equation (5-2).

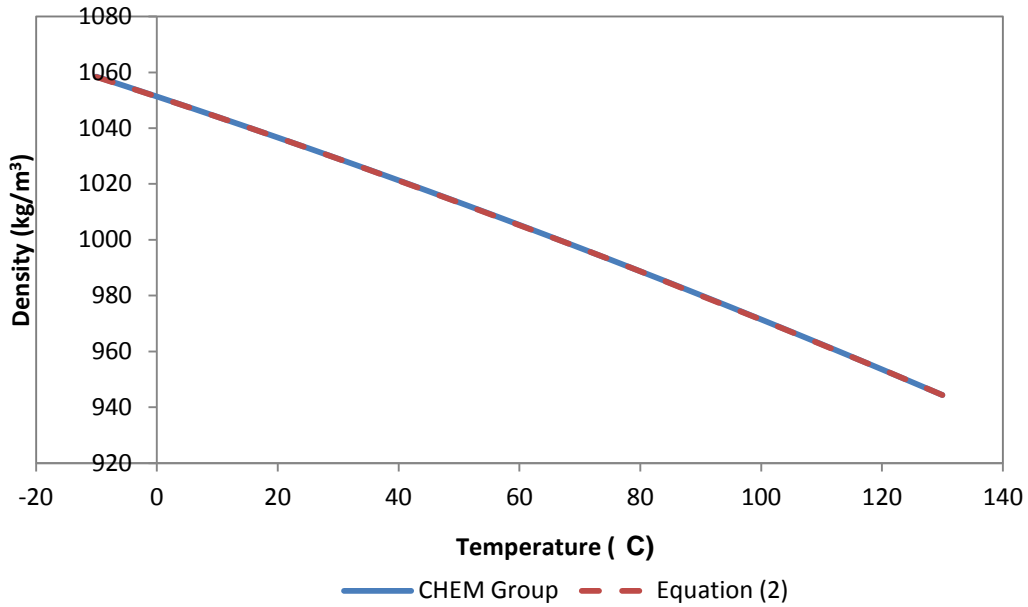


Figure 5-3: Comparison of PG density with temperature by CHEM Group data and equation result

5.6.3. Energy Consumption, Generation and Efficiency Equations for Equipment in House-A

5.6.3.1. Wall Mounted Mini Gas Boiler

Figure 5-4 displays the schematic view of the gas boiler with the inputs / outputs and the locations of all installed sensors.

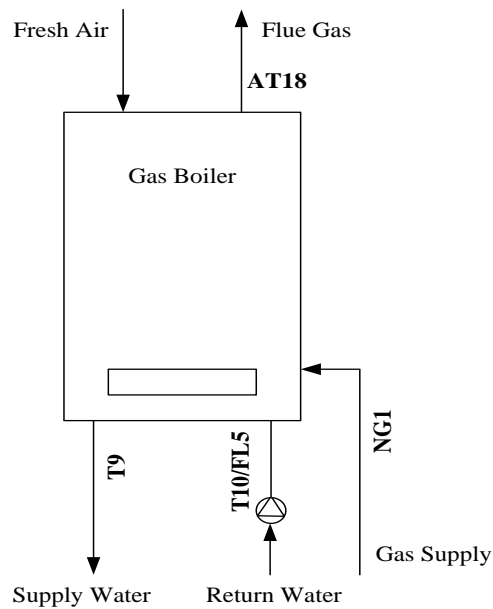


Figure 5-4: Schematic view of gas boiler with related sensors of House-A

Thermal power generation is obtained using Equation (5-4):

The water flow rate reading is in U.S. GPM (converted to L/s), the temperature readings are in °C and the supply gas flow rate is in l/min. By substituting the obtained values from different sensors into Equation (5-4), the equation can be rewritten as followed:

Boiler efficiency is achieved using Equation (5-6):

The higher heating value¹ (HHV) of natural gas is 37.8 —.

5.6.3.2. Domestic Hot Water Tank (DHWT)

Figure 5-5 displays the schematic view of the DHWT with the inputs / outputs and the locations of all installed sensors.

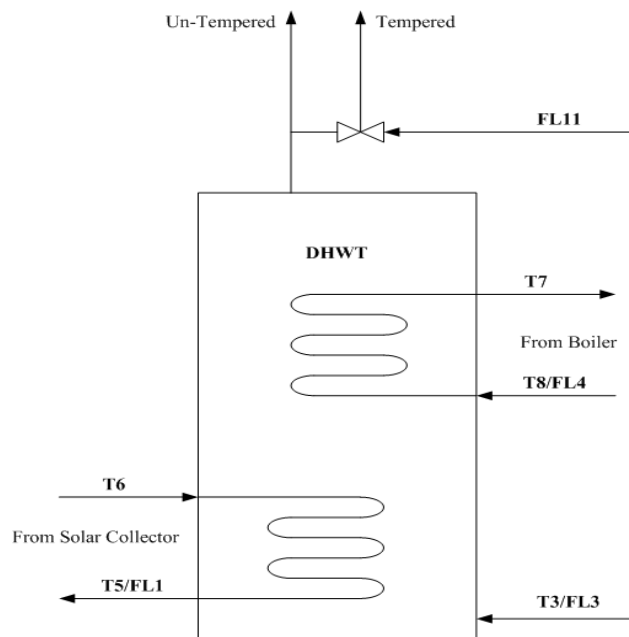


Figure 5-5: Schematic view of DHWT with related sensors of House-A

¹ High heating value of natural gas is taken from Union Gas website <http://www.uniongas.com/aboutus/aboutng/composition.asp>

Thermal power supplied to the DHWT by the boiler is obtained by using:

—

The water flow rate reading is in U.S. GPM and the temperature readings are in °C. By substituting the value of density from Equation (5-1) and the constant value for the specific heat of water, the value for the supplied thermal power to the tank would be:

Thermal power supplied to the house load by the DHWT is also achieved from Equation (5-7). By substituting the value of density from Equation (5-1) and the constant value for the specific heat of water, the value for this thermal power would be:

5.6.3.3. Flat Plate Solar Thermal Collector

Figure 5-6 displays the schematic view of the flat plate solar collector with the inputs/ outputs and the locations of all installed sensors. The sensors locations are close to the solar preheat tank and therefore, do not measure the exact fluid's temperature at entrance and exit points of the solar thermal collector.

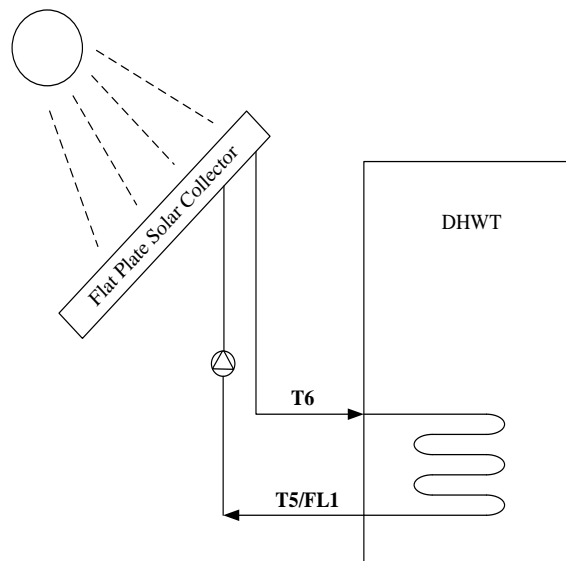


Figure 5-6: Schematic view of flat plate solar collector with related sensors of House-A

Total amount of heat generation can be achieved using Equation (5-10):

The propylene glycol solution flow rate reading is in U.S. GPM and the temperature readings are in °C. By substituting the value of density and specific heat for the solution from Equation (5-2) and Equation (5-3), the value for the thermal power would be:

The efficiency of the solar collector can be obtained using Equation (5-12):

Where A is the aperture area of the collector (2.33 m^2) and I_t is the solar radiation on the tilted surface (25°) of the collector. The solar radiation can be obtained using two sets of pyranometers, one vertical and one with the tilt angle of 25° , which is the same tilt angle as the collector have, and give the global solar radiation (direct and diffuse) in W/m^2 .

5.6.3.4. Drain Water Heat Recovery (DWHR)

Figure 5-7 displays the schematic view of the DWHR system with the inputs / outputs and the locations of all installed sensors. It should be mentioned that the flow rates are not measured at the cold and hot side inlets of the unit. For the location of the flow rate sensors, refer to Figure 4-2.

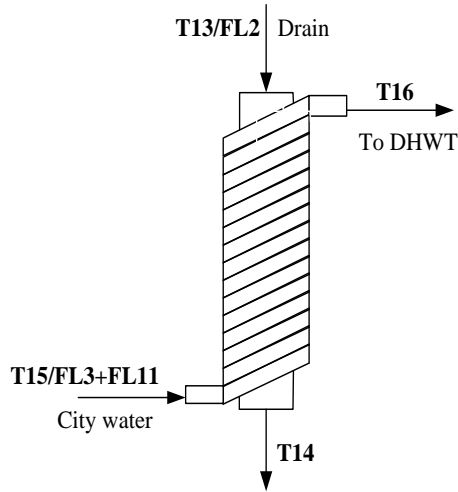


Figure 5-7: Schematic view of House-A DWHR system with related sensors

Total amount of heat recovery by DWHR system can be achieved using Equation (5-13):

$$\text{---}$$

The water flow rate readings are in U.S. GPM and the temperature readings are in °C. T_{16} and T_{15} are the outlet and inlet temperatures on the cold side of the DWHR system. By substituting the value of density from Equation (5-1) and the constant value for the specific heat of water, the heat recovery by the system would be as in Equation (5-14):

$$\text{---}$$

The actual effectiveness of the system can be obtained using Equation (5-15):

$$\text{---}$$

C_{min} is the minimum heat capacity rate; that is the lesser of C_{hot} or C_{cold} . \dot{m}_c is the water flow rate (kg/min) and c_p is the water heat capacity (kJ/kg.°C). With the DWHR setup of House-A, the cold side heat capacity rate is always the lesser one.

5.6.4. Energy Consumption, Generation and Efficiency Equations for Equipments in House-B

5.6.4.1. Solar Preheat Tank

Figure 5-8 displays the schematic view of the solar preheat tank with the inputs / outputs and the locations of all installed sensors.

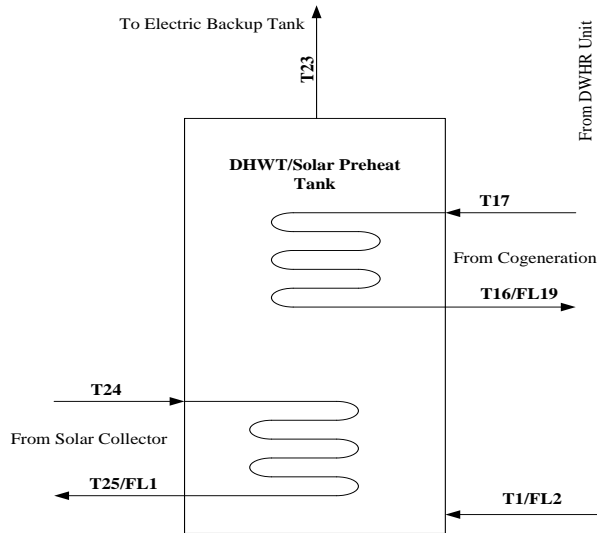


Figure 5-8: Schematic view of solar preheat tank with related sensors of House-B

Thermal power supplied by the solar preheat tank is calculated by using Equation (5-7).

The water flow rate reading is in U.S. GPM and the temperature readings are in °C. By substituting the value of density from Equation (5-1) and the constant value for the specific heat of water, the value for the supplied thermal power by the tank would be:

5.6.4.2. Electric Backup Tank

Figure 5-9 displays the schematic view of the electric backup tank with the inputs / outputs and the locations of all installed sensors.

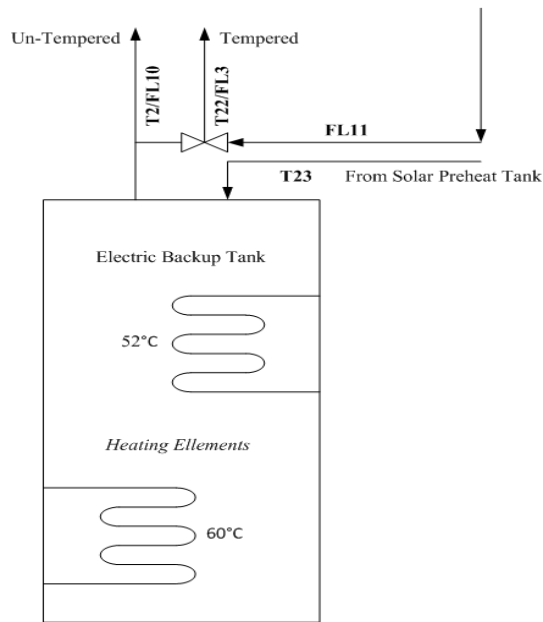


Figure 5-9: Schematic view of electric backup tank of House-B with related sensors

Thermal power supplied by the electric tank is calculated by using Equation (5-7).

The water flow rate reading is in U.S. GPM and the temperature readings are in °C. By substituting the value of density from Equation (5-1) and the constant value for the specific heat of water, the value for the supplied thermal power by the tank would be:

$$\text{Thermal Power} = \rho \cdot C_p \cdot \dot{V} \cdot (T_{\text{Tempered}} - T_{\text{Un-Tempered}})$$

Efficiency of the tank is calculated using Equation (5-18):

$$\text{Efficiency} = \frac{\text{Thermal Power}}{\text{Electrical Power}}$$

5.6.4.3. Evacuated Tube Solar Thermal Collector

Figure 5-10 displays the schematic view of the evacuated tube solar collector with the inputs / outputs and the locations of all installed sensors.

Thermal power and efficiency calculation equations are the same as for the flat plate solar collector. The propylene glycol solution flow rate reading is in U.S. GPM and the temperature readings are in °C. The values for the thermal power and collector efficiency can be obtained from Equations (5-19) and (5-20).

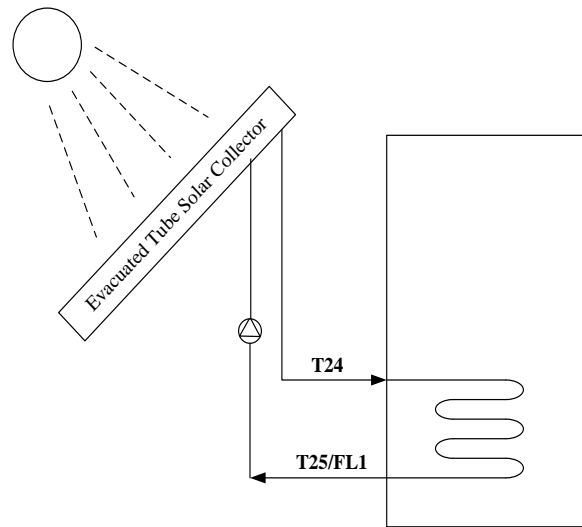


Figure 5-10: Schematic view of evacuated tube solar collector with related sensors in House-B

A is the aperture area of the collector (2.11 m^2) and I_t is the solar radiation on the tilted surface (25°) of the collector. The evacuated tube solar thermal collector is south facing and with the same tilt angle of 25° .

5.6.4.4. Drain Water Heat Recovery (DWHR)

Figure 5-11 displays the schematic view of the DWHR system with the inputs / outputs and the locations of all installed sensors. Again, the flow rates are not measured at the cold and hot side inlets of the unit. For the location of these sensors, refer to Figure 4-3.

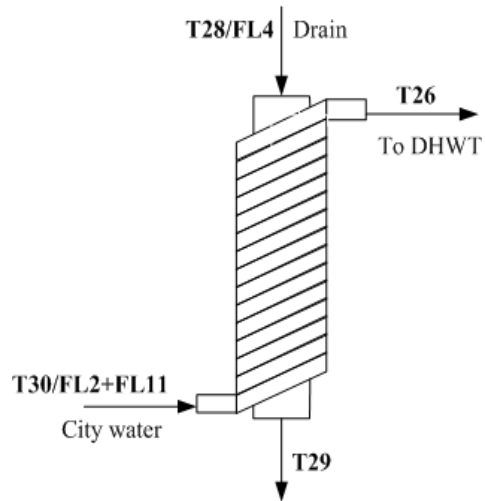


Figure 5-11: Schematic view of House-B DWHR system with related sensors

Again, the water flow rate readings are in GPM and the temperature readings are in °C. The total amount of heat recovered by the system can be calculated using Equation (5-21):

$$\text{-----} \quad \text{-----} \quad \text{-----}$$

The actual effectiveness of the system can be obtained using the same equation, Equation (5-15), as provided for the other system, installed in House-A.

Chapter 6 : Data analysis

No permanent occupant lives in the twin houses due to the nature of the project. However, the houses are open to the public for visit, and staff can work inside during the day. Therefore, both houses have occupants during weekdays. The real time data being collected is similar to that in the typical family environment except for household activities such as cooking, bathing and laundry. As mentioned earlier, the hot water dumping schedule for a typical Canadian household of four has been implemented in the houses to simulate the daily hot water consumptions.

6.1. Drain Water Heat Recovery System

DWHR systems are used to recuperate part of the energy contained in drain water and are efficient in reducing the amount of energy needed for DHW heating. Other than energy savings, there are several other benefits which a DWHR system can provide to a homeowner or to a utility which is supplying for the DHW heater. These benefits are reduction of the peak hot water demand and the possibility of selecting a smaller electric water tank. Other than these benefits, if the hot water heater uses a primary energy source which produces greenhouse gases, the addition of a DWHR system will reduce these emissions in direct proportion to the reduction in the water heater's gross energy consumption.

The DWHR systems used in the twin Archetype houses are composed of a main tube over which a series of smaller pipes are enrolled to form a closely wrapped spiral coil as seen in Figure 6-1. Both main tube and spiral coil are made out of copper to enhance heat transfer between the two fluid streams. Drain water flows inside the main tube and the surface tension and gravity causes the falling films to spread and adhere to the inner wall of the tube, while incoming cold water from the cold inlet mains circulates inside the coil. Thus, there are two walls separating potable water from wastewater in accordance with most building codes. The flow through the curved pipe is known as Dean Flow. In the spiral form pipes, centrifugal forces generate a secondary flow that consists of two counter rotating cells, generally known as Dean roll-cells (Kalb & Seader, 1974). The presence of this secondary flow permits more homogeneous temperature distributions within the fluid, thus inducing higher average heat transfer coefficients.

The nature of this system implies that there must be simultaneous water flow in the drain pipe and in the coil in order to maximize the heat recovery from the drain water. Therefore, the

DWHR will work less efficiently when used in conjunction with the use of baths, dishwasher or washing machines.



Figure 6-1: General View of a Drain Water Heat Recovery System (Zaloum et al., 2007)

6.1.1. Performance of DWHR Systems

DWHR systems can be classified as counter flow heat exchangers. In order to calculate the performance and the amount of heat transfer for any heat exchanger, there are two methods: the Logarithmic Mean Temperature Difference (LMTD) and Number of Heat Transfer Units (NTU)-effectiveness. Both methods will be described briefly here.

6.1.1.1. Logarithmic Mean Temperature Difference

The logarithmic mean temperature difference is a measure of temperature difference along heat exchangers. The disadvantage of this method is that all outlet temperatures need to be known.

LMTD for counter flow heat exchanger is as follows:

$$\frac{(T_{h1} - T_{c2}) - (T_{h2} - T_{c1})}{\ln \left(\frac{T_{h1} - T_{c2}}{T_{h2} - T_{c1}} \right)}$$

The heat transfer rate will be:

where “UA” is the overall heat transfer coefficient and F is the correction factor. F is 1 or close to 1 for counter flow heat exchangers with one shell and a single tube pass.

6.1.1.2. NTU-Effectiveness

The second method for calculating the rate of heat transfer and overall heat transfer coefficient of these heat exchangers is the NTU-effectiveness method. The NTU is a measure of the heat transfer size of heat exchangers; that is, the larger the NTU, the closer it approaches its thermodynamic limit. This method is useful when outlet temperatures are not known.

where C_{min} is the minimum heat capacity rate; that is the lesser of C_h or C_c . C_h is the water mass flow rate (kg/sec) and c_p is the water heat capacity (kJ/kg.°C). The capacity heat ratio is determined as follows:

where C_{max} is the greater of C_h or C_c .

The DWHR system can be characterized as a counter-flow heat exchanger. Knowing the hot side inlet water temperature $T_{h,i}$, cold side outlet water temperature $T_{c,o}$ and cold side inlet water temperature $T_{c,i}$, the actual effectiveness (ϵ) and the actual heat transfer rate (q) can be determined from the expressions below:

Using the actual effectiveness and the specific heat ratio, NTU can be determined.

(for unbalanced flows).

(for balanced flows).

The overall heat transfer coefficient can then be obtained:

—

The method used to obtain the heat transfer for this project is the NTU-effectiveness method.

6.1.2. DWHR Systems in the Twin Archetype Houses

The DWHR units at the TRCA twin houses are identical. The units are 3 inches in diameter and 36 inches (91.44 cm) in length. Both units have 3/8" (0.95 cm) (Type-L) wrap tubes with four parallel wraps. The units are manufactured by Renewability Inc. and the model is PowerPipe™ R3-36. The general specifications of the units are as listed in Table 6-1, and Figure 6-2 shows the DWHR unit in House-B. Both units are located on the first floor of both houses and can capture heat from the drain water of the shower(s) and bathroom sink(s) on the second and third floors. The two units can preheat the cold water to the solar storage tanks.

Table 6-1: General specifications of Power-pipe R3-36 DWHR

	Item Specifications	Assembled Specifications
Depth (in)	7	7
Height (in)	40	36
Width (in)	4	4
Weight (lbs)	23	16.2



Figure 6-2: Overview of PowerPipe R3-36 unit in House-B and the wrapped tubes view

The piping configurations in the houses have been designed in a way that routes all cold water going to solar hot water tanks through the DWHR units; in other words, the DWHR units can preheat the cold water intended to go to hot water taps. If both cold and hot taps are opened together, the DWHR's cold side flow rate would be lower than that of the hot side.

Two sets of Pt.100 temperature sensors, which are of the RTD probe type, have been installed on the cold-side inlet and outlet of the units, and two surface-mount Pt.100 temperature sensors (surface mount type) have also been installed on the inlet and outlet of the main drain pipes. The flow rate sensors on the main water line to the houses are used to read the drain water flow rate. The DHW loop flow rate sensors in the two houses are all GEMS turbine flow rate sensors. According to the specific type of the sensors being used, these sensors are capable of reading a wide range of flow rates from as low as 0.5 l/min to 30 l/min. The selection of a specific type of sensor depends on the flow rate range on each desired pipe line. The real-time collected data from all relevant sensors will be used to determine the performance and effectiveness of the unit. The amount of flow rate to the hot water solenoid valves in both houses is equal to the sum of the readings from the flow rate sensors which are located on the DWHR unit's cold side (preheated) outlet branches to the tempering valve and to the solar tank(s).

6.1.3. Daily Water Draw Profiles

Daily hot water draw for the two houses is in the range of 220 l/day to 250 l/day. The end use water temperature is in the range of 40°C to 45°C. The daily hot water draw profile used in this study is the 5-second-water-draw profile based on the IEA Annex 42 schedule by the International Energy Agency (Knight et al., 2007). The hourly hot water draw profile is shown in Figure 6-3.

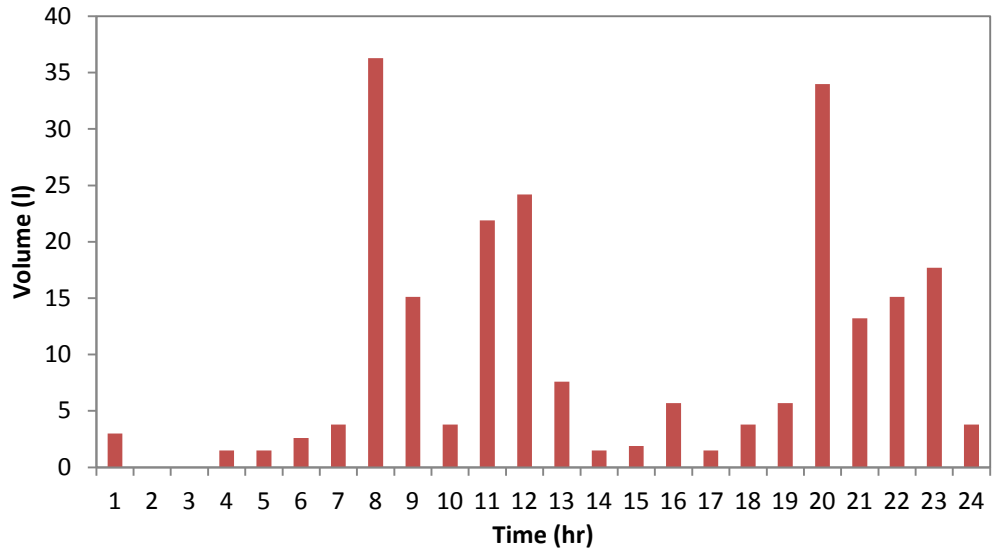


Figure 6-3: Average daily hot water draw profile

Figure 6-4 displays the minutely hot water usage pattern with 225 litres of water consumption.

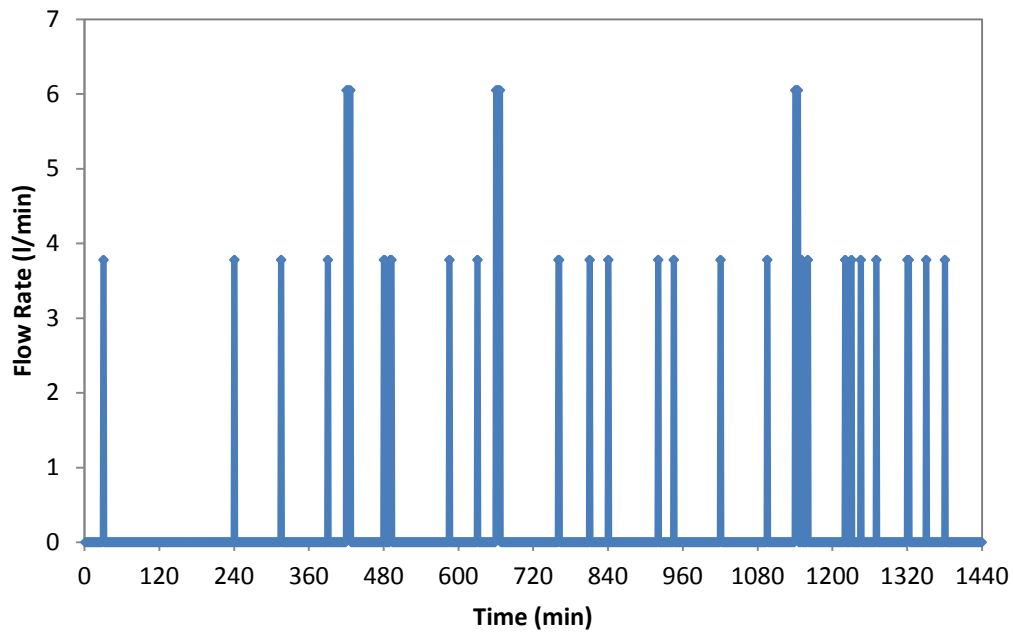


Figure 6-4: High Resolution Daily Hot Water Draw Pattern

About 40% of the daily hot water usage is from showers (Jordan & Vajen, 2001). The daily hot water consumption for simultaneous water draw sources is assumed to be about 180 liters (Hendron & Burch, 2007). As stated before, the archetype houses' water mains are drawn from the local wells and the monthly average water main temperatures have been measured at the site. The monthly average water main temperatures are as shown in Figure 6-5.

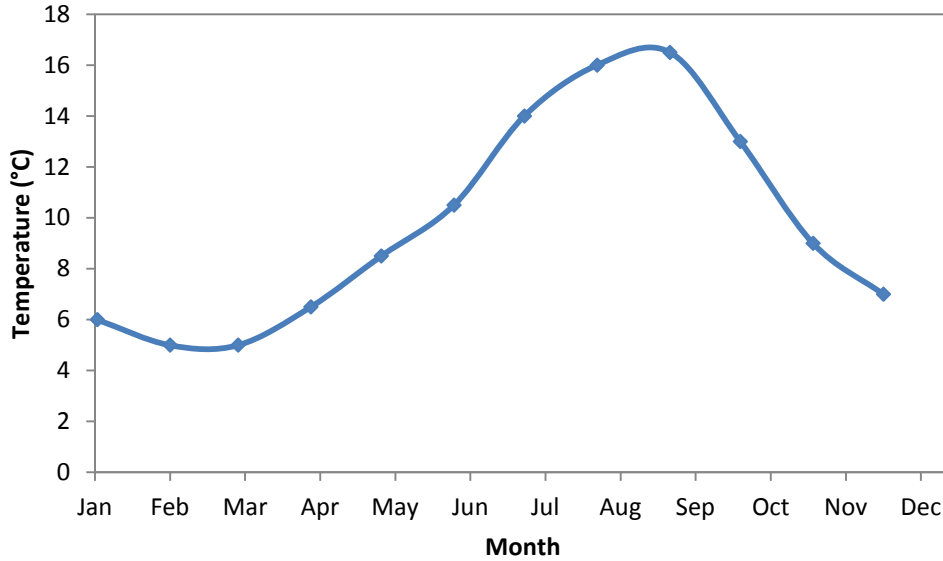


Figure 6-5: Average measured water mains temperatures to the Archetype Houses

6.1.4. Operational Performance of DWHR Systems

After determining the daily domestic hot water draw profile for the houses, the monthly DHW energy consumption is also needed to be sought out; this is achieved by Equation (5-11):

$$q = \dot{m} c_p \Delta T$$

where:

- q Energy required for the DHW heating (kJ/month)
- \dot{m} Mass flow rate of water (kg/day)
- c_p Specific heat of water (kJ/kg·C)
- ΔT Difference in temperature of hot water tank set-point and monthly temperature of entering cold water

Adding the DWHR systems to the piping systems of the houses would result in lesser energy consumed by the water heaters to heat the water to the desired set-point temperature. The two DWHR systems are setup in a way that they preheat the water going to the hot water taps. With this setup, the minimum heat capacity rate is always equal to the cold side heat capacity rate. As a result, the effectiveness of the DWHR units can be determined using the Equation (6-12). All temperatures are measured at the cold and hot side inlets / outlets of the DWHRs:

It should be noted that _____ and 3°C is the temperature drop from the solenoid valves outlet to the inlet of the two DWHR systems.

The overall efficiency of the units can be determined through Equation (6-13):

Next, the operational curves of the unit will be presented, which will give more insight into the behaviour of the system under different operational conditions. Furthermore, the effects of various parameters like the drain water temperature, drain water flow rate and cold side inlet water temperature on the performance of the DWHR system will be investigated. It should be stated that the inlet water has pressure fluctuations which are due to the fact that the water supply to the house is delivered from the local wells located at the Kortright Centre, and pressure may constantly vary when there are other water usages throughout the centre.

Table 6-2 shows the averaged flow rates and temperatures for a typical shower with 390 seconds duration during the winter testing period.

Table 6-2: Averaged flow rates and temperatures during a shower event in February (DWHR is cooled down)

Cold side inlet temperature (°C)	Cold side outlet temperature (°C)	Hot side inlet temperature (°C)	Hot side outlet temperature (°C)	Drain water flow rate (lit/min)	Tempered line from DHW tank temperature (°C)	Tempered line flow rate (lit/min)
15.2	27.0	38.5	24.9	6.85	46.8	5.60

Hot and cold side temperatures variations for this shower are displayed in Figure 6-6. For this event, the DWHR unit is in a cooled down state. The cold side inlet temperature continuously decreases from the stagnated water within the pipes temperature, which is the room temperature, to 5.5°C of running water. Although the drain water temperature increases until it reaches its steady point, the cold side outlet temperature shows an initial increase and then continuous dropping. This is due to cold side inlet temperature's continuous decrease. The cold side water temperature difference is always increasing until the cold side inlet temperature is settled (5.5°C for February). Figure 6-6 also shows that the DWHR unit is capable of boosting the inlet water temperature by 16 °C.

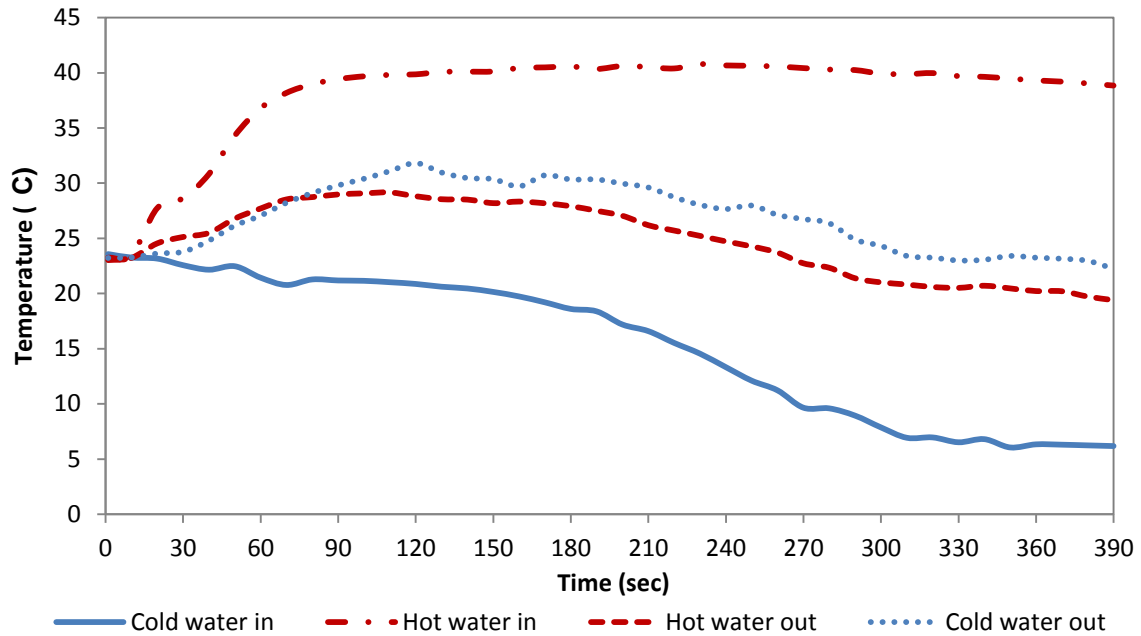


Figure 6-6: DWHR cold side and hot side temperatures variations for a typical shower in February

Figure 6-7 shows the DWHR unit's instantaneous effectiveness and drain water inlet temperature curves. The average effectiveness for this shower event is approximately 47%.

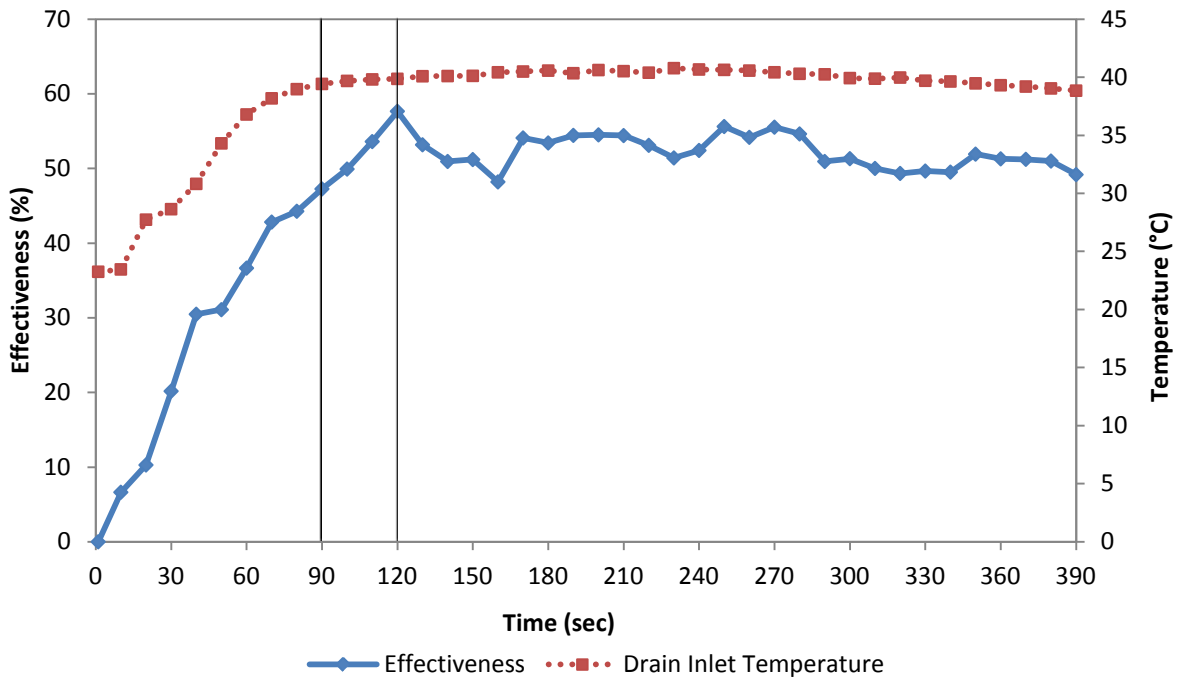


Figure 6-7: DWHR's instantaneous effectiveness and inlet drain water temperature changes for a shower in February

Figure 6-8 displays the heat recovery rate trend line for this shower event. The average heat recovery rate is approximately 4.55 kW. The data points show constant increase in the heat

recovery rate until it gradually reaches its steady state. The steady heat recovery rate varies between 6 kW and 7 kW. The total amount of energy recovered by the unit for this shower is about 0.49 kWh.

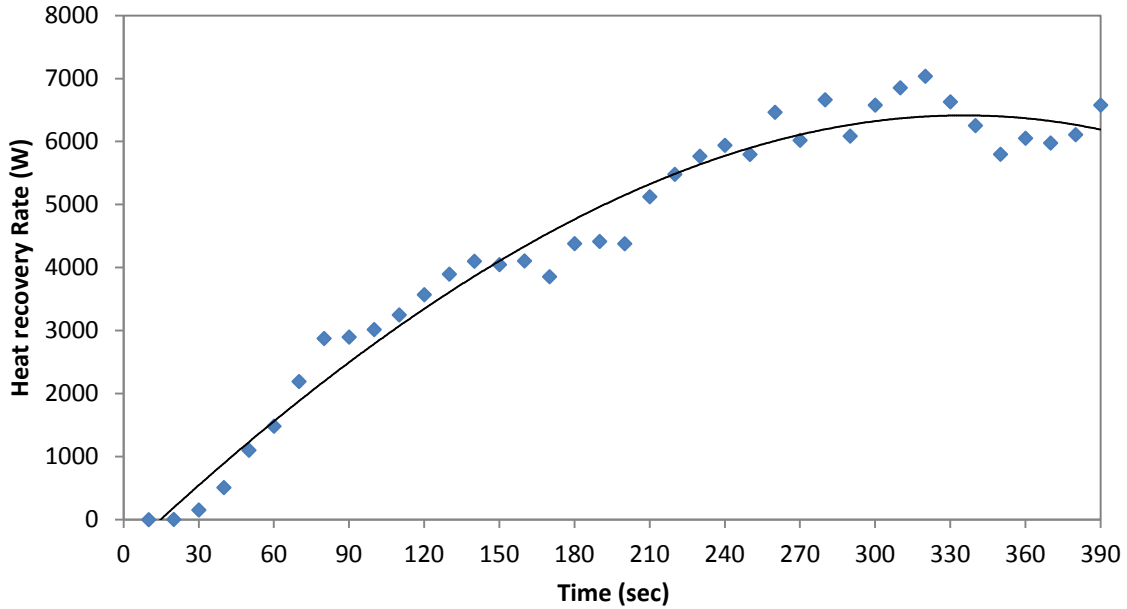


Figure 6-8: DWHR heat recovery rate curve for a typical shower in February

DWHR systems can be more beneficial if a simultaneous hot water dumping event occurs after the system has reached its thermodynamics limits. In such a case, the unit is already heated and the heat recovery rate would quickly reach its steady value. Table 6-3 shows the averaged flow rates and temperatures for a sink usage with 150 seconds. The DWHR is not completely cooled down for this case.

Table 6-3: Averaged flow rates and temperatures during a sink usage (DWHR is not cooled down)

Cold side inlet temperature (°C)	Cold side outlet temperature (°C)	Hot side inlet temperature (°C)	Hot side outlet temperature (°C)	Drain water flow rate (lit/min)	Tempered line from DHW tank temperature (°C)	Tempered line flow rate (lit/min)
13.0	24.9	37.4	20.8	4.54	47.6	3.80

Figure 6-9 shows the DWHR unit’s instantaneous effectiveness and drain water inlet temperature curves. The water draw has started while the unit is not completely cooled down and, therefore, the instantaneous effectiveness for this event settles quicker, compared to the case when the unit is completely cooled down. This clearly shows that the DWHR unit is more advantageous when a simultaneous water draw occurs while the unit is warmed up. The effectiveness for this case is

approximately 55%, due to lower drain flow rate. The DWHR unit is capable of boosting the inlet water temperature by almost 16°C.

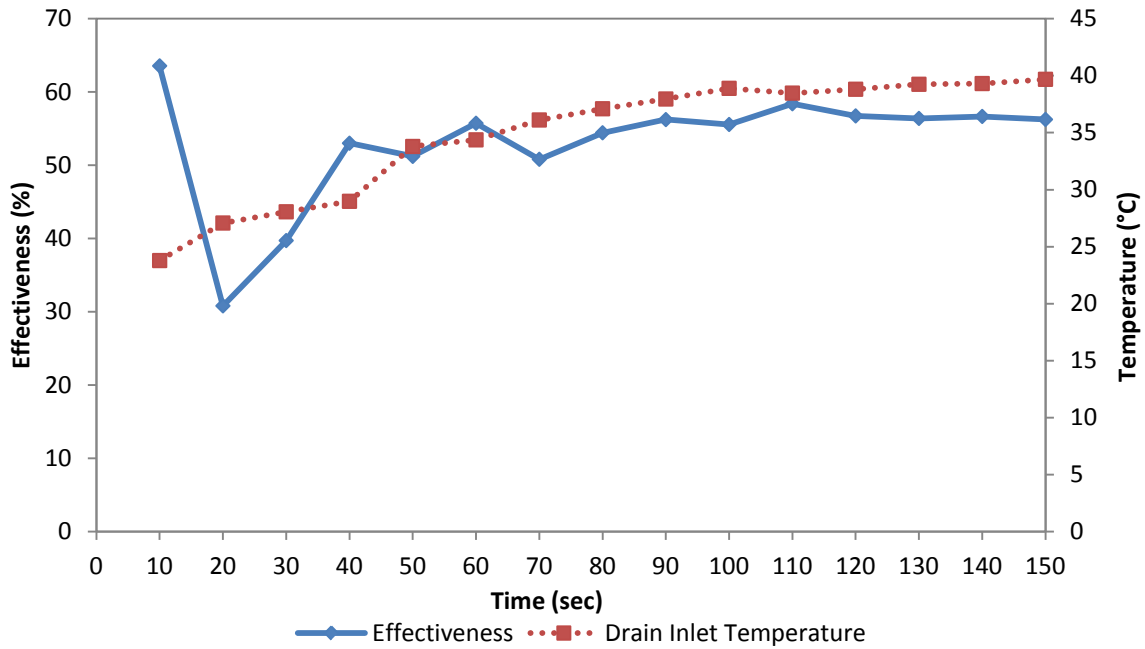


Figure 6-9: DWHR’s effectiveness and inlet drain water temperature changes for a sink usage with the completely warmed up unit in February

Figure 6-10 displays the heat recovery rate trend line for this sink event. The average heat recovery rate is around 3.1 kW. Even for a short water dumping period, the amount of recovered energy is approximately 0.13 kWh. By comparing the data points from

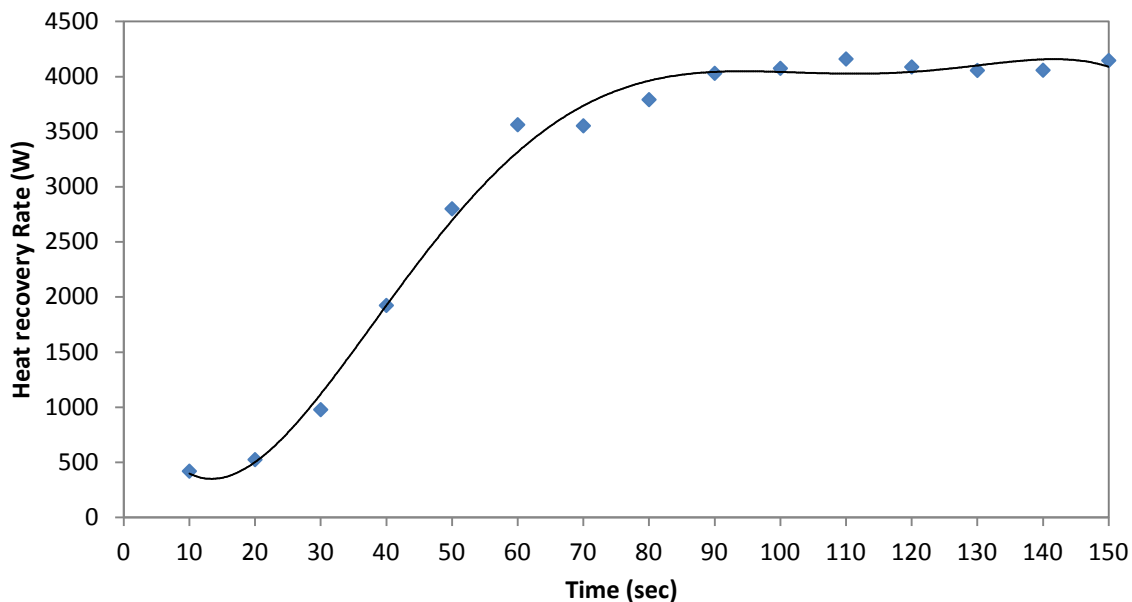


Figure 6-10: DWHR heat recovery rate curve for a sink usage with the completely warmed up unit in February

Figure 6-8 and Figure 6-10, it can be concluded that for the shower case, the settled heat recovery rate is about 6.5 kW while for the sink usage with lower drain flow rate (4.54 lit/min compared to the 6.85 lit/min for the shower case), the heat recovery rate is approximately 4 kW. Next, another shower event in the summer testing period is presented to compare the impact of the fresh inlet water temperature on the performance of the DWHR systems. Table 6-4 shows the averaged flow rates and temperatures for a typical shower with 400 seconds duration during the summer testing period in the month of August.

Table 6-4: Averaged flow rates and temperatures during a shower event in August (DWHR is cooled down)

Cold side inlet temperature (°C)	Cold side outlet temperature (°C)	Hot side inlet temperature (°C)	Hot side outlet temperature (°C)	Drain water flow rate (lit/min)	Tempered line temperature (°C)	Tempered line flow rate (lit/min)
19.8	29.5	39.5	28.4	6.85	47.5	5.70

The drain water temperature and flow rate are very close to the shower event for the winter testing period and as a result, the impact of the inlet water temperature is comparable. Figure 6-11 displays the hot side and cold side temperature variations for this shower. For this water draw event, the DWHR unit is also in a cooled down state. The first noticeable fact from Figure 6-11 is that the DWHR unit is capable of boosting the inlet water temperature by almost 13°C compared to the 16°C increase of the inlet water temperature for the winter testing period.

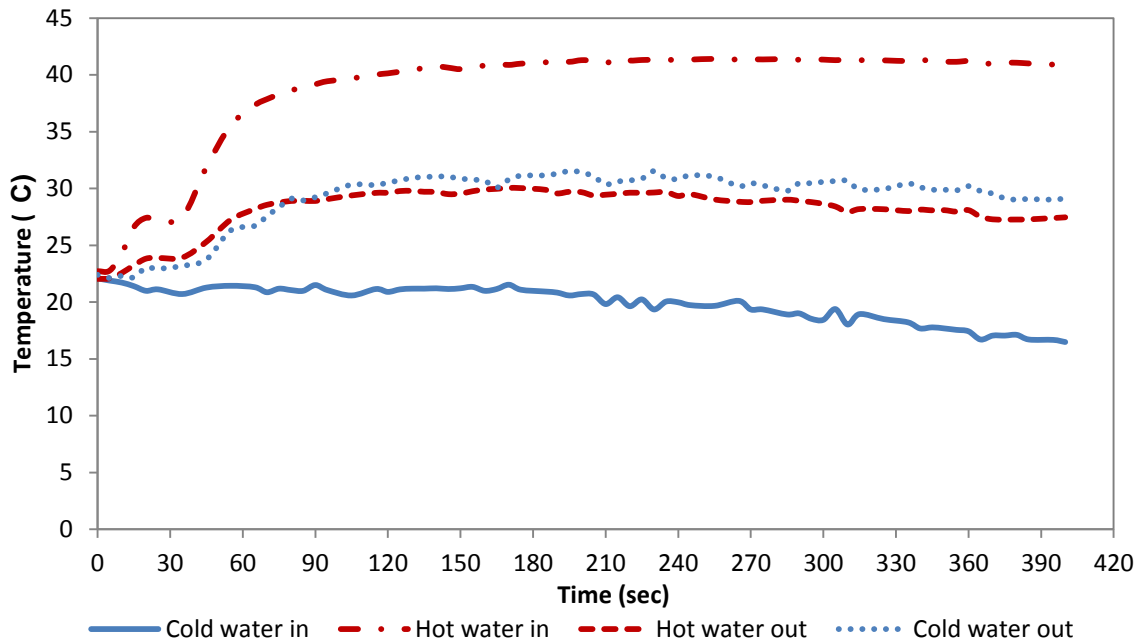


Figure 6-11: DWHR cold side and hot side temperatures variations for a typical shower in August

Figure 6-12 displays the heat recovery rate trend line for this shower event. The average heat recovery rate is approximately 3.75 kW. The heat recovery rate shows the same trend as the winter period testing case. The steady heat recovery rate varies between 4.5 kW and 5 kW, compared to 6.5 kW for the winter shower event. The total amount of energy recovered by the unit for this shower is approximately 0.43 kWh.

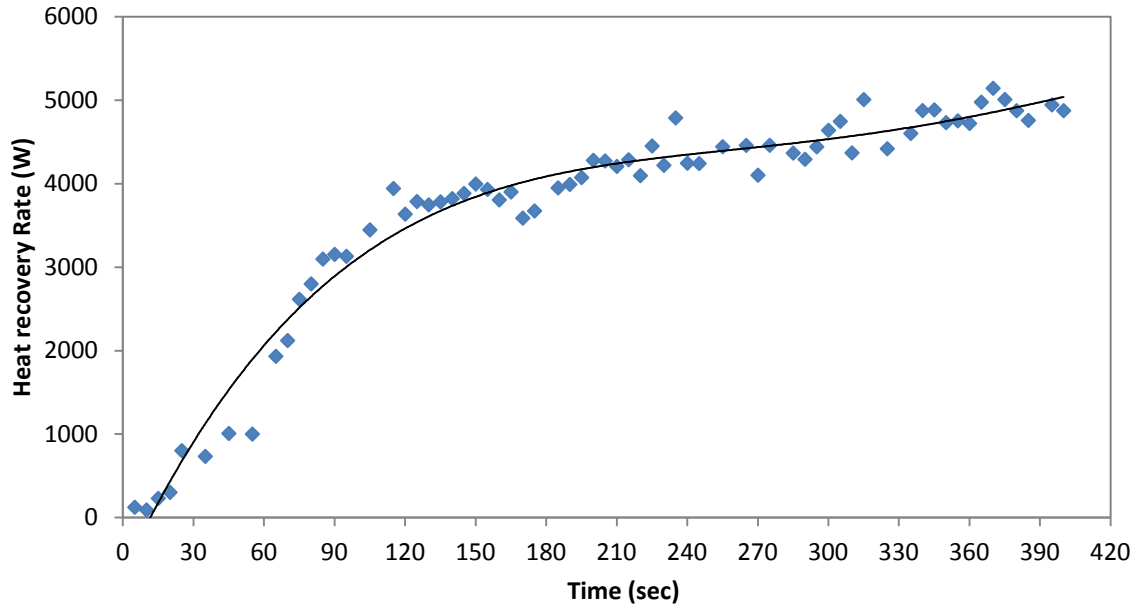


Figure 6-12: DWHR heat recovery rate curve for a typical shower in August

By comparing the two shower events with almost the same drain flow rate and temperature and time duration, it is concluded that the DWHR units have a higher heat transfer rate and are capable of recovering more heat, when used in colder months with lower inlet water temperatures. The inlet water temperature value however, does not have a significant influence on the DWHR units' effectiveness, as displayed in Figure 6-13.

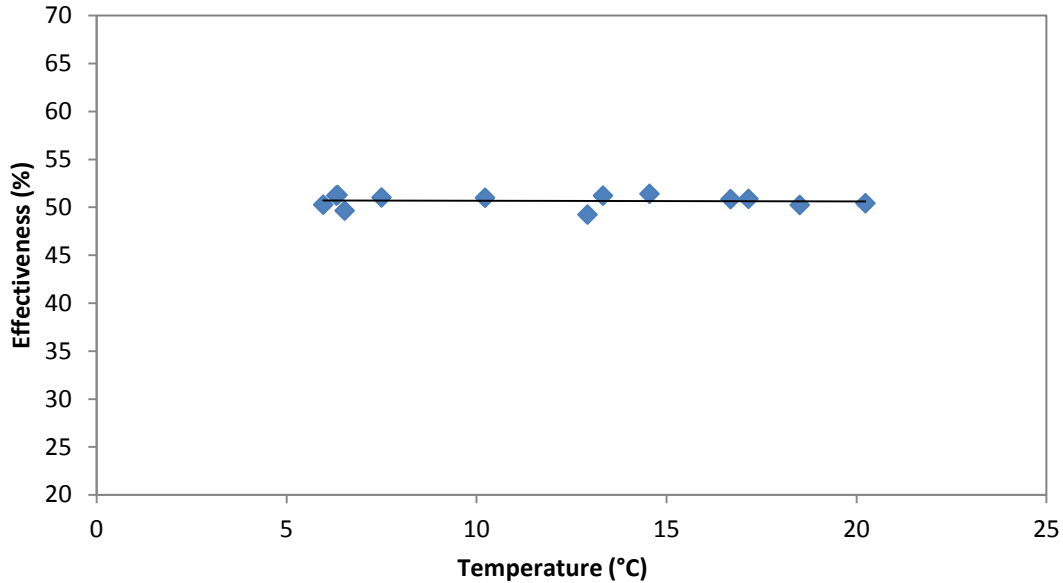


Figure 6-13: Effectiveness as a function of inlet water temperature for similar drain water flow rates

The performance of DWHR units can be measured in terms of NTU and effectiveness. As stated earlier, NTU is a measure of the heat transfer size of a heat exchanger. On the other hand, the effectiveness is the ratio of the actual rate of heat transfer to the maximum possible rate of heat transfer. The performance of DWHR units have been measured from the NTU and effectiveness versus drain water flow rate curves for different flow rates from different events and after the DWHR units are warmed up (about 90 to 100 seconds from the drain water dumping initiation) and have reached their steady state. Figure 6-14 displays effectiveness versus different flow rates for two different coil-over-drain water flow rate ratios of 0.8 and 1. The obtained trend is valid for flow rates of up to 8 lit/min. As seen, the increase in the coil-over-drain flow rate ratio leads to lower effectiveness of the DWHR units. This is in accordance with previous studies conducted by other researchers (Bernier et al., 2004). The effectiveness differences for the two flow-rate-ratio cases stated earlier, are approximately 5%.

Figure 6-15 shows the effectiveness versus drain flow rate of the TRCA DWHR unit for coil-over-drain water flow rate of 0.8 and 1.0, with the obtained curve from the same DWHR unit by another study (Zaloum et al., 2007). Comparing the two sets of data reveals higher effectiveness for the TRCA unit. This difference is approximately 5% to 6% for flow rates higher than 6 lit/min. Comparing the three sets of data from Figure 6-14 and Figure 6-15 justifies the TRCA DWHR units' higher effectiveness compared to the above mentioned study.

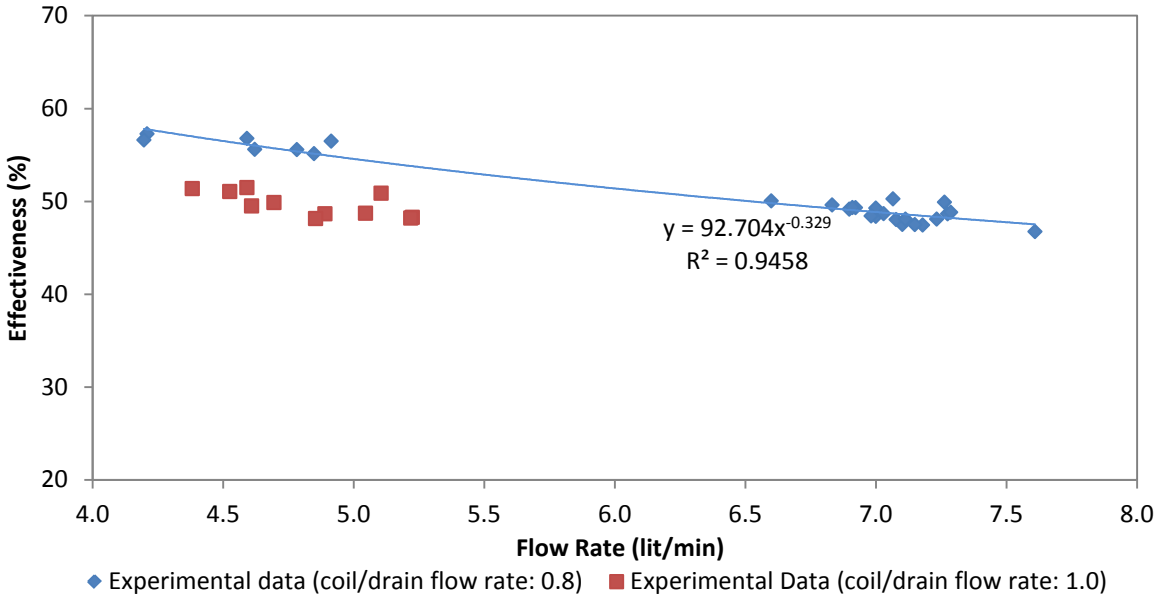


Figure 6-14: Effectiveness as a function of drain flow rate for different coil/drain flow rate ratio

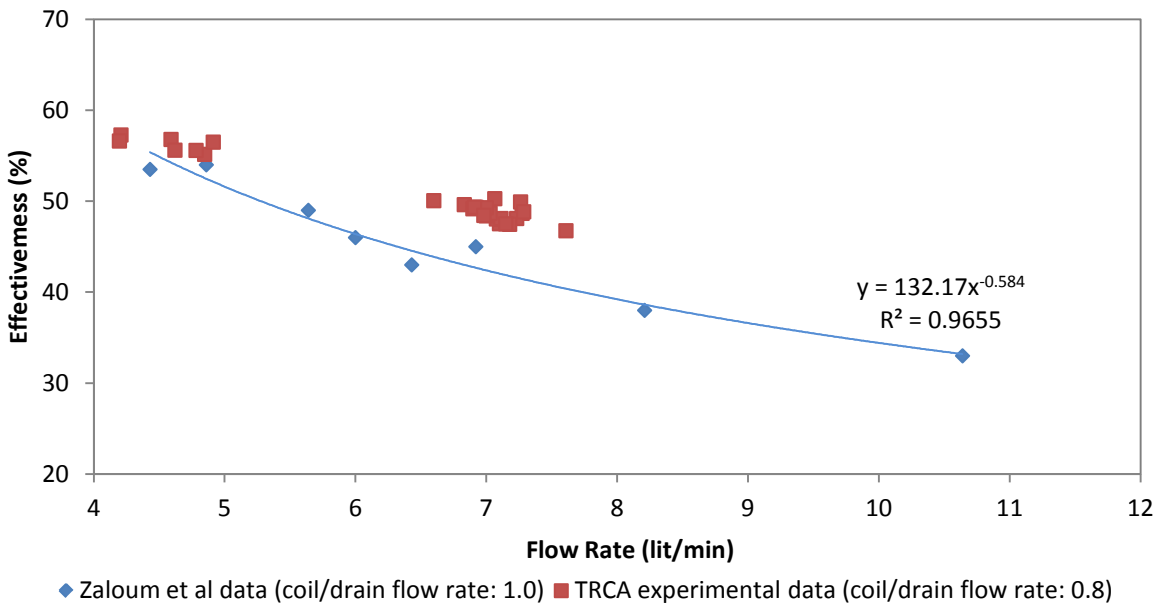


Figure 6-15: Effectiveness as a function of drain flow rate from TRCA experimental results and the study by Zaloum et al. (2007)

Figure 6-16 displays the NTU versus different flow rates data points for two different coil-over-drain water flow rate ratios of 0.8 and 1. Again, it can be seen that the NTU is higher when the coil-over-drain flow rate ratio is smaller. Comparing Figure 6-14 and Figure 6-16 clearly shows that the NTU curve correlates better than the effectiveness curve. This is in accordance with the study performed on the performance of different types of DWHR units (Zaloum et al., 2007). It

should be stated here that the NTU versus flow rate curves for these system can be used for modelling the units for energy and cost savings calculations.

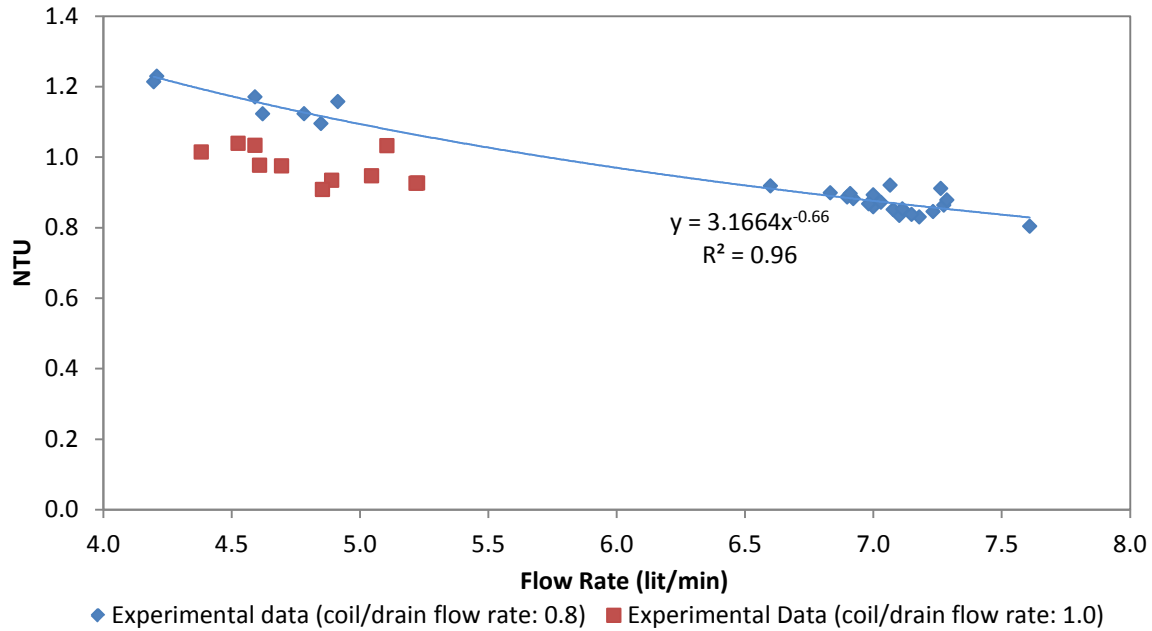


Figure 6-16: NTU vs. drain flow rate for different coil/drain flow rate ratio

Finally, the effect of drain water temperature on the effectiveness of the DWHR units is also investigated. Figure 6-17 displays the DWHR unit effectiveness as a function of drain water temperature for the cases when the units are warmed up; drain flow rates are within the same range (4.2 to 5.2 lit/min), and the coil-over-drain flow rate ratio is 0.8.

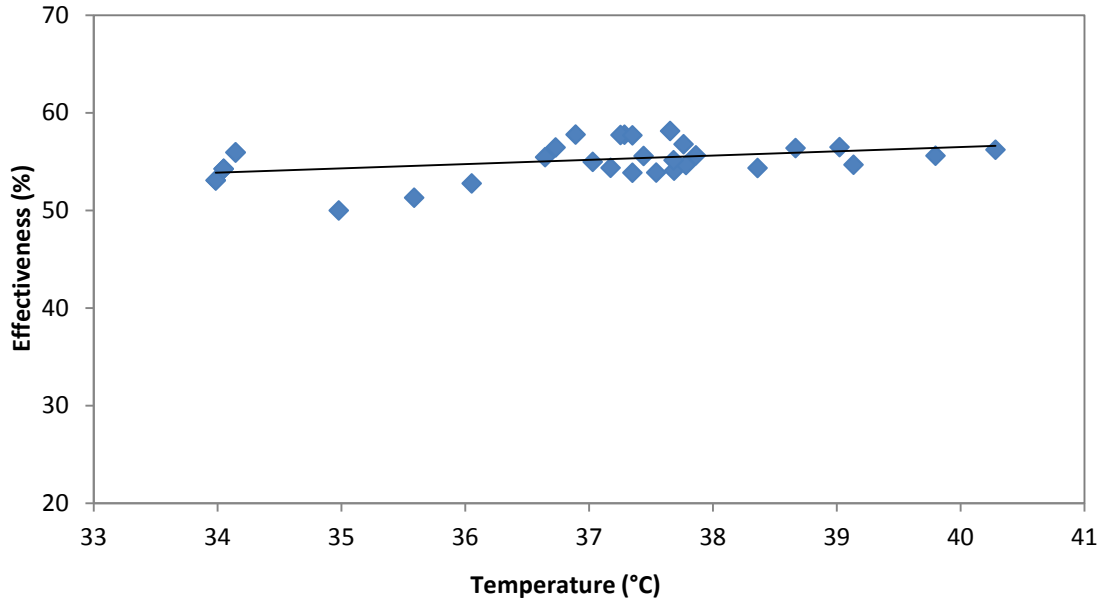


Figure 6-17: Effectiveness as a function of drain water temperature for different drain flow rates with coil/drain ratio of 0.8

Although the effectiveness increases a bit with the increase of drain temperature, this temperature does not have a significant effect on the effectiveness of the DWHR units. From what has been seen from the performance data of the DWHR systems, the main factors that have impact on the effectiveness of the systems, are the drain water flow rate and coil / drain tube flow rate ratio.

Another important factor in determining the performance of DWHR units is to determine the time required for the unit to completely cool down. Using the actual (transient) effectiveness of the DWHR system, instead of the steady state effectiveness, will better represent the transient behaviour of the DWHR system in energy simulating models. A damping factor, f , can be used to multiply the value of the steady state effectiveness to obtain the actual effectiveness, ϵ (Bernier et al., 2004):

When the unit is in operating mode, the value of f can be achieved as followed:

$$\text{---}$$

is the time constant in operating mode. From the collected data during the operating periods of the DWHR unit at the TRCA twin Archetype Houses, it was concluded that the units require a settling time of 90 to 100 seconds before a steady output is obtained. Based on this settling time and the 50% average steady state effectiveness for showers, the average value for is set to 40

seconds. Figure 6-18 displays the comparison of the transient effectiveness prediction of the DWHR using Equation (6-14), with the effectiveness values from experimental data for a shower event, when the DWHR is in a fully cooled down state.

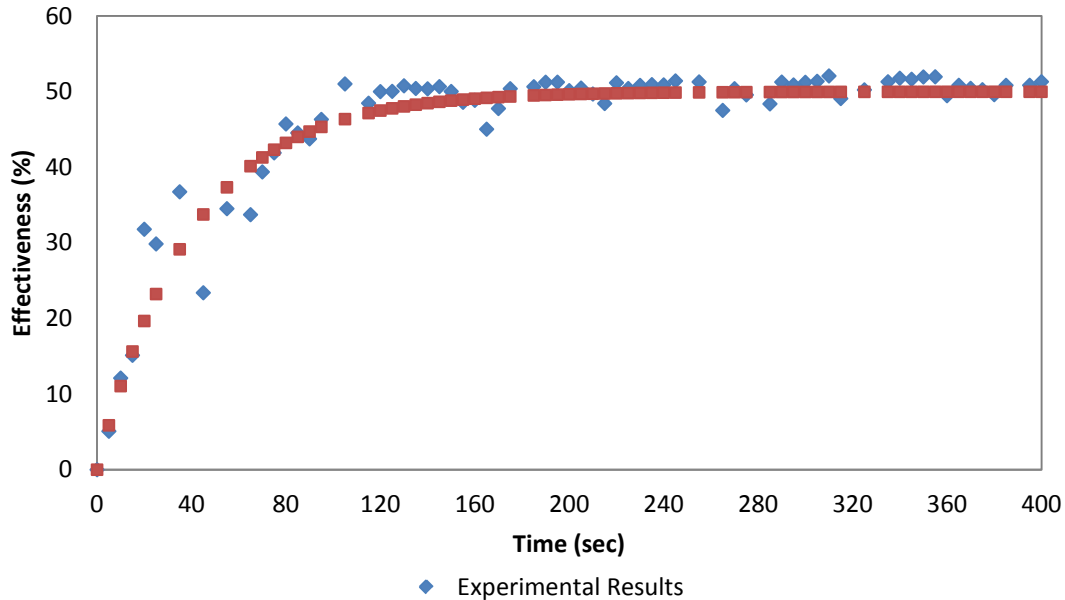


Figure 6-18: Comparison of the predicted effectiveness of the DWHR with the experimental results

As seen in Figure 6-18, the theoretical approach prediction is quite close to the experimental values, especially when the unit is in its steady state.

When the unit is in standby mode, the value of f can be achieved as follows:

—

is the time constant in standby mode. From the collected data the total cool down time for the units was determined to be approximately 1.5 hours. Based on this time and several other cooling time slots (from 10 minutes to 90 minutes) after different water dumping events, the was determined to be 3000 seconds.

6.1.5. Extrapolated Data

As stated earlier, the DWHR systems work best when fresh water demand and drain water flow are simultaneous. The simultaneous, daily hot water draw has been assumed to be about 180 liters. Thus, the DWHR systems can recuperate the heat from 180 litres of drain water. The average amounts of daily heat recoveries have been measured for winter (March) and summer (August) testing periods. Incorporating the fresh water supply temperatures from Figure 6-5, and,

assuming that the end use hot water temperature is between 42°C and 44°C, the heat recovery amounts for each month are sought out. Table 6-5 displays the monthly energy recovery by the DWHR systems, obtained from the experimental data.

Table 6-5: Monthly heat recovery by DWHR systems

Month	Q (kWh) / day	# of days	Q (kWh)
January	2.41	31	74.64
February	2.44	28	68.32
March	2.47	31	76.64
April	2.38	30	71.26
May	2.25	31	69.62
June	2.12	30	63.49
July	1.89	31	58.58
August	1.76	31	54.56
September	1.73	30	51.83
October	1.95	31	60.58
November	2.21	30	66.40
December	2.34	31	72.63
		Total	788.54

If the water heating source is electricity and assuming that the DHW tank is operating with 79% efficiency, the addition of a similar DWHR system with similar water draw conditions would result in annual cost savings of \$107.2, based on the 2011 rate of electricity at \$0.136/kWh (London Economics LLD, 2011). With the electricity based, GHG emission factor of 0.16 kg/kWh equivalent CO₂ (Environment Canada, 2011), the annual GHG emissions reduction would be approximately 126.2 kg. With the DWHR unit’s purchase and installation cost of almost \$600, the payback period for using this unit would be 5.6 years.

If the water heating source is natural gas and the assuming that the gas boiler is operating with 56% efficiency, the addition of this DWHR system would result in annual heat recovery of 2.84 GJ. With the 2011 rate of natural gas at \$0.458/m³ (Statistics Canada, 2011) and knowing that 27 m³ of natural gas can produce about 1 GJ of Energy (NRCan, 2009), the annual DHW energy consumption cost savings would be \$35.1. With the natural gas based, GHG emission factor of 1.879 kg/m³ equivalent CO₂ (Environment Canada, 2011), the annual GHG emissions reduction

would be approximately 144.1 kg. Similarly, the payback period of this unit, when used with a system that has gas boiler as the auxiliary heating source would be approximately 17 years.

From monitoring the data for the winter and summer testing periods, the DWHR fresh side exit temperatures for shower events are obtained. The obtained exit temperatures are then extrapolated to achieve the monthly DWHR exit temperatures for the whole year. Using the measured incoming cold water and the DWHR exit temperatures, the monthly DHW energy demand for the pre-heated fresh water supply can be found, using Equation (6-17):

—

Figure 6-19 displays the monthly average inlet and outlet temperatures of the DWHR units for a typical shower event of 450 seconds in duration, with shower temperature of 42°C and the monthly fresh inlet water temperatures to the houses. As seen in this figure, DWHR inlet temperatures are slightly higher than the fresh water mains temperatures, which is due to the presence of stagnated water within the water mains. Figure 6-19 also clarifies that DWHR systems are more advantageous in raising the inlet water temperature during colder months, with lower water mains temperatures.

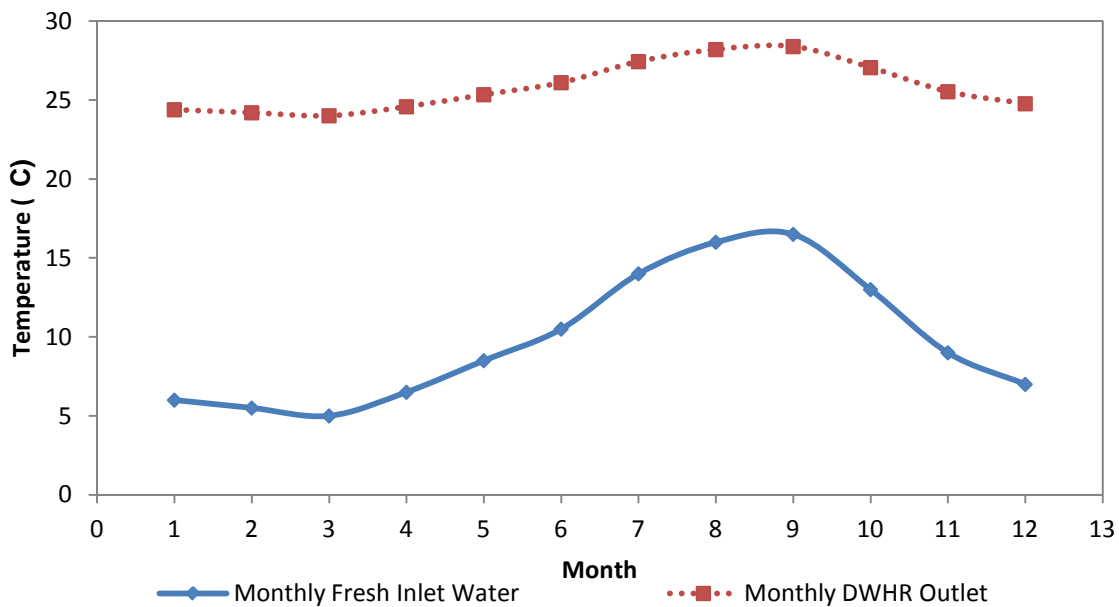


Figure 6-19: DWHR systems inlet and outlet temperatures profile

The overall efficiency of the DWHR units for the entire year can be determined through Equation (6-12). With the set point temperature of 56°C (average of 52°C and 60°C for the lower

and upper heating elements of the electric backup tank), the overall efficiency is calculated to be approximately 28.6% and 24% for the lowest and highest inlet water temperatures, respectively. The average overall efficiency for the entire year would be 26.8%. With the overall efficiency known, the DWHR units' outlet temperatures for different shower temperatures can be achieved through Equation (6-18).

The outlet temperatures can then be used to determine the amount of energy that can be recaptured by the DWHR units, using Equation (6-17).

6.2. Solar Thermal Collectors

The TRCA Archetype houses are each equipped with a solar thermal collector. The two solar collectors are of different types, manufactured by Viessmann Solar Thermal Collectors Manufacturing Ltd. The solar collector in House-A is a flat plate collector, and the one in House-B is an evacuated tube collector. Both collectors are south facing and are installed on the south side of the twin houses with an inclination angle of 25° with respect to the horizontal base. The specifications of the two solar collectors are as listed in Table 6-6.

Table 6-6: Viessmann solar collectors' specifications in TRCA Archetype Houses (Viessmann Ltd., 2010)

Collector	Type	Gross Area (m ²)	Absorber Area (m ²)	Aperture Area (m ²)	Dimensions			Weight (kg)
					Width (mm)	Height (mm)	Depth (mm)	
 Vitosol 100	SV1	2.51	2.32	2.33	1056	2380	90	52
 Vitosol 200	SD2	2.88	2.05	2.11	1418	2031	143	51

The solar loop liquid for the two systems is propylene glycol (PG) solution with 60% propylene glycol and 40% water. The solar preheat tanks for the two systems have the exact same specifications (Vitocell 100-B by Viessmann). The two domestic hot water (DHW) tanks are

indirect-fired dual coil DHW tanks which allow for the integration of a solar system with an auxiliary heating system. The capacity of the tanks is 300 liters, and the heat absorbed by the solar collectors is transferred to the DHW via the lower heat exchanger coils. The indirect coil in the upper area of the House-A DHW tank is heated by a gas boiler, and the one in the House-B preheat tank is heated by GSHP desuperheater or the cogeneration system upon DHW demand. The DHW tanks are protected against corrosion by Ceraprotect enamel coating and an additional cathode which can be either magnesium or impressed current anode.

It is found in ASHRAE (1999) that the performance of any solar thermal system depends on,

- the heating load,
- the amount of solar radiation, and
- the solar thermal system characteristics.

The European Commission Directorate General for Energy and Transport (2004) broadly mentioned that the most important factors affecting the performance of a solar domestic hot water system are:

- the collector area and efficiency
- the volume of storage tank
- the system design of heat exchanger and controller
- the solar radiation and air temperature
- the load, i.e., cold water temperature, volume, demand temperature.

ASHRAE (1999) has also mentioned that the collector operation is regulated by a controller with the following glycol cycle: 1) overheating protection and 2) auxiliary heating when it is required. A similar differential controller is used in the two systems, which regulates the above operations. The solar hot water systems are controlled in a way that the glycol loop pump starts when the temperature difference between the solar collector header output and the solar preheat tank water temperature exceeds 6.7°C .

The instantaneous efficiency of this solar thermal collector can be calculated through Equations (5-12), (5-20) and (6-19).

According to the European Commission Directorate General for Energy and Transport (2004) recommendations, the efficiency curve for a solar collector should be presented as the second order polynomial Equation (6-19) of the reduced temperature difference, T^* ($T^* = (T_m - T_a)/I$).

(6-19)

In Equation (6-18), η_0 is the optical efficiency, U_L is thermal loss coefficient in $W/(m^2.K)$, U_r is thermal loss coefficient in $W/(m^2.K^2)$, and I is the solar irradiance, at the tilt angle of 25° . T_m is the mean temperature of the propylene glycol solution in the solar loop in $^\circ C$ and T_a is the ambient temperature in $^\circ C$.

Unlike the European Commission Directorate General for Energy and Transport, the Solar Rating and Certification Corporation (SRCC Document, 1994) and the California Solar Initiative Program (The California Public Utilities Commission (CPUC), 2009), has utilized a different approach for the reduced temperature difference. In this approach, $T^* = (T_{in}-T_a)/I$ where T_{in} = inlet temperature ($^\circ C$) of PG.

The values need for determining the collectors' efficiencies are listed in Table 6-7, as provided by the manufacturer and have been determined in accordance with the EN 12975 standard.

Table 6-7: Efficiency equation variables of the two Solar Collectors in TRCA houses (Viessmann Ltd., 2010)

Collector	Optical Efficiency (%)	Thermal Loss Coefficients		Specific Heat Capacity (kJ/ m ² K)	Max. Idle Temperature ($^\circ C$)
		(W/m ² K)	(W/m ² K ²)		
Vitosol 100 (SV1)	81.0	3.48	0.0164	6.4	221
Vitosol 200	83.8	1.18	0.0066	25.5	300

For the winter testing period, the three-week time frame of March 4th to March 24th of 2011 and for the summer testing period, the four-week time frame of August 1st to August 28th of 2011 have been used for evaluating the performance of the two solar thermal collectors. For each solar thermal collector, individual performance data is presented, and the performance comparison is followed afterwards.

The system control for both solar loops is a simple differential controller. The solar loop pumps start to run when the temperature difference between the solar preheat tanks' sensors, located inside the heat exchanger coil and close to the outlet port of the tanks, and the solar collector outlet reaches $6.7^\circ C$ and stops when the temperature difference falls below $4.5^\circ C$. There is also a high limit cut-off that would stop the pumps when solar preheat tank's hot water outlet temperature exceeds $95^\circ C$.

6.2.1. Flat Plate Solar Thermal Collector

As stated earlier, the flat plate solar thermal collector installed in House-A is Vitosol 100 by Viessmann. The main component of this collector is the copper absorber that is coated with Sol-titanium which ensures a high absorption of solar radiation and low emission of thermal radiation. The heat transfer medium channels the absorber heat through a copper pipe which is fitted to the absorber. The absorber is encased in a highly insulated collector housing, which consists of an aluminum frame for minimizing heat losses. The high quality thermal insulation provides temperature stability and is free from gas emission (Vitotech technical guide, 2010). The cover of the solar panel is made of a glass with very low iron content to reduce reflection losses. Figure 6-20 shows the main components of the flat plate solar collector.

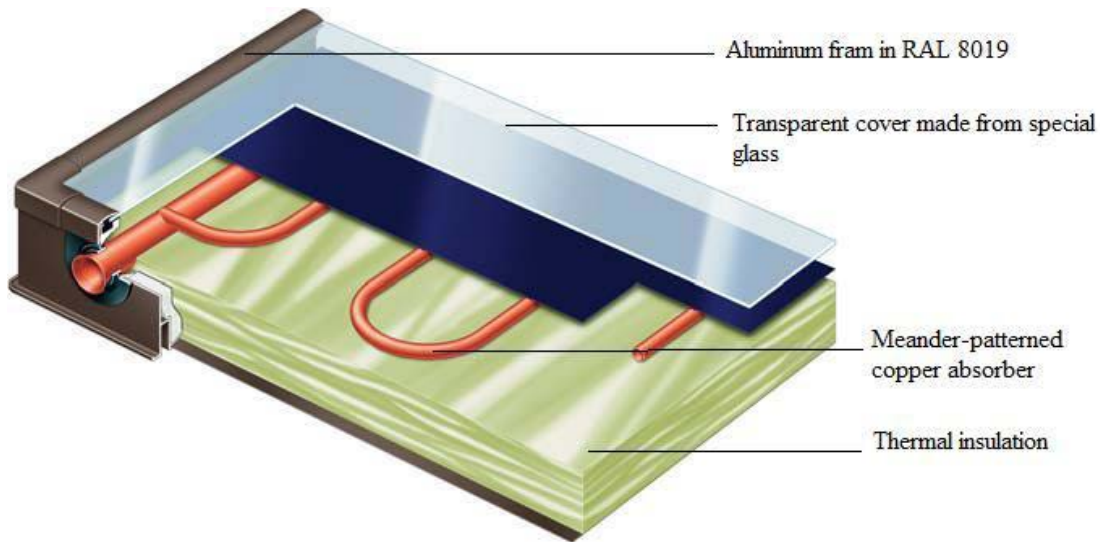


Figure 6-20: Main components of a flat plate Solar Collector (Viessmann Ltd., 2010b)

Figure 6-21 displays the collector efficiency and solar irradiance curves for a typical sunny day. From the collected data, average solar radiation on tilted surface and ambient temperature were found to be of 630 W/m^2 and -1°C (average daytime measurements from 8:00 am till 6:00 pm). As seen, the efficiency and solar radiation curves variations have similar pattern when the collector surface is not covered by snow to allow solar radiation reach the absorber.

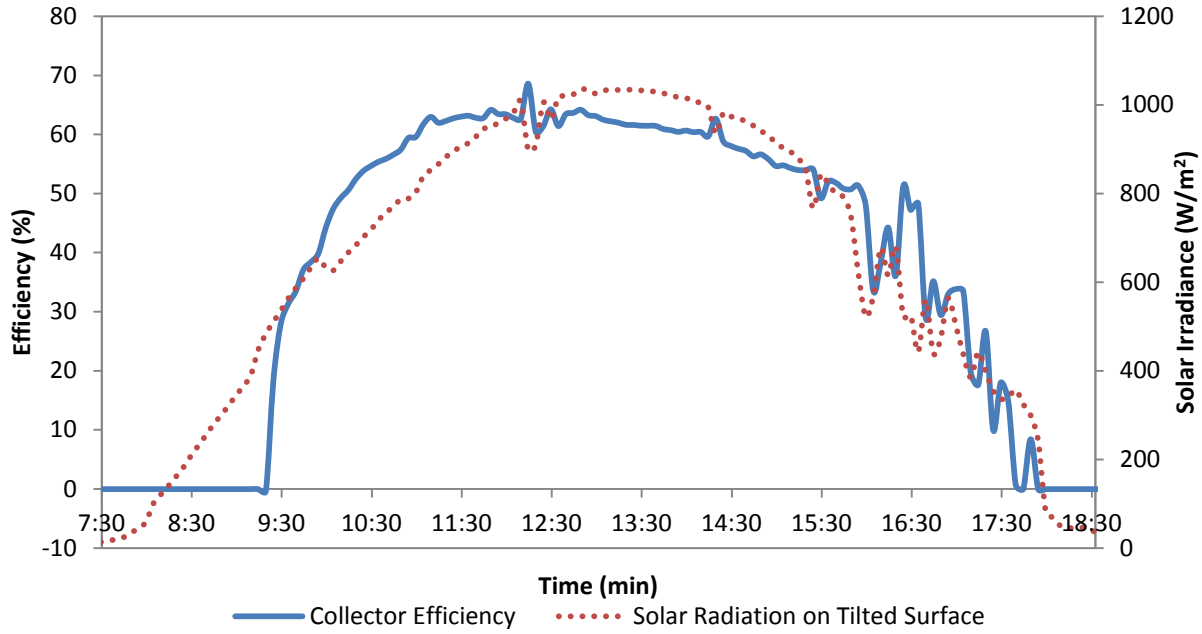


Figure 6-21: Flat plate solar collector efficiency curve changes with solar radiation (Mar/14/2011)

Figure 6-22 shows the average daily values of solar preheat tank inlet and outlet temperature and the thermal energy provided by the collector for the winter testing period.

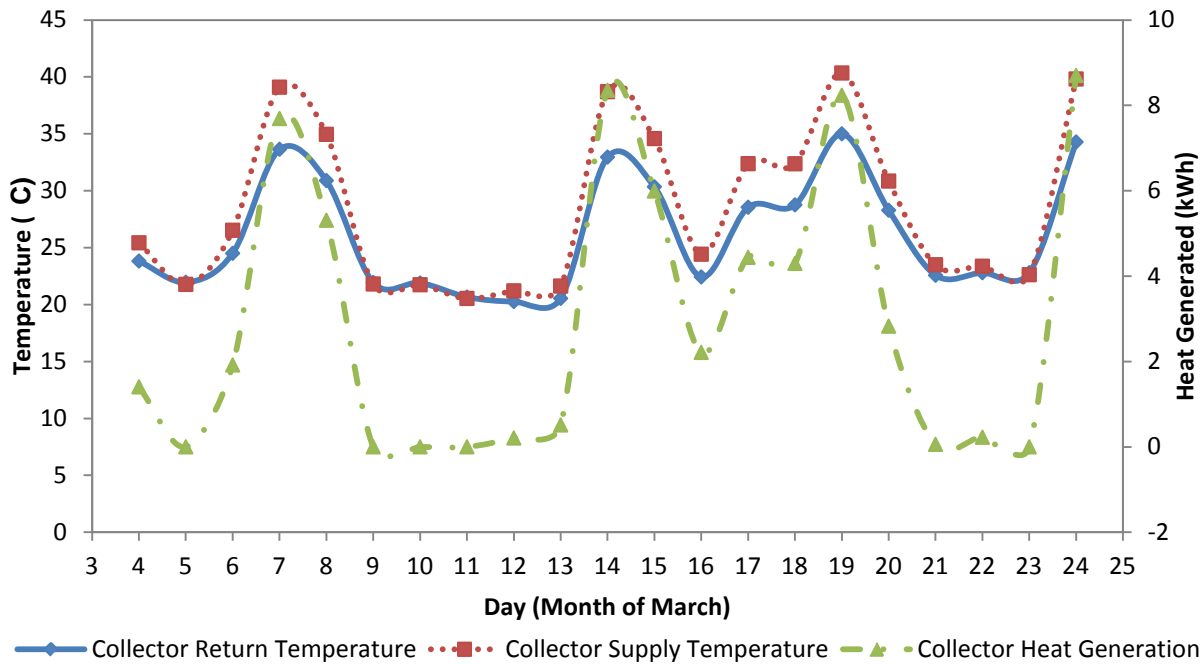


Figure 6-22: Figure 3: Solar loop inlet and outlet temperature and thermal energy output of flat plate collector

Figure 6-23 and Figure 6-24 show the solar collector efficiency changes with average daily solar radiation during the two testing period which shows similar patterns.

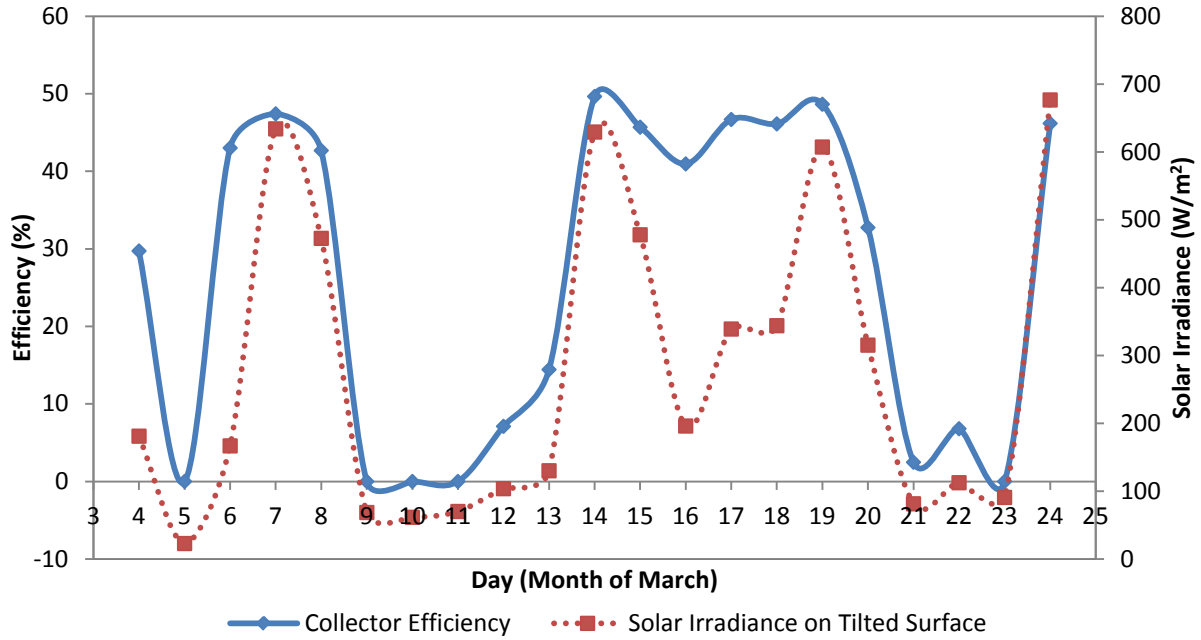


Figure 6-23: Flat plate solar collector efficiency changes with solar radiation on tilted surface in winter

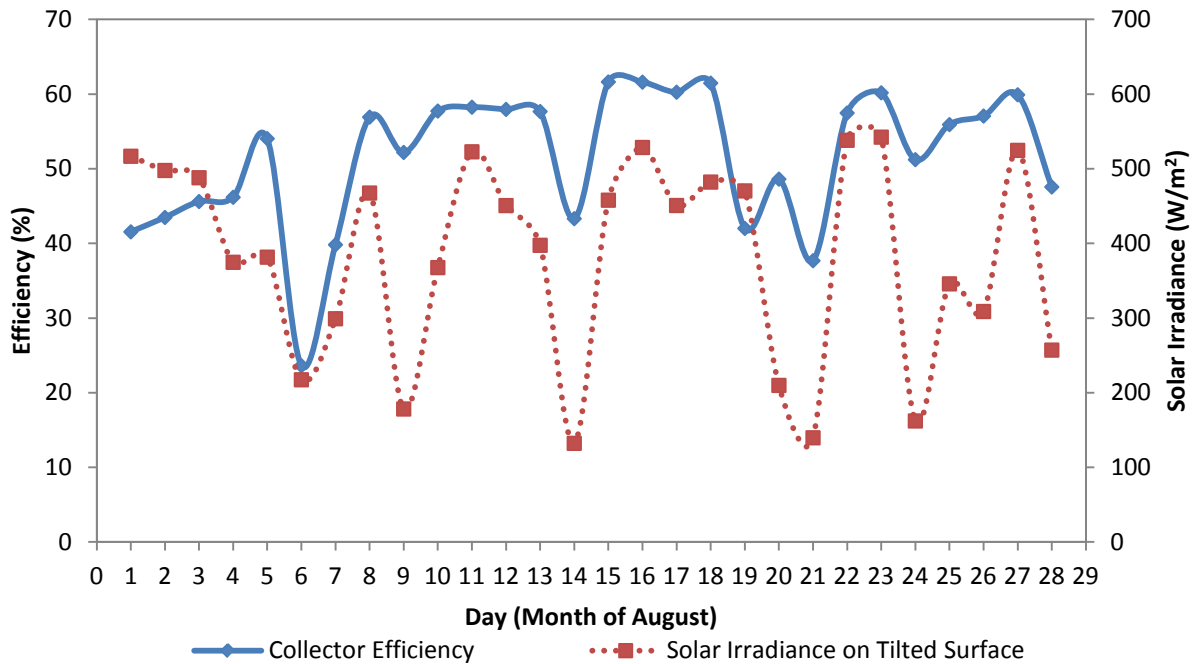


Figure 6-24: Flat plate solar collector efficiency changes with solar radiation on tilted surface in summer

Figure 6-25 and Figure 6-26 show the thermal energy output by the solar collector and solar loop pump electrical energy consumption changes with average daily solar radiation for the two testing periods. By comparing the two figures, higher heat generation by the solar collector in summer is obvious, but solar pump consumption is almost similar, as obtained from the data.

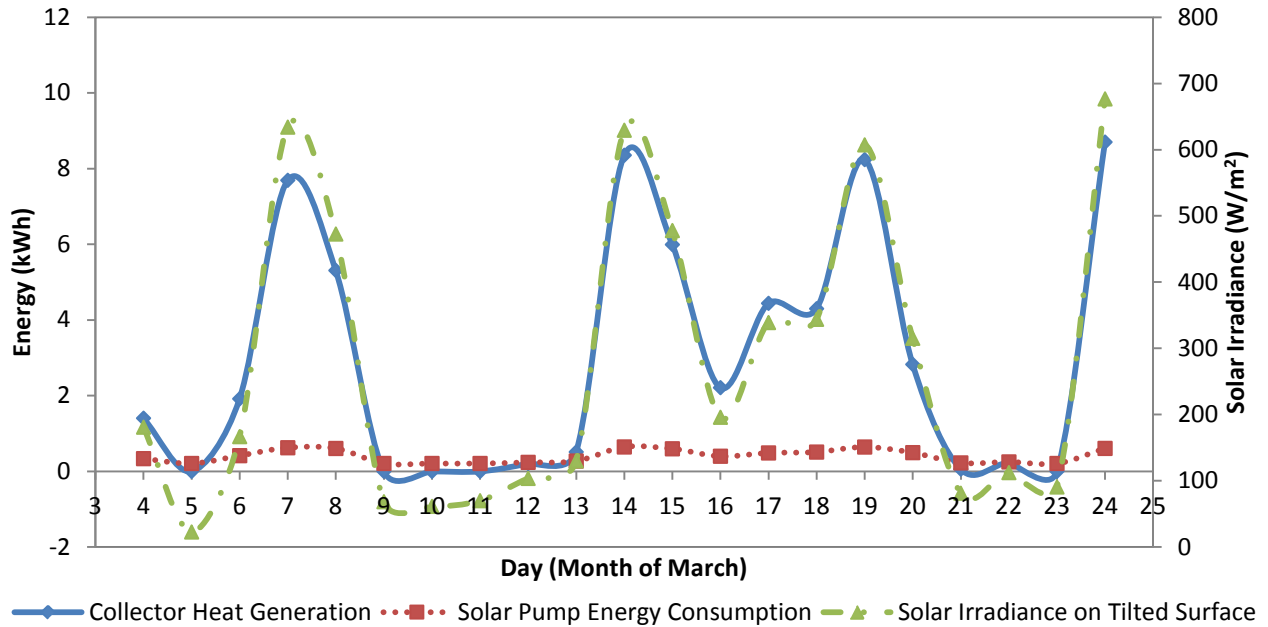


Figure 6-25: Flat plate solar collector thermal energy output and solar pump energy consumption variations with solar radiation in winter

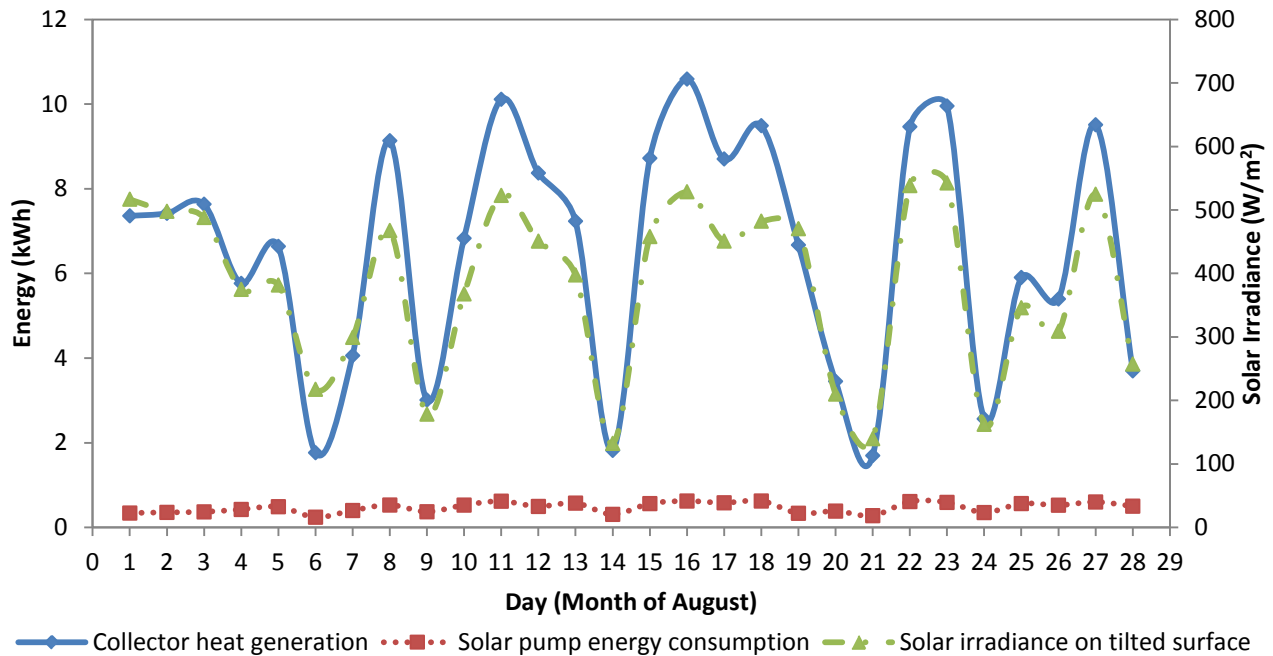


Figure 6-26: Flat plate collector thermal energy output and solar pump energy consumption variations with solar radiation in summer

Figure 6-27 displays the instantaneous collector efficiency curve versus temperature difference ($T_m - T_a$) comparison between the manufacturer data, Equation (6-18), and the efficiency from Equation (5-12) for the winter and summer testing periods.

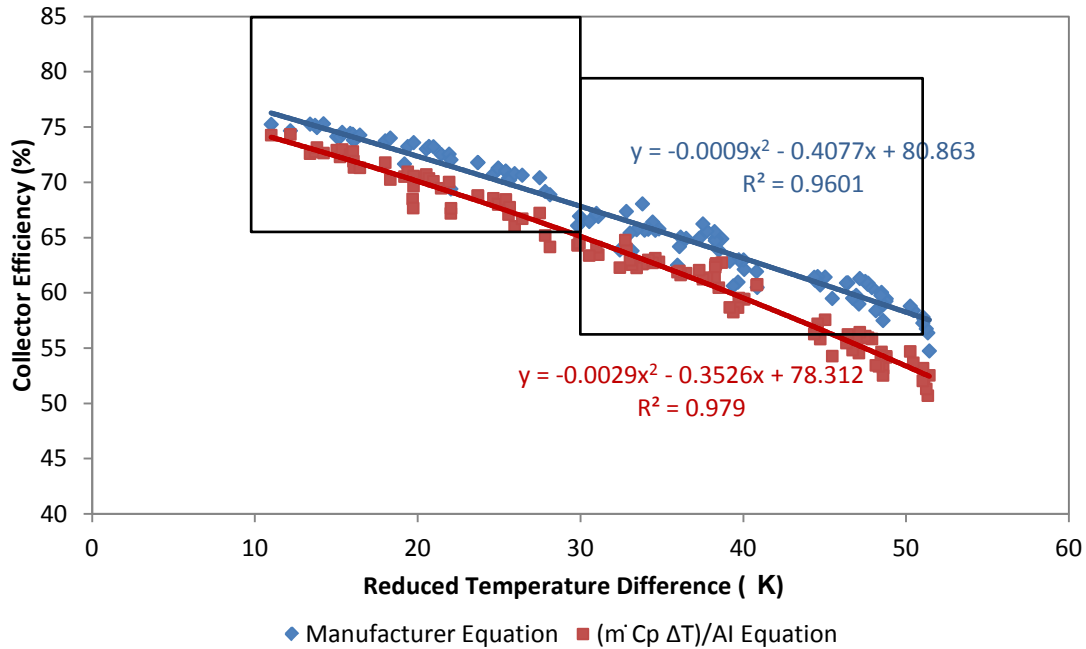


Figure 6-27: Flat plate collector instantaneous efficiency curve vs. reduced temperature difference for winter and summer testing periods

During both periods, efficiency of the collector decreases with the increase of reduced temperature difference, which is due to decrease in the ambient temperatures or lower solar irradiance on the collector surface (low sun radiation availability or collector surface covered by snow). The efficiencies are within the solar heating system for DHW at higher coverage range (30°C to 50°C temperature difference) for the winter testing period, and are within the solar heating system for DHW at low coverage range of 10°C to 30°C temperature difference for summer period, as specified by the manufacturer. As seen in Figure 6-27, collector efficiencies from Equation (5-12) are closer to the trend line from manufacturer data during the summer testing period. It should be noted that the manufacturer’s curve is obtained under controlled operating conditions, and the collector’s inlet and outlet temperature are measured exactly at the inlet and outlet point of the collector; whereas in the case of House-A’s collector, the two temperatures are measured at the inlet and outlet of the DHW tank and temperature drops certainly occurs due to thermal losses from the solar loop’s piping system. Using the curves in Figure 6-27, k_1 , and k_2 values from experimental data were found to be 78.3%, 2.82 W/m²K

and $0.023 \text{ W/m}^2\text{K}^2$. This was derived by assuming that the solar irradiance is 800 W/m^2 , as specified by the manufacturer.

The energy amounts provided by the flat plate solar collector and the solar pump electrical consumptions for the two testing periods are listed in Table 6-8. The solar collector's overall efficiency can be achieved by taking into account the solar loop pump's electricity consumptions.

Table 6-8: Total and average deliverable energy by the flat plate collector during winter and summer periods

	Period (Days)	Collected Energy by Collector (kWh)	Pump Electricity Consumption (kWh)	Available Energy on Tilted Collector Surface (kWh)	Collector Efficiency (%)	Collector Overall Efficiency (%)
Winter Total	21	62.4	8.4	157.9	---	---
Winter Average Daily	–	2.97	0.40	7.52	39.5	37.5
Summer Total	28	183.0	13.1	346.5	---	---
Summer Average Daily	–	6.54	0.47	12.38	52.8	50.9

6.2.2. Evacuated Tube Solar Thermal Collector

The evacuated tube solar collector installed in House-B is Vitosol 200 by Viessmann which consists of 20 evacuated glass tubes. An absorber with sol-titanium is an integral part of the tubes which ensures high absorption of solar radiation and low emission of thermal radiation. The vacuum in the tubes ensures optimum thermal insulation. Convection losses between the tubes and the absorber are also eliminated (Viessmann Ltd., 2010). Figure 6-28 shows the main components of the evacuated tube solar collector. Pure water is used inside the copper tube as the heat transfer media from the absorber to the condenser, i.e. to Propylene Glycol as shown in Figure 6-29.

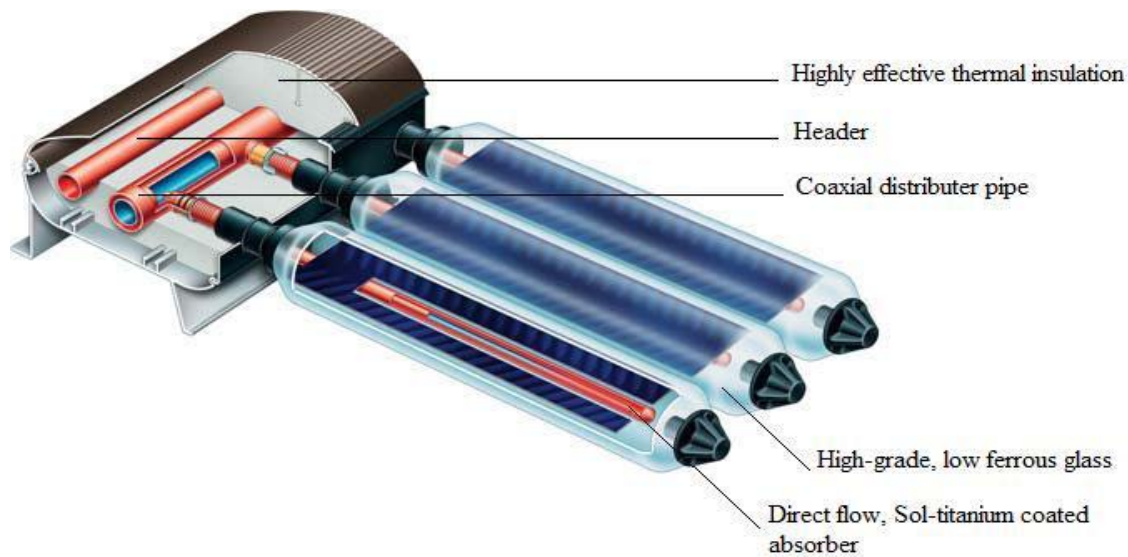


Figure 6-28: Main components of an evacuated tube solar collector (Viessmann Ltd., 2010b)

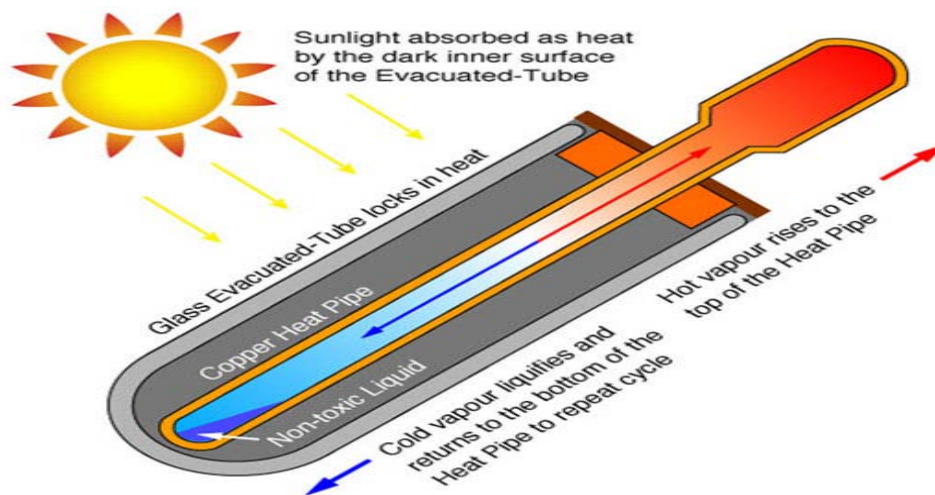


Figure 6-29: Heat absorption mechanism from the solar energy in a Evacuated Tube Solar Collector (<http://www.echomaterico.net/blog/?p=497>)

During winter testing period, three evacuated tubes were not operating properly, due to damaged vacuum seals. Thus, the absorber and aperture areas were modified accordingly. The damaged tubes were replaced after the winter testing period. Figure 6-30 displays the collector efficiency and solar irradiance curves for the same sunny day (Mar/14/2011) with the average solar radiation on tilted surface of 630 W/m^2 and the ambient temperature of -1°C . As seen, although the efficiency and solar radiation curves variations follow similar patterns, there is back flow during the early operation time of the collector and that there are more oscillations in the

efficiency curve in comparison to the flat plate collector. The early morning back flows are a common occurrence with this solar collector which is even greater during colder months. This is due to the fact that during early mornings, the heat starts to build up in the collector header and the differential controller senses this temperature difference between the header and the solar preheat tank water temperature and forces the pump to start. As the pump runs, the “initial” heat is carried away and the temperature difference falls below the lower dead band temperature and the pump is stopped. This phenomenon causes heat loss from the solar preheat tank, especially during winter months when the solar radiation values are relatively lower and the ambient temperature is much lower.

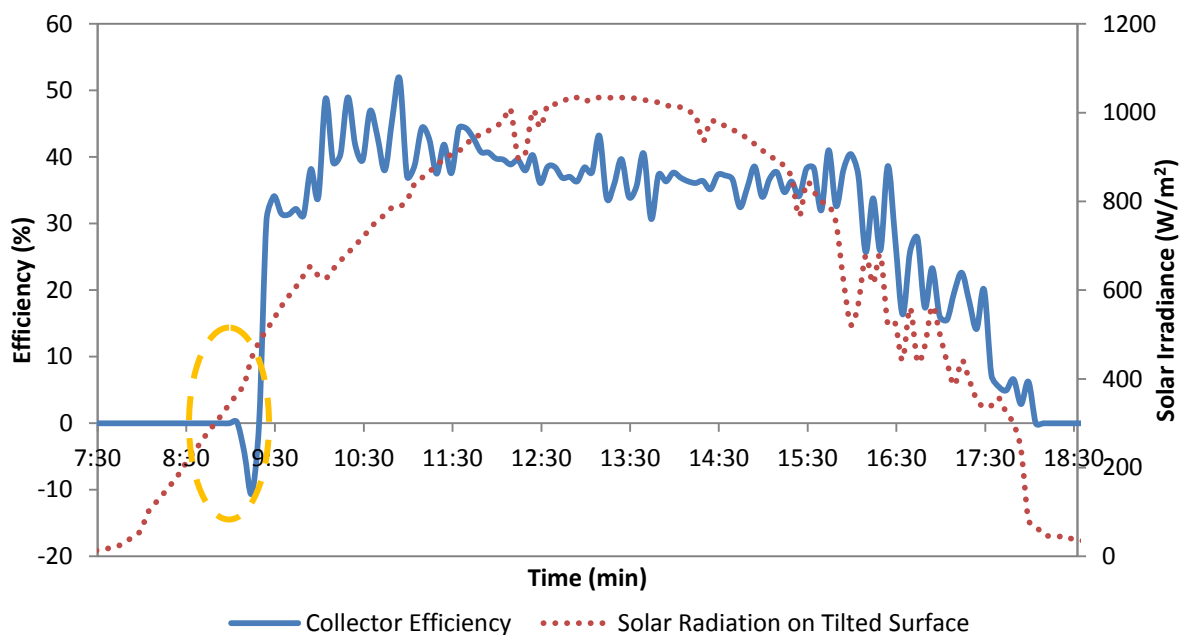


Figure 6-30: Evacuated tube solar collector efficiency curve changes with solar radiation (Mar/14/2011)

Figure 6-31 shows the solar collector efficiency changes with average daily solar radiation during the winter testing period, which for most of the times shows similar patterns. As outlined in Figure 6-31, solar collector has a very low efficiency (less than 5%) for a sunny day with average solar radiation of over 600 W/m^2 which is in an indication that the collector surface is covered by snow and/or ice. Generally, there are more times that the evacuated tube surface is covered by snow, compared to the flat plate collector. The reason for this is that the vacuum tubes have very high thermal insulation, which in return does not allow the snow on the surface of the tubes to be melted, and sun would be the only source for melting the snow. The geometry of these collectors is also in a way that causes the snow and ice to get stuck in between the tubes.

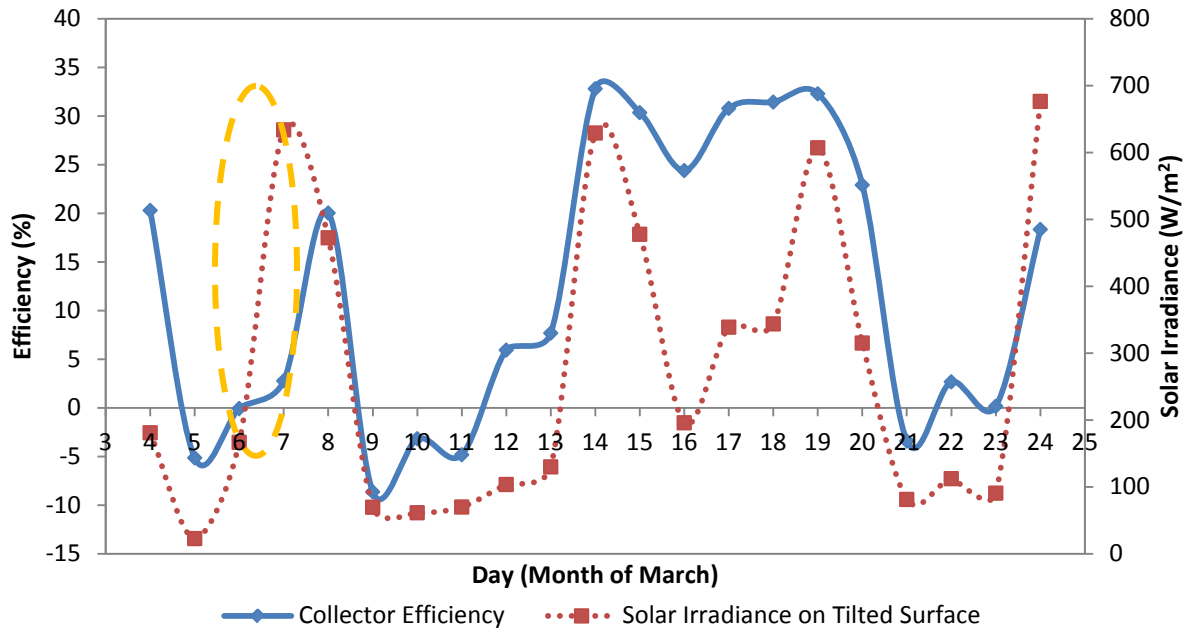


Figure 6-31: Evacuated tube solar collector efficiency changes with solar radiation on tilted surface in winter

Figure 6-32 displays the solar collector efficiency changes with average daily solar radiation during the summer testing period which shows similar patterns.

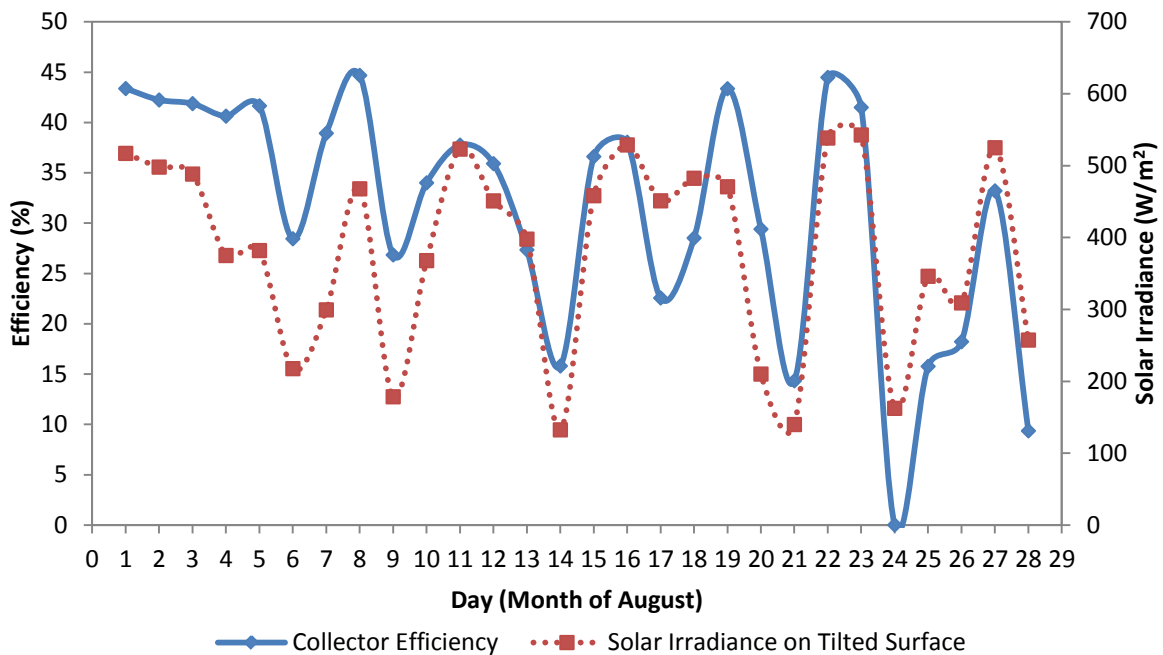


Figure 6-32: Evacuated tube solar collector efficiency changes with solar radiation on tilted surface in summer

Figure 6-33 and Figure 6-34 show the thermal energy output by the solar collector and solar loop pump electrical energy consumption changes with average daily solar radiation.

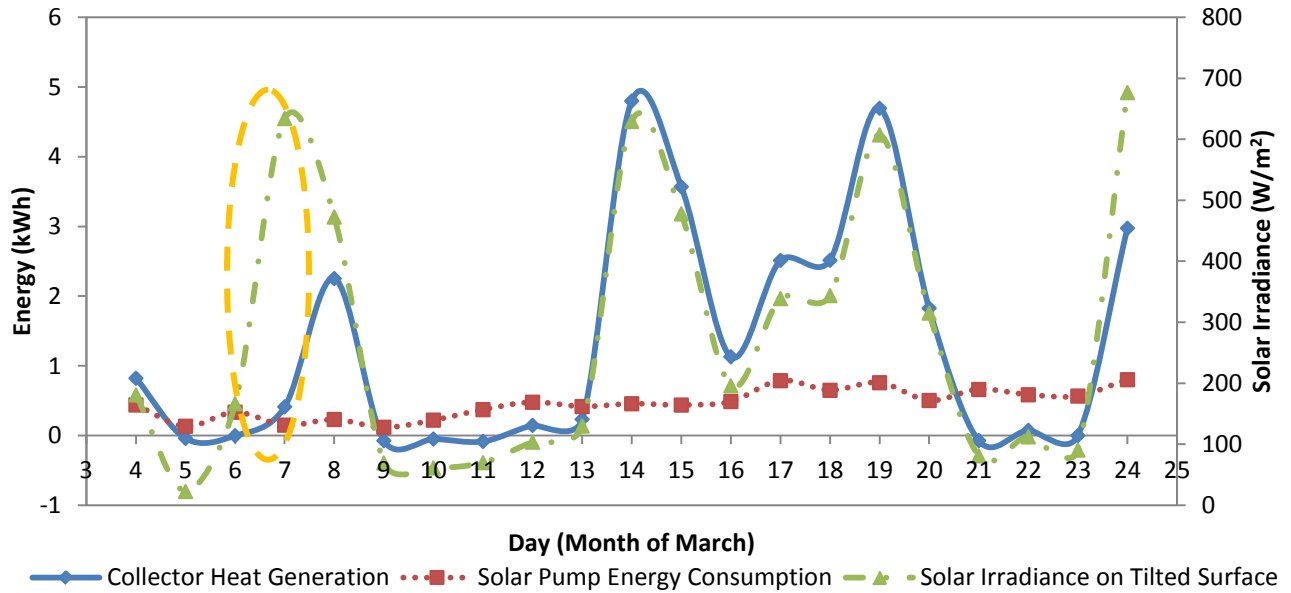


Figure 6-33: EVT collector thermal energy output and solar pump’s energy consumption variations with solar radiation in winter

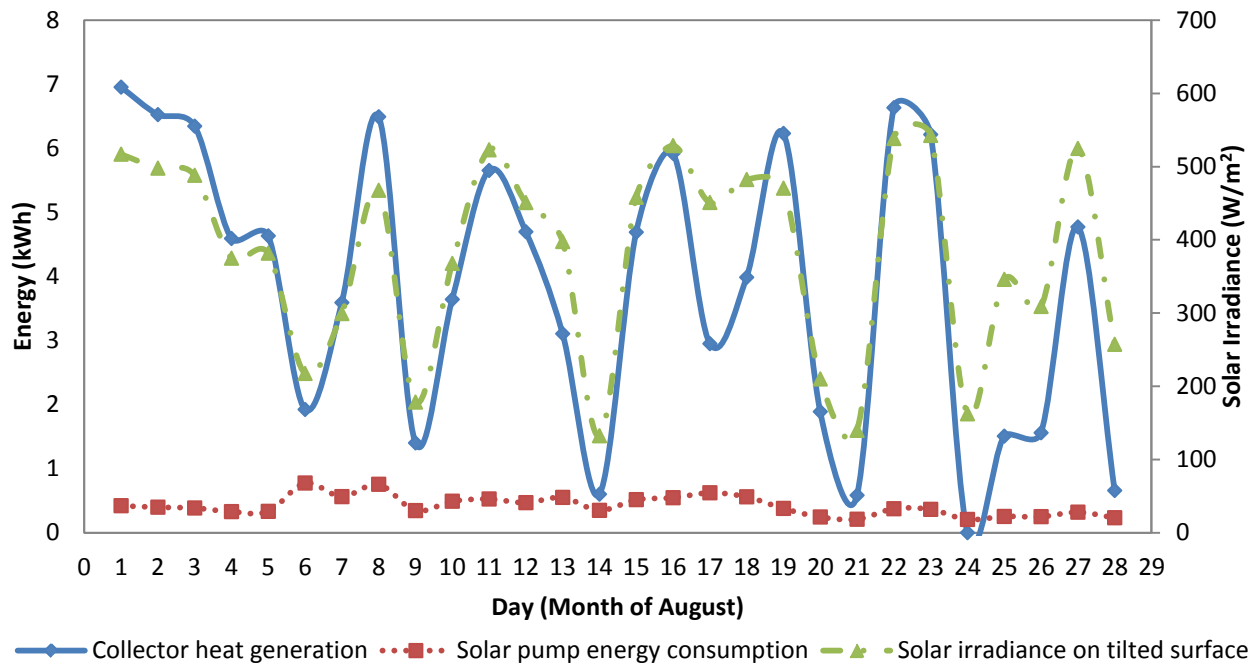


Figure 6-34: EVT collector thermal energy output and solar pump’s energy consumption variations with solar radiation in summer

Although daily thermal energy output shows relatively similar patterns with the average daily solar radiation variations in winter period, electrical energy consumption variations does not

seem to follow this pattern. The reason for this is that the solar loop pump needs to circulate the PG solution more, during antifreeze cycles, to prevent freezing of the water at the collector's header.

Figure 6-35 and Figure 6-36 display the instantaneous collector efficiency curve versus reduced temperature difference ($T_m - T_a$) comparison between the manufacturer data, Equation (6-18), and the efficiency from Equation (5-20) for the two testing periods.

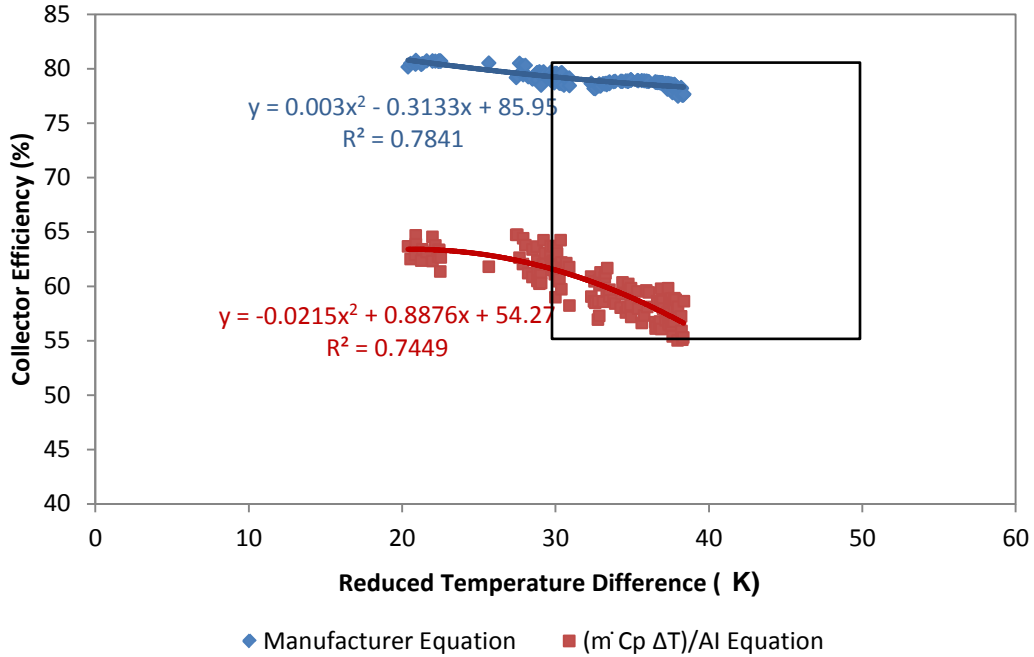


Figure 6-35: EVT collector instantaneous efficiency curve vs. reduced temperature difference for winter period

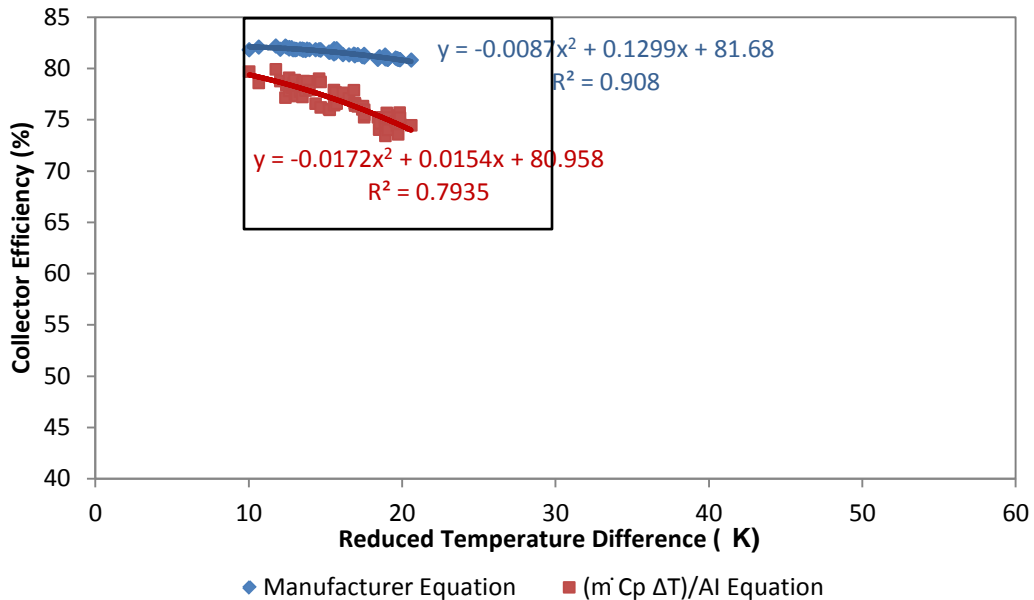


Figure 6-36: EVT collector instantaneous efficiency curve vs. reduced temperature difference for summer period

In both periods, efficiency decreases with the increase of reduced temperature difference. There is a significant difference between the efficiency curves from the two equations for the winter testing period. The main reasons are the loss of three evacuated tubes due to vacuum seals damage as stated earlier, lower available solar radiation, surface of the collector's tubes being covered by snow/ice, and lower ambient temperatures. For the winter testing period, the efficiencies are within the range of both solar heating system for DHW at higher coverage range and solar heating system for DHW at low coverage range of 10°C to 30°C. The efficiencies are within the solar heating system for DHW at low coverage range, during the summer testing period. Similar to what mentioned for the flat plate solar thermal collector, the manufacturer's curve is obtained under controlled operating conditions, and the collector's inlet and outlet temperature are measured exactly at the inlet and outlet points of the collector; whereas in the case of House-B's collector, the two temperatures are measured at the inlet and outlet of the solar preheat tank and temperature drops certainly occurs due to thermal losses from the solar loop's piping system. The two sets of collector efficiency curves are not displayed in a single figure, simply due to the three sets of damage tubes which were replaced with new tubes before the beginning of the summer testing period. Using the curves in Figure 6-36, k_1 , and k_2 values from experimental data were found to be 81.0%, 0.12 W/m²K and 0.138 W/m²K². This was derived by assuming that the solar irradiance is 800 W/m², as specified by the manufacturer.

The energy amounts provided by the evacuated tube solar thermal collector and the solar pump electrical consumptions for the two testing periods are as listed in Table 6-9.

Table 6-9: Total and average deliverable energy by the EVT collector during winter and summer periods

	Period (Days)	Collected Energy by Collector (kWh)	Pump Electricity Consumption (kWh)	Available Energy on Tilted Collector Surface (kWh)	Collector Efficiency (%)	Collector overall Efficiency (%)
Winter Total	21	30.4	18.0	146.8	---	---
Winter Average Daily	–	1.38	0.82	6.67	20.7	18.4
Summer Total	28	107.8	11.8	313.0	---	---
Summer Average Daily	–	3.85	0.42	11.18	34.4	33.2

6.2.3. Solar Thermal Collectors' Performance Comparison

In this part, the daily heat generation by the two solar collectors during the two testing periods will be discussed. Figure 6-37 and Figure 6-38 display the thermal energy output of the two collectors and the solar irradiance effect, during winter and summer testing periods.

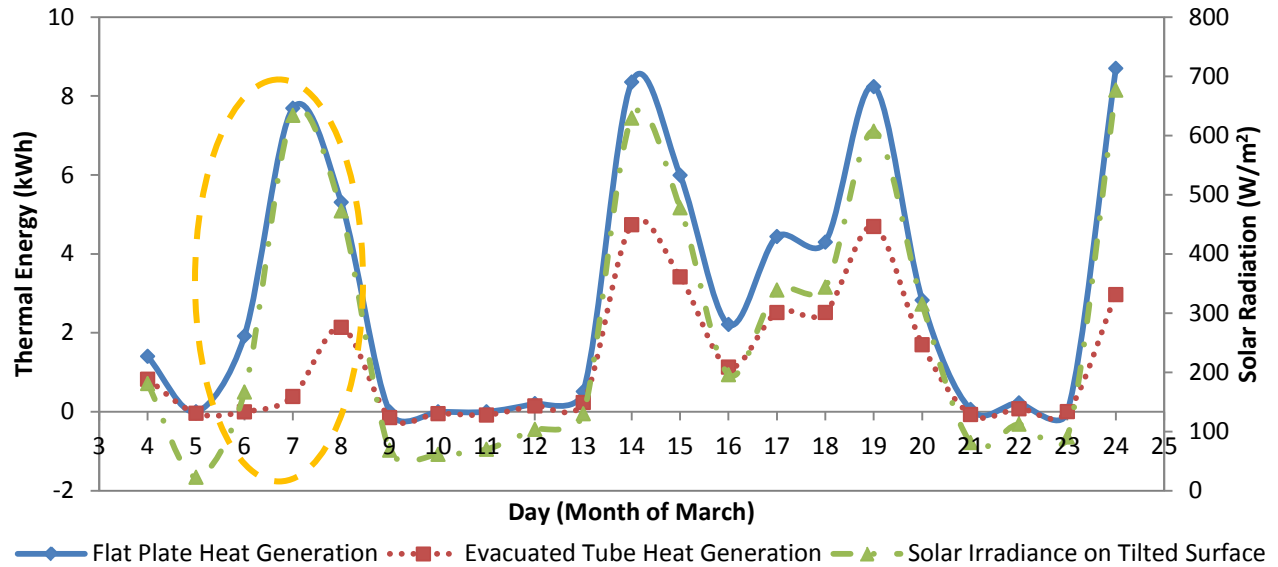


Figure 6-37: Solar collectors' daily thermal energy output variations with solar radiation in winter

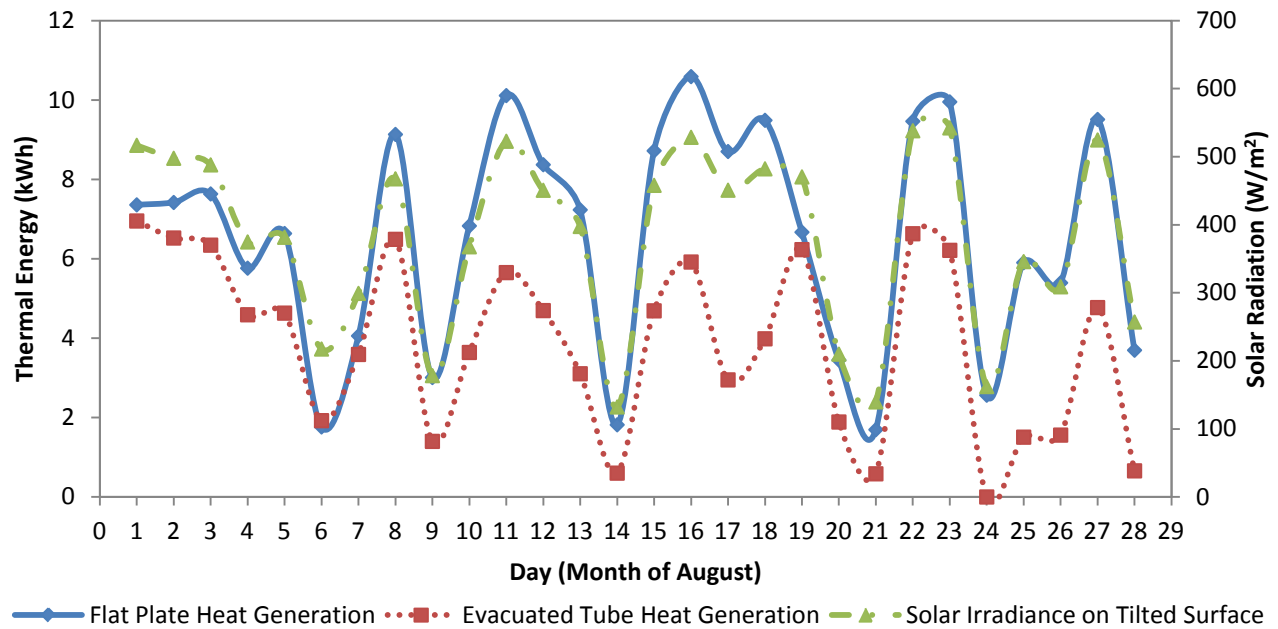


Figure 6-38: Solar collectors' daily thermal energy output variations with solar radiation in summer

From these two figures, it is evident that the thermal energy output of both collectors, follow the same pattern as the average daily solar irradiance does, especially during summer. As seen in the highlighted part of Figure 6-37, flat plate collector will soon start generating heat after a snowy day and snow does not cover its surface for long which is to the smooth surface of the collector and the inclination angle. Evacuated tube collector surface however, is longer covered by snow and is slower in beginning the heat generation.

The daily thermal energy output by the two solar thermal collectors can be easily compared from Figure 6-39 and Figure 6-40. In general, the flat plate collector has higher daily thermal energy output during both testing periods.

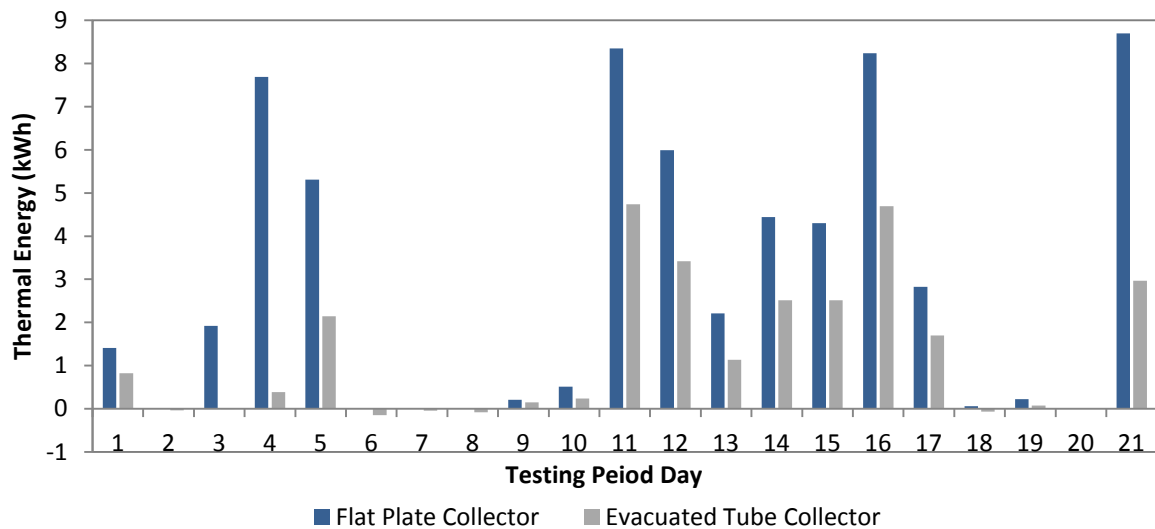


Figure 6-39: Daily thermal energy output from solar thermal collectors in winter testing period

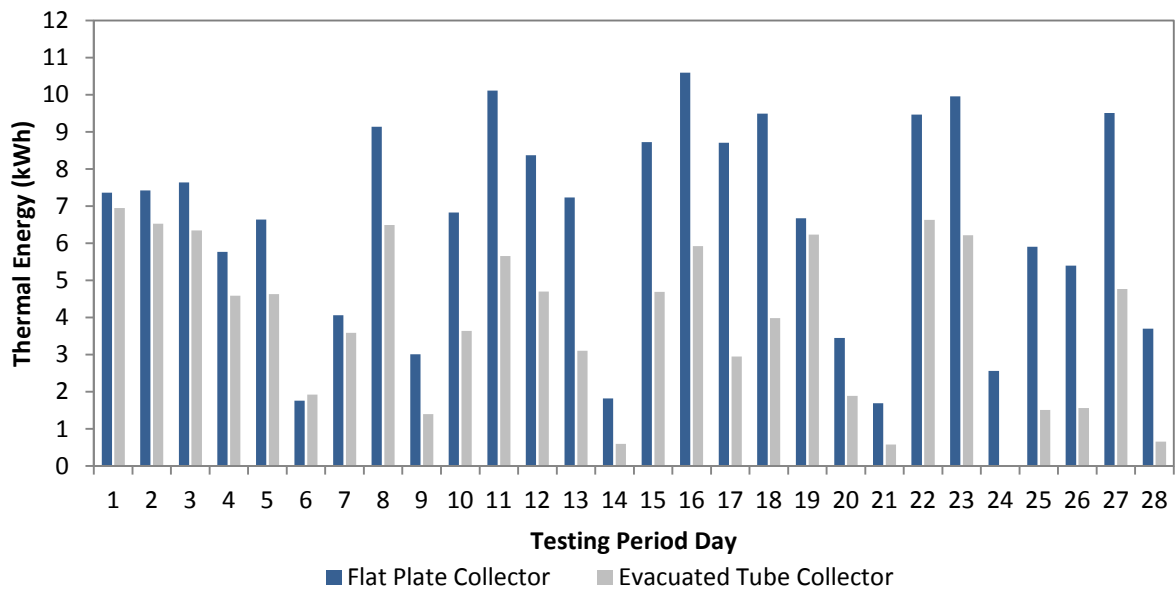


Figure 6-40: Daily thermal energy output from solar thermal collectors in summer testing period

Figure 6-41 shows the cumulative thermal energy output by the two collectors for the three-week winter testing period. Total thermal energy output from the flat plate collector is 62.4 kWh, which is more than twice of that of the evacuated tube collector at 30.4 kWh.

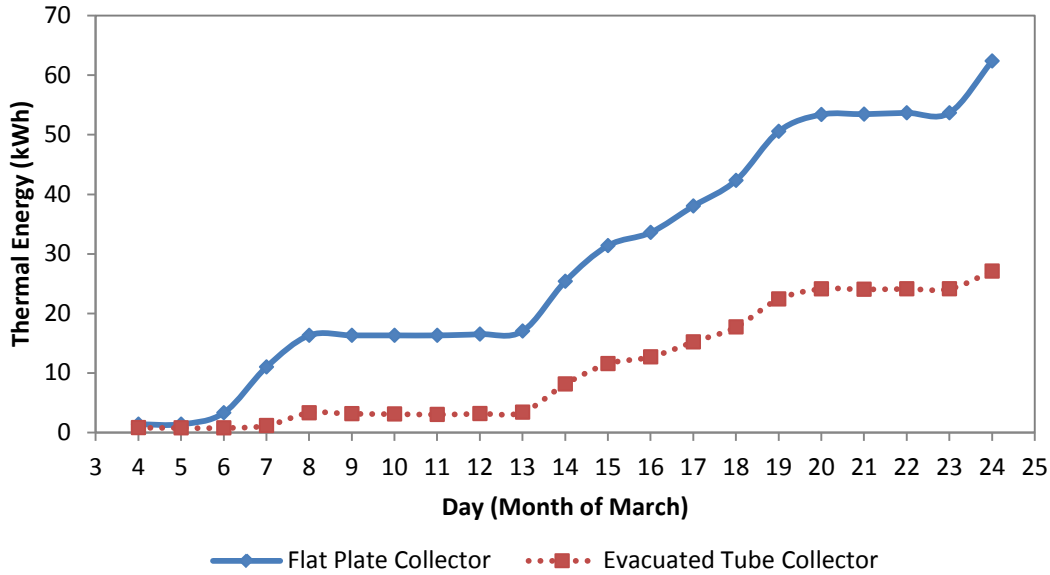


Figure 6-41: Cumulative thermal energy output by the two solar thermal collectors in winter

Figure 6-42 shows the cumulative thermal energy output by the two collectors for the four-week summer testing period. Total thermal energy output from the flat plate and evacuated tube collectors are 183 kWh and 107.8 kWh, respectively. In other words, for the same period, the flat plate collector can produce 70% more heat, compared to the evacuated tube collector.

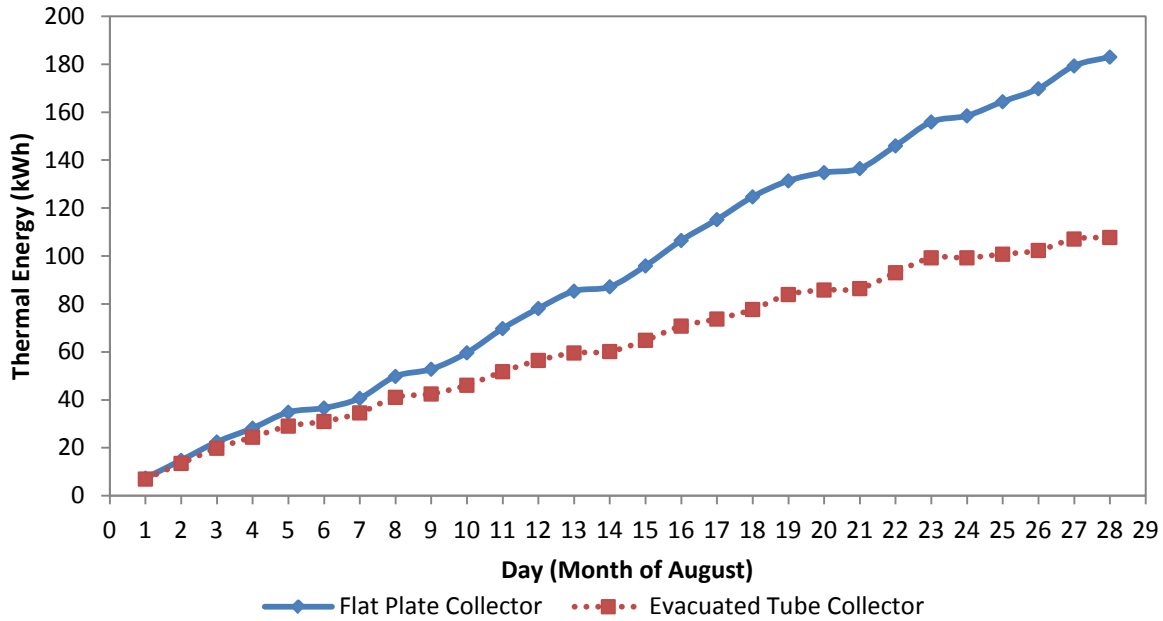


Figure 6-42: Cumulative thermal energy output by the two solar thermal collectors in summer

6.2.4. Extrapolated Data

The thermal energy output of the solar thermal collectors with respect to average daily solar irradiance on the collectors' surfaces, is obtained for winter and summer testing periods. The annual thermal energy outputs of the collectors can be derived, using the average daily solar radiations, obtained from TRNSYS 16. In this software, the weather data for metropolitan Toronto have been generated using Meteonorm version 5, published by METEOTEST (<http://www.meteotest.com>). 52 different cities and locations for Canada have been selected for which, solar radiation data has been recorded at related primary stations. TRNSYS "data reader" component serves the purpose of reading weather data at regular time intervals from a data file, converting it to a desired system of units and processing the solar radiation data to obtain tilted surface radiation and angle of incidence for an arbitrary number of surfaces (Solar Energy Laboratory of University of Wisconsin, 2005). The sky model for diffuse radiation parameter, used for calculating the diffuse radiation on tilted surfaces, has been set to 4, representing the Perez model. This model is considered to be the best available model and is TRNSYS default. The tracking mode parameter is also set as 1.

Figure 6-43 displays the annual cumulative thermal energy output of the two solar thermal collectors.

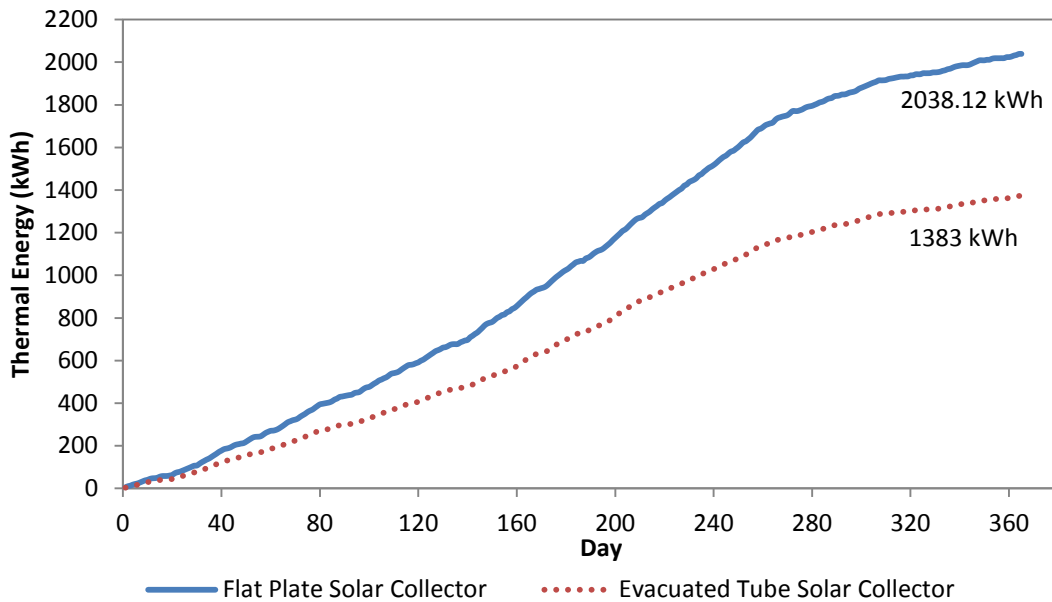


Figure 6-43: Annual cumulative thermal energy output by the two solar thermal collectors

The thermal energy output of the flat plate and evacuated tube collectors are calculated to be 2038.12 kWh and 1383 kWh, respectively. This clearly shows that the flat plate collector has better performance, compared to the evacuated tube one, and is capable of providing almost 47% more thermal energy during a typical year in metropolitan Toronto.

Figure 6-44 shows the overall monthly thermal energy output by the two solar collectors. It is evident that the thermal energy outputs of the two collectors follow similar trends throughout a typical year. Another important observation is that, the thermal energy output differences are higher during warmer months, with higher monthly solar irradiances.

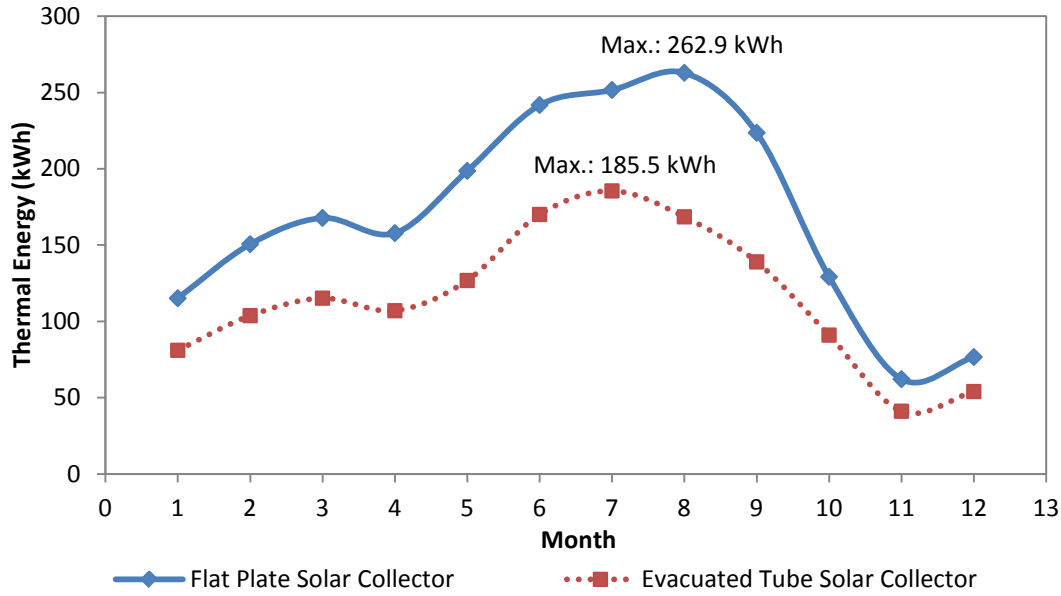


Figure 6-44: Monthly thermal energy output by the two solar thermal collectors

6.3. Overall Performance of the Archetype Houses’ SDWH Systems

The overall daily performance of the two SDWH systems, including the heat generation by auxiliary heating sources (electric backup heating tank and mini gas boiler) and the two solar thermal collectors, plus the daily heat recovery amounts by the DWHR systems have been obtained for the two testing periods. Using the fresh water supply temperatures, as displayed in Figure 6-5, and the average daily solar irradiance from TRNSYS, and, assuming that the end use hot water temperature is between 42°C and 44°C, the annual heat generation by the auxiliary and renewable sources and the heat recovery amounts can be achieved. The monthly heat recovery and thermal energy output by the two solar thermal collectors have already been mentioned in previous sections of this chapter.

Figure 6-45 displays the average monthly energy consumption of the mini gas boiler in House-A and flat plate solar thermal collector’s thermal energy output. As seen in this figure, the two series have opposite trends.

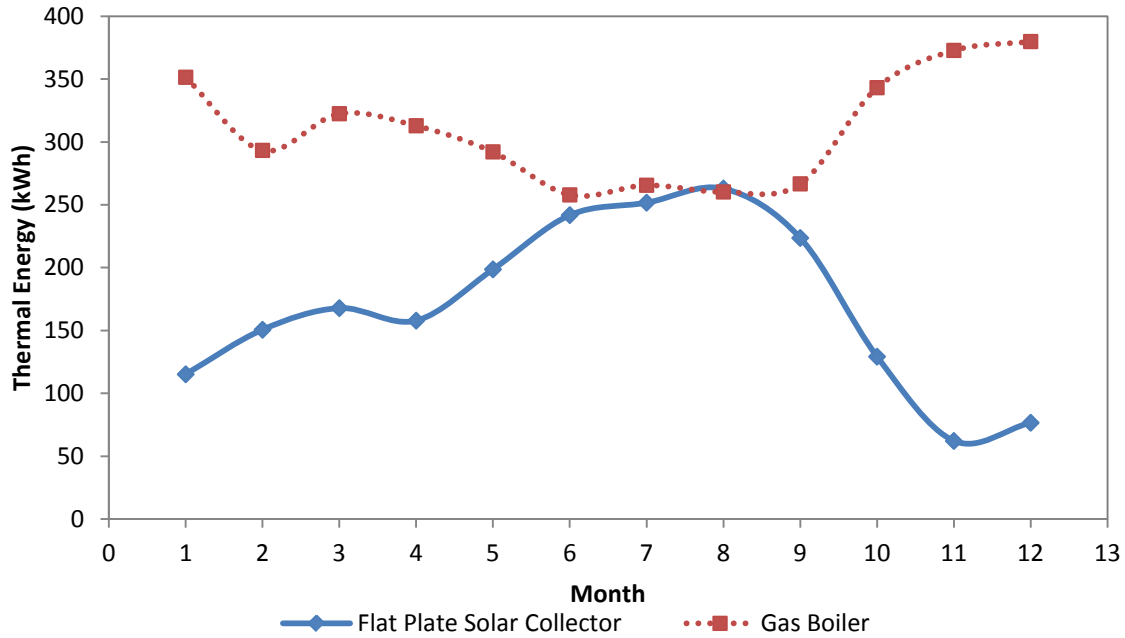


Figure 6-45: Comparison of thermal energy output of flat plate collector and energy consumption of gas boiler

Figure 6-46 displays the average monthly electricity consumption of the electric heating backup tank in House-B and evacuated tube solar thermal collector’s thermal energy output. As what was observed with the case for House-A, these two also have opposite trends.

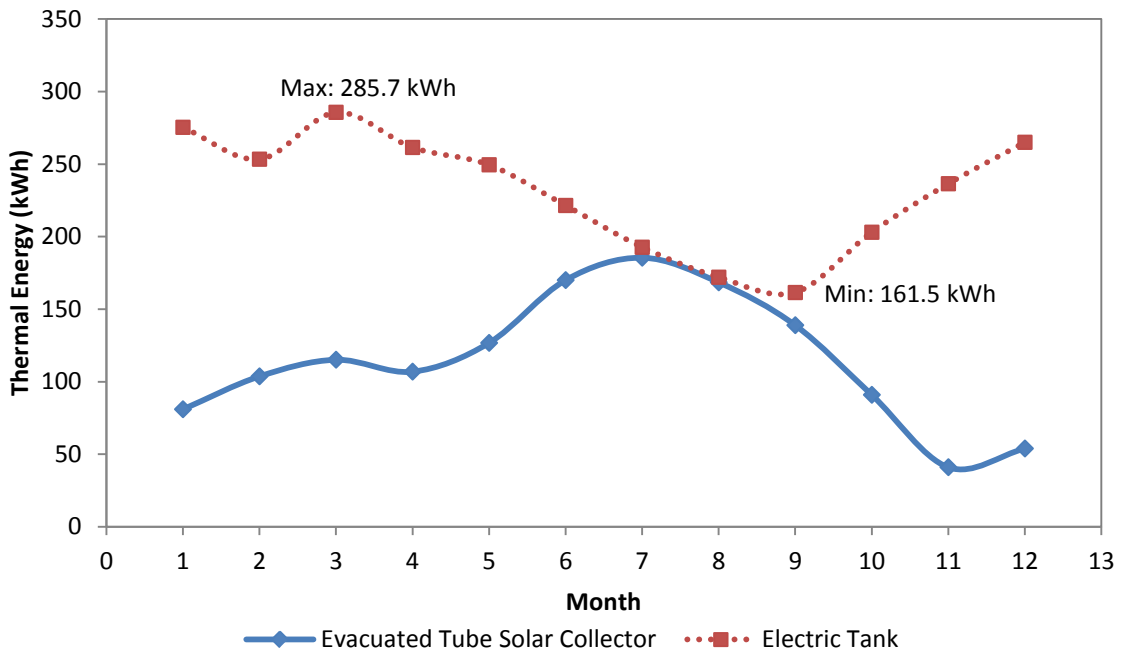


Figure 6-46: Comparison of thermal energy output of evacuated tube collector and energy consumption of electric tank

The annual energy consumption by the gas boiler, heat generation by the flat plate solar thermal collector and heat recovery by the DWHR unit in House-A, are listed in Table 6-10. It should be mentioned that the average efficiency of the boiler, with respect to the thermal energy supplied to the DHW tank, was found to be 55.5%.

Table 6-10: Annual energy consumption, generation and recovery by SDWH system's components of House-A

Heat Generation by Flat Plate Solar Collector (kWh)	Energy Consumption by Mini Gas Boiler (kWh)	Heat Recovery by DWHR (kWh)
2038.12	3718.69	788.54

Similarly, the annual energy consumption by the electric backup tank, heat generation by the evacuated tube solar thermal collector and heat recovery by the DWHR unit in House-B, are listed in Table 6-11. The average efficiency of the electric backup tank, obtained from the two testing periods, is found to be approximately 78.8%.

Table 6-11: Annual energy consumption, generation and recovery by SDWH system's components of House-B

Heat Generation by Evacuated Tube Solar Collector (kWh)	Energy Consumption by Electric Backup Tank (kWh)	Heat Recovery by DWHR (kWh)
1383.02	2777.92	788.54

Chapter 7 : TRNSYS Simulations

In this chapter, the SDHW systems for the two Archetype houses will be modeled using TRNSYS. Once the models are validated with the experimental results, the models can then be used to achieve the benefits from such systems, in lowering annual energy required for DHW production, costs and GHG emissions in major Canadian cities. First, a brief description of the software will be represented.

TRNSYS is a complete and extensible simulation environment for the transient simulation of systems, including multi-zone buildings (Solar Energy Laboratory of University of Wisconsin, 2005). It is used by engineers and researchers around the world to validate new energy concepts, from DHW systems to the design and simulation of buildings and their equipment, including control strategies, occupant behaviour, alternative energy systems (wind, solar, photovoltaic, hydrogen systems) and thermal comfort. One of the key factors in TRNSYS success over the last 25 years is its open, modular structure. The source code of the kernel as well as the component models are delivered to the end users. This simplifies extending existing models to make them fit the user's specific needs. The DLL-based architecture allows users and third-party developers to easily add custom component models, using many common programming languages (C, C++, PASCAL, FORTRAN, etc.). In addition, TRNSYS can be easily connected to many other applications, for pre- or post-processing or through interactive calls during the simulation (e.g. Microsoft Excel, Matlab, COMIS, etc.). TRNSYS applications include:

- Solar systems (solar thermal and PV)
- Low energy buildings and HVAC systems with advanced design features (natural ventilation, slab heating/cooling, double facade, etc.)
- Renewable energy systems
- Cogeneration, fuel cells
- Anything that requires dynamic simulation

A TRNSYS project is typically setup by connecting components graphically in the Simulation Studio. Each Type of component is described by a mathematical model in the TRNSYS simulation engine and has a set of matching Proforma's in the Simulation Studio The proforma has a black-box description of a component: inputs, outputs, parameters and etc.

7.1. Twin Houses SDWH Systems Modeling

The two SDWH systems of the Archetype houses were modeled, using TRNSYS-16. Figure 7-1 shows the TRNSYS model of House-B SDWH system. Standard components from TRNSYS library were used, except for the DWHR unit for which a new model was created. The new DWHR model was created by modifying the existing counter-flow heat exchanger model. As described earlier, the two systems are configured in a way that the DWHRs only preheat the water to solar preheat tanks. The DWHRs are also modeled in a way to recuperate heat only during simultaneous water draw and water dumping events. Various technical parameters related to different components were collected from technical data sheets and input into these components. The major components of the two systems will be described briefly.

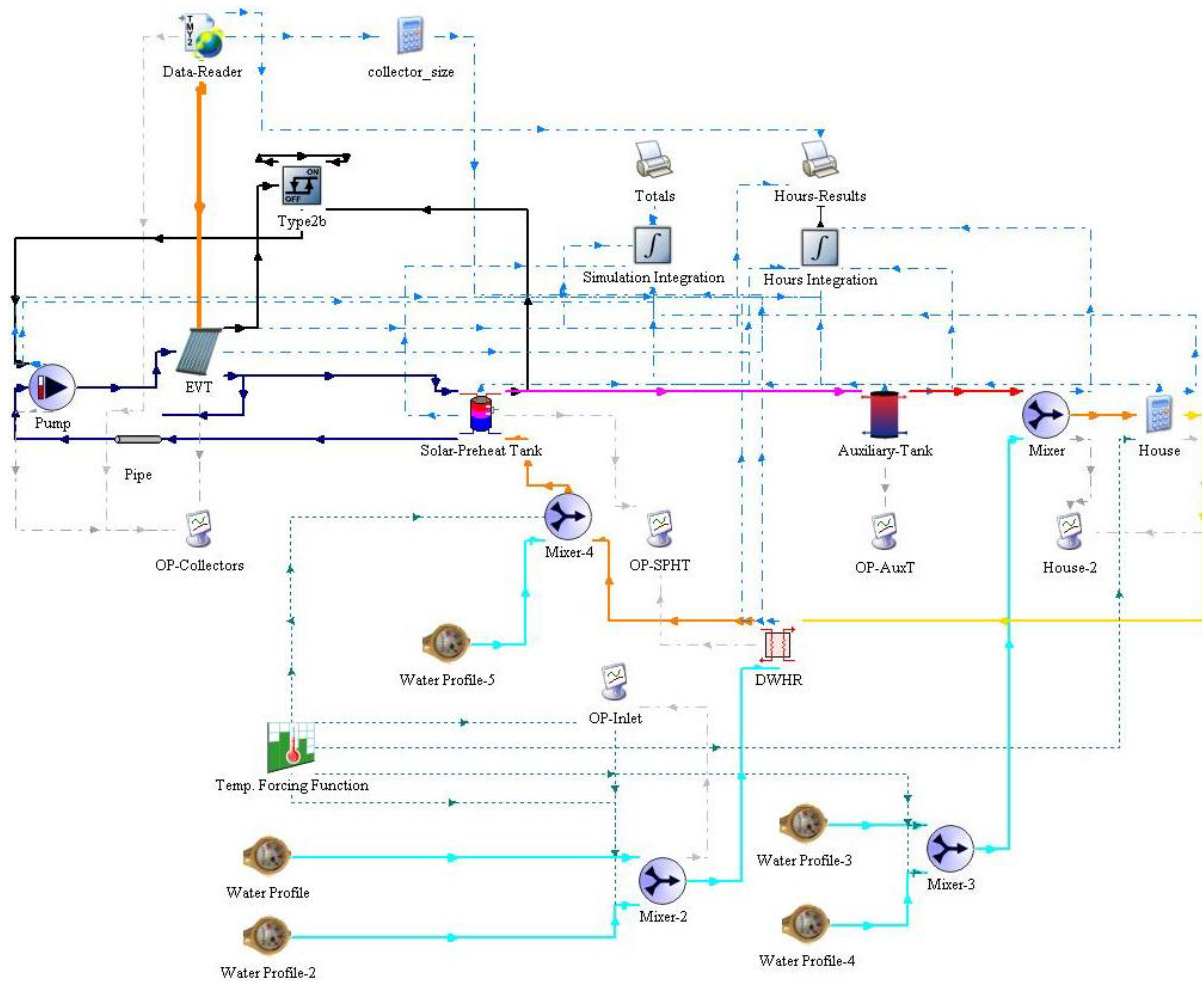


Figure 7-1: TRNSYS model overview of SDWH system of House-B

- Solar Preheat Tank(s): The model used for the tank is Type 60t, and is assumed to be a stratified tank with a volume of 300 litres with two immersed heat exchangers. Both heat exchanger coils are 0.025 m in diameter. The upper heat exchanger area is 0.9 m² with 6 litres of liquid content and the lower one has an area of 1.5 m² with 10 litres of liquid content. The upper and lower heat exchanger coils of the tank in House-A are connected to the mini gas boiler and solar collector loop, respectively. The lower heat exchanger coil of the tank in House-B is connected to the solar collector loop, and it is assumed that no other auxiliary heating source is hooked up to the tank, via the upper coil.
- Solar Loop Circulation Pump(s): The pumps are used to circulate the propylene glycol solution within the solar loops. The model used is Type 110, which is a variable speed pump that is able to maintain any outlet mass flow rate between zero and a rated value. The rated flow rate for the pump is 120 kg/hr and the rated power is 50 W. A differential controller with hysteresis (Type 2b) is used to activate the pump. The pumps start to run when the temperature difference between the solar preheat tank sensors, located inside the lower heat exchanger coils and close to the outlet ports of the tanks, and the solar collectors' outlet, reaches 6.7°C and stops when the temperature difference is less than 4.5°C.
- DWHR: A new model, by modifying the existing counter-flow heat exchanger model, was created for the DWHRs used for the SDHW systems. DWHRs are assumed to be a counter flow heat exchanger. This model is based on the work done by Zaloum et al. (2007). According to their report, different DWHR units can be characterized by the NTU vs. flow rate curve due to the fact that the units flow rates, inlet and outlet temperatures are the most important variables in determining the performance of the units. The correlation is in the format shown in Equation (7-1):

From the actual data collected from the DWHR units at the site, the two coefficients for the NTU vs. flow rate correlation formula for different flow rates for simultaneous hot water draw events and with coil / drain water flow rate ratio of 0.8 (for all simultaneous water draw events), were determined to be:

= Drain water flow rate (lit/min)

$$A_1 = 3.166$$

$$A_2 = 0.66$$

Once the curve for the NTU is obtained, the units' effectiveness and heat transfer rate can be achieved, as shown in Chapter 6.

- Gas Boiler: The model used for this component is auxiliary heater Type 6. The maximum heating rate is set to 84000 kJ/hr. From the collected data, the average annual efficiency of 55.5% is used for the heater. The set point temperature for the hot water within the DWH loop, between the boiler and DHW tank, is set to 78°C.
- Auxiliary Tank (Electric heating backup tank): The tank is assumed to be a stratified tank with a volume of 184 litres. The tank is modelled by assuming that it consists of eight fully mixed equal volume segments with an equal height of 0.15 m. Each segment has an assigned node. The type used to model the tank is Type 4a with two electric resistance heating elements. The first element is located in the eighth node with node one being the top most node with a set point temperature of 52°C and a dead band of 5°C and with a maximum heating rate of 3000 W. The second element is located in the fourth node with a set point temperature of 60°C and a dead band of 5°C and with a maximum heating rate of 3000 W. It should be noted that node one is the top most node.
- Solar Thermal Collector(s): The model used for the flat plate collector is Type 1b. The aperture area of 2.32 m² is set for the collector area. Flow rate at test conditions is 0.02 kg/s-m². The values for the optical efficiency and thermal loss coefficients are input, were derived from experimental analysis (as specified in Table 6-7. The model used for the evacuated tube collector is Type71. The aperture area of 2.11 m² is set for the collector area. Flow rate at test conditions is 0.02 kg/s-m². The values for the optical efficiency and thermal loss coefficients are again input, as specified in Table 6-7. Unlike Type1b, Type 71 needs an external file for the IAM data. Total number of 7 data points for the IAM for transverse and longitudinal directions are selected.

The same water draw profile of 225 lit/day, as shown in Figure 6-4 for high resolution daily hot water draw, and the end use hot water temperature of 43 °C that has been implemented in the TRCA archetype houses is used in the two TRNSYS models. The average monthly water temperatures are also the measured values from the twin houses water mains. The TRNSYS models performances must be validated first, and it is only then that they can be used to predict the energy consumption / producing of such systems and their components in other locations, with different weather data and monthly water mains temperatures.

7.2. House-A SDWH System

The thermal energy output results from flat plate solar thermal collector in TRNSYS model is compared with the experimental thermal energy output data, as seen in Figure 7-2. It can be concluded from Figure 7-2 that TRNSYS model's thermal energy output prediction is quite close to experimental results.

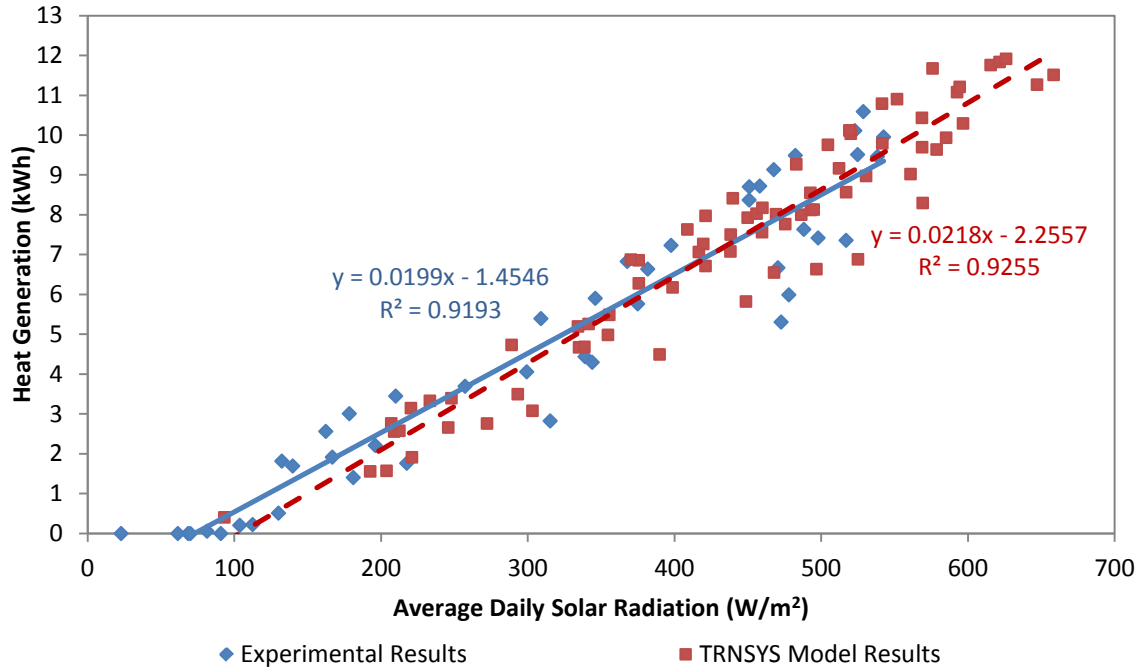


Figure 7-2: Comparison of experimental and TRNSYS model thermal energy output of flat plate solar thermal collector

The sum of the annual thermal energy output from TRNSYS model and experimental data is 2012.5 kWh and 2038.1 kWh, respectively which shows an approximate difference of 1.3%. Figure 7-3 shows the flat plate collector's monthly thermal energy output comparison of the TRNSYS model and the experimental data.

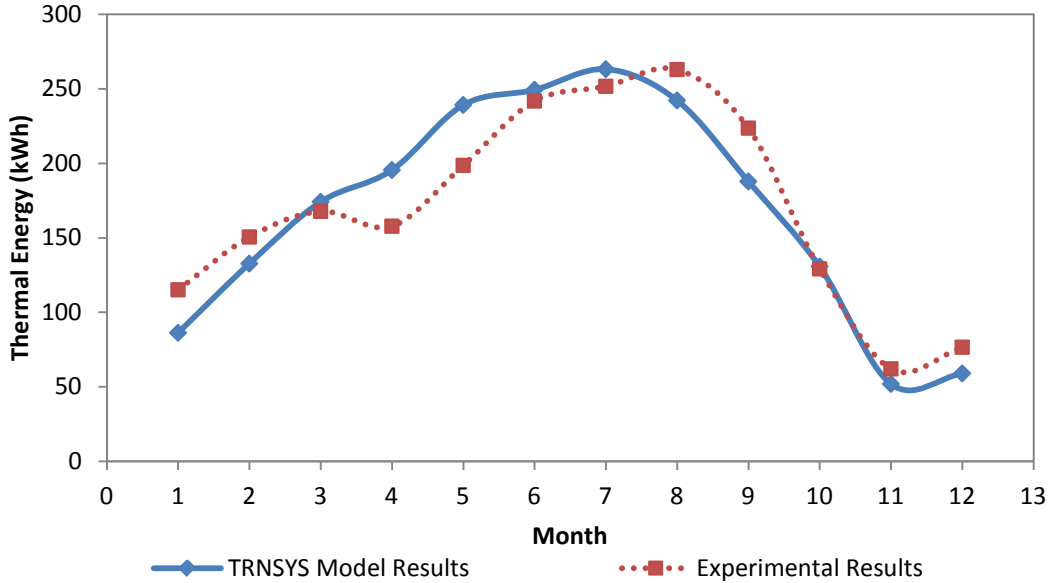


Figure 7-3: Monthly thermal energy output of flat plate collector from experimental data and TRNSYS model

As seen in Figure 7-3, there are differences in monthly thermal energy outputs, obtained from the two series, with major differences for the months of April, May, August and September. The reason for this is that the weather data file of TRNSYS has the average data, obtained over thirty years, and the simulation results might vary from the experimental, under severe weather conditions. Figure 7-4 illustrates the monthly heat recovery by the DWHR unit from the experimental data and TRNSYS model.

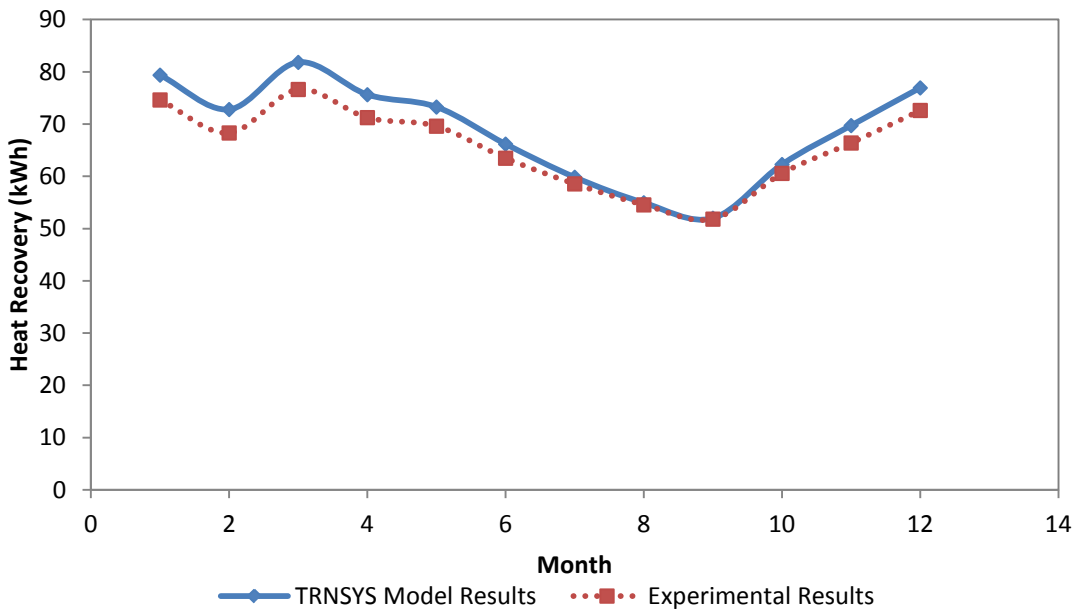


Figure 7-4: Monthly heat recovery by DWHR from experimental data and TRNSYS model

The annual heat recovery by the unit from TRNSYS model and experimental is 824.9 kWh and 788.5 kWh, respectively. This shows a 4.6% difference for the annual heat recovery from the two approaches.

Table 7-1 lists the annual energy consumption by the gas boiler, heat generation by the flat plate solar thermal collector and heat recovery by the DWHR unit, from both TRNSYS model and the experimental data.

Table 7-1: Comparison of the annual performance of the SDWH system's components of House-A

	Heat Generation by Flat Plate Solar Collector (kWh)	Energy Consumption by Mini Gas Boiler (kWh)	Heat Recovery by DWHR (kWh)
Experimental Data	2038.12	3718.69	788.54
TRNSYS Model	2012.45	3690.50	824.87
Percentage Difference (%)	1.3	0.8	4.6

7.3. House-B SDWH System

The TRNSYS model performance of House-B is also validated with the thermal energy output experimental data, as seen in Figure 7-5.

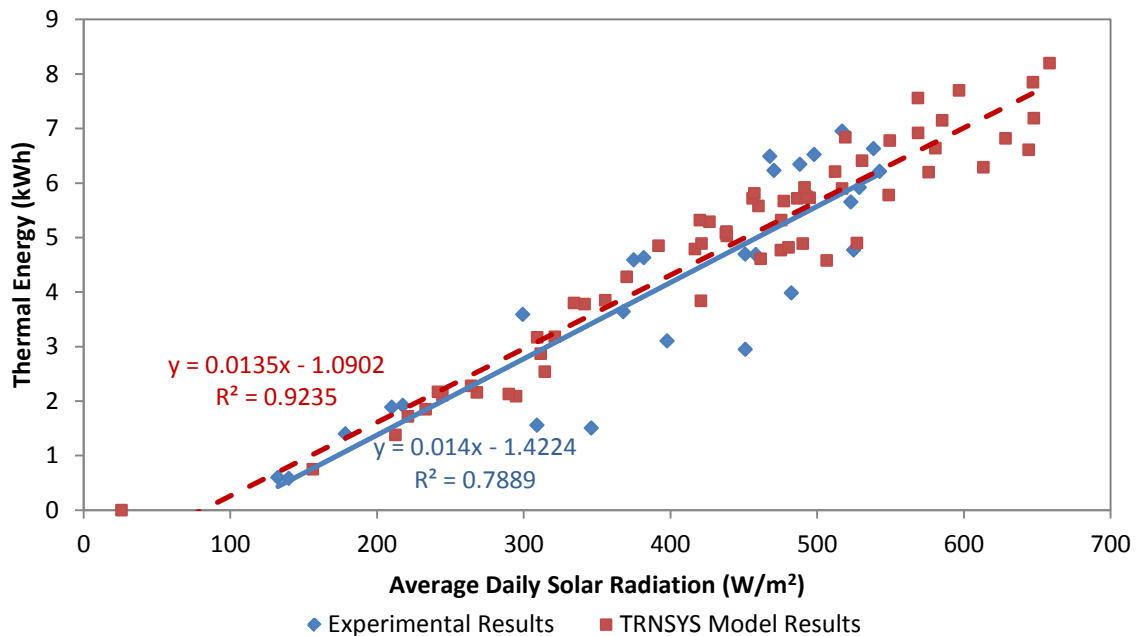


Figure 7-5: Comparison of experimental and TRNSYS model thermal energy output of evacuated tube solar thermal collector

Figure 7-6 shows the evacuated tube collector’s monthly thermal energy output comparison of the TRNSYS model and the experimental data.

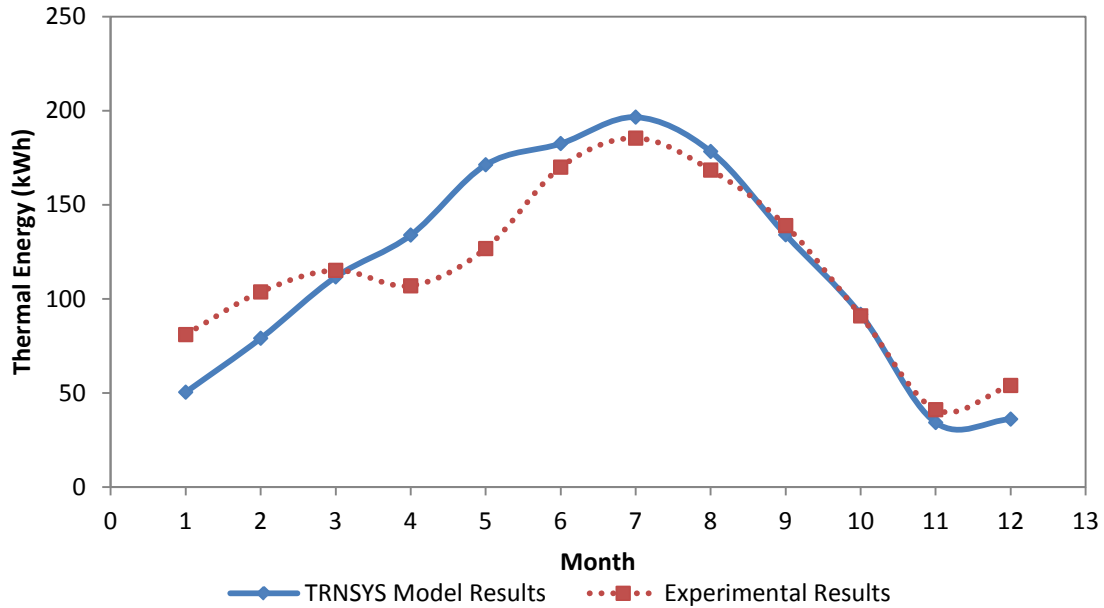


Figure 7-6: Monthly thermal energy output of evacuated tube collector from experimental data and TRNSYS model

The annual thermal energy output for the TRNSYS model and experimental data are 1400.8 kWh and 1383 kWh, respectively which shows a difference of 1.3%. As seen in this figure, there are differences in monthly thermal energy outputs, obtained from the two series, with major differences for the months of January, February, April and May.

The annual energy consumption by the electric backup tank, heat generation by the evacuated tube solar thermal collector and heat recovery by the DWHR unit, from both TRNSYS model and the experimental data are listed in Table 7-2. It should be mentioned the solar loop pump of House-A’s SDHW system energy consumption from experimental data and TRNSYS model are 142.4 kWh and 148.5 kWh, respectively. Similarly, energy consumption of House-B’s SDHW system solar loop pump from experimental data and TRNSYS model are 174.3 kWh and 180.6 kWh, respectively.

Table 7-2: Comparison of the annual performance of the SDWH system's components of House-B

	Heat Generation by Evacuated Tube Solar Collector (kWh)	Energy Consumption by Electric Backup Tank (kWh)	Heat Recovery by DWHR (kWh)
Experimental Data	1383.02	2777.92	788.54
TRNSYS Model	1400.76	2713.52	824.87
Percentage Difference (%)	1.3	2.3	4.6

7.4. SDWH Systems Performance in Major Canadian Cities

Now that the two SDWH systems performance are validated, the two models can be used to investigate the performance of such systems in five major Canadian cities, including: Toronto, Montreal, Halifax, Edmonton and Vancouver. TRNSYS simulations of the two systems are performed, using the weather data files for the six mentioned cities, from the weather data files of TRNSYS. The average water mains temperatures should also be implemented in the models. There is no documented data on the average monthly water mains temperatures for Canadian cities. Average monthly inlet water temperature has been compiled for different American cities, with regards to the average monthly ambient temperatures (NAHB Research Center, 2002). Using the average monthly ambient temperature for five major Canadian cities, from national climate data and information archive (Environment Canada, 2000) as input, the average monthly water mains temperatures for these cities were obtained Figure 7-7 displays the average monthly water mains temperature variations for the five major cities mentioned above.

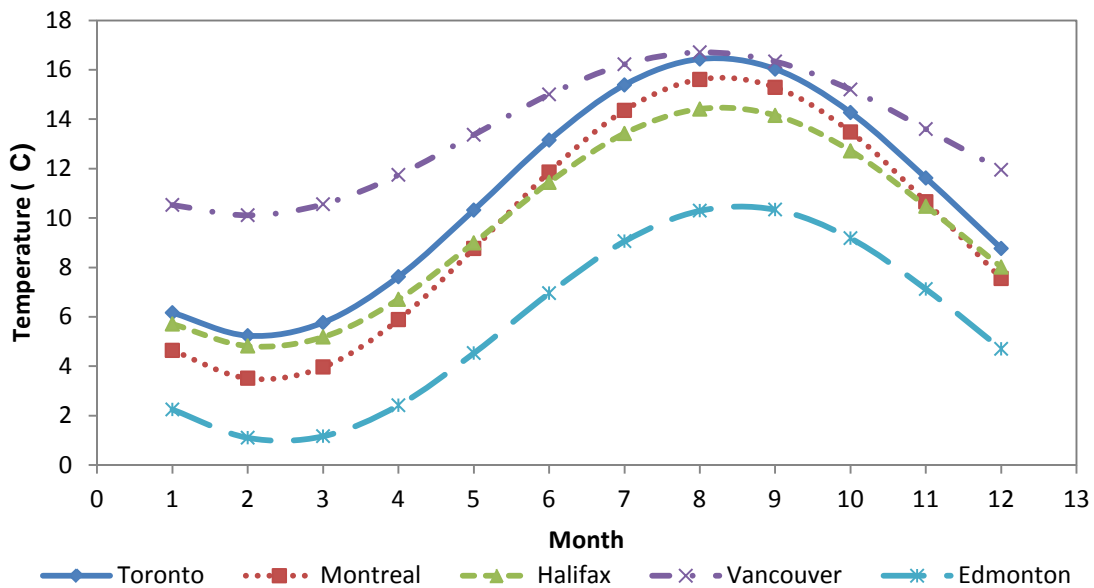


Figure 7-7: Monthly water mains temperatures for six Canadian major cities

The summary of the annual thermal energy production by the conventional and renewable heating sources, and the heat recovery by the DWHRs for the two SDWH systems are listed in Table 7-3 and Table 7-4. It should be noted that the base case, without DWHR and flat plate solar thermal collector for the system in House-A and without DWHR and evacuated tube collector for the system in House-B, would be 5468 kWh and 4452 kWh, respectively.

Table 7-3: Annual performance of the House-A, SDWH system's components in different Canadian cities

City	Heat Generation by Flat Plate Solar Collector (kWh)	Energy Consumption by Mini Gas Boiler (kWh)	Heat Recovery by DWHR (kWh)
Toronto, ON	2011	3637	793
Montreal, QC	1970	3618	829
Halifax, NS	1878	3491	828
Vancouver, BC	1818	3564	720
Edmonton, AB	2039	3763	941

Table 7-4: Annual performance of the House-B, SDWH system's components in different Canadian cities

City	Heat Generation by Evacuated Tube Solar Collector (kWh)	Energy Consumption by Electric Backup Tank (kWh)	Heat Recovery by DWHR (kWh)
Toronto, ON	1391	2681	793
Montreal, QC	1351	2748	829
Halifax, NS	1286	2784	828
Vancouver, BC	1249	2681	720
Edmonton, AB	1402	2853	941

The maximum values for each category of the two SDWH systems are also highlighted. For both systems, city of Edmonton has the highest values for energy consumptions by the gas boiler and the electric backup tank and heat recovery by the DWHRs, which are due to colder monthly ambient temperatures and lower water mains temperatures, as seen in Figure 7-7.

Using the average efficiencies of 55.5% and 78.8% for the gas boiler and electric backup tank, the annual operational cost / savings, for providing 225 lit/day of DHW with the end use water temperature of 43°C from different components of the two SDWH systems are tabulated in Table 7-5 and Table 7-6. The annual cost / savings for the SDWH system of House-A are based on the 2010 average natural gas rate for the residential sector of different provinces (Statistics Canada, 2011), as defined in Table 7-5.

Table 7-5: Annual cost / savings by House-A SDWH system's components in different Canadian cities

City	Cost of Natural Gas per m ³ (¢)	Savings by Flat Plate Solar Collector (\$)	Cost of Energy Consumption by Mini Gas Boiler (\$)	Savings From Heat Recovery by DWHR (\$)
Toronto, ON	45.75	161.12	161.73	63.52
Montreal, QC	57.70	199.04	202.91	83.76
Halifax, NS	N/A*	—	—	—
Vancouver, BC	50.20	159.81	93.04	63.33
Edmonton, AB	26.86	95.94	98.26	44.26

* Natural gas is not available for Atlantic Canada, including the province of Nova Scotia.

Based on the results from Table 7-5, with the SDWH system of House-A, the city with the minimum fuel cost would be Vancouver. The highest savings by the flat plate solar thermal collector and DWHR system happen in Montreal.

The annual cost / savings for the SDWH system of House-B are based on the 2009 average electricity rate for the residential sector of different provinces (London Economics LLD, 2011), as defined in Table 7-6.

Table 7-6: Annual cost / savings by House-B SDWH system's components in different Canadian cities

City	Cost of Electricity per kWh (¢)	Savings by Evacuated Tube Solar Collector (\$)	Cost of Energy Consumption by Electric Backup Tank (\$)	Savings from Heat Recovery by DWHR (\$)
Toronto, ON	13.6	240.00	364.68	136.82
Montreal, QC	6.6	113.18	181.38	69.43
Halifax, NS	11.8	192.51	328.46	124.05
Vancouver, BC	6.5	103.06	174.29	59.42
Edmonton, AB	12.9	229.47	368.02	154.02

Based on the results from Table 7-6, with the SDWH system of House-B, the city with the minimum fuel cost would be Vancouver again. The highest savings by the evacuated tube solar thermal collector and DWHR system happen in Toronto and Edmonton, respectively.

The annual GHG emissions from the two systems and the GHG savings from the renewable energy components are also tabulated in Table 7-7 and Table 7-8. With the 2009 GHG emission factors per kilogram equivalent CO₂ for natural gas known (Environment Canada, 2011), the annual GHG emissions and the overall savings in GHG emissions from different components of the SDWH system of House-A will be as shown in Table 7-7.

Table 7-7: Annual GHG emission by House-A SDWH system's components in different Canadian cities

City	GHG Emission Factor per m ³ (kg)	GHG Emission Savings by Flat Plate Solar Collector (kg)	GHG Emission by Mini Gas Boiler (kg)	GHG Emission Savings by DWHR (kg)
Toronto, ON	1.879	661.73	664.24	260.89
Montreal, QC	1.878	647.84	660.42	272.63
Halifax, NS	1.891	622.01	641.75	274.35
Vancouver, BC	1.916	609.97	663.71	241.71
Edmonton, AB	1.918	685.06	701.61	316.03

Based on the results from Table 7-7, with the SDWH system of House-A, the city with the minimum GHG emissions would be Halifax. The city with the highest savings in GHG emissions from the flat plate solar collector and DWHR system would be Edmonton.

Using the 2009 GHG emission factors per kilogram equivalent CO₂ for electricity (Environment Canada, 2011), the annual GHG emissions and the overall savings in GHG emissions from different components of the SDWH system of House-B will be as shown in Table 7-8.

Table 7-8: Annual GHG emission by House-B SDWH system's components in different Canadian cities

City	GHG Emission factor per kWh (kg)	GHG Emission Savings by Evacuated Tube Solar Collector (kg)	GHG Emission by Electric Backup Tank (kg)	GHG Emission Savings by DWHR (kg)
Toronto, ON	0.160	282.35	429.04	160.97
Montreal, QC	0.002	3.43	5.50	2.10
Halifax, NS	0.784	1279.07	2182.30	824.18
Vancouver, BC	0.015	23.78	40.22	13.71
Edmonton, AB	0.880	1565.36	2510.53	1050.66

Based on the results from Table 7-8, with the SDWH system of House-B, the city with the minimum GHG emissions would be Montreal. The city with the highest savings in GHG emissions, from the evacuated tube solar collector and DWHR system would be Edmonton.

The best and worst cases for using the two SDWH systems can now be determined. With respect to the SDWH system of House-A (natural gas), It is clear from Table 7-5 and Table 7-7 that the worst performance, with regards to annual fuel costs and GHG emissions, are Montreal and Edmonton, respectively. With the high cost of natural gas in Montreal, the use of this system

would be most advantageous. This can be clearly seen in Figure 7-5, which shows highest savings from the flat plate solar collector and DWHR occur in Montreal.

With respect to the SDWH system of House-B (electricity) and from the results from Table 7-6 and Table 7-8, the worst performance, with regards to annual fuel costs and GHG emissions, happens in Edmonton. The best city for using such system is Toronto, which shows the highest savings by the evacuated tube solar collector and second best savings by the DWHR. In addition, Toronto also shows relatively low annual GHG emission by the electric backup tank.

Chapter 8 : Author's Contribution and Conclusion

This thesis project is based on the performance analysis of two solar domestic water heating systems are part of the twin sustainable Archetype houses built at Kortright Conservation Centre of Toronto and Region Conservation Authority (TRCA) in Vaughan, Ontario, Canada. In this regard, the author has finished the following activities:

- Validating the collected data from all related sensors, through cross-checking and performing calibration, if required.
- Implementing the high resolution hot water draw profile for the two houses, installing the two sets of solenoid valves for dumping water, adjusting the flow rates for each valve (total of 6 valves in each house).
- Thermal performance analysis of all the related components of the two SDHW systems, and comparing the results with the manufacturer's data (where applicable) and available publications.
- Obtaining the whole year performance and benefits of the two SDHW systems and their individual components in reducing the annual energy demand, cost and GHG emissions
- Creating TRNSYS models of the two systems and validating the results with the experimental data. Using the two models as a tool to obtain the benefits from such system in major Canadian cities.

8.1. Conclusions

Domestic water heating is estimated to be the second largest energy end-use for Canadian households, which accounts for about 18% of total residential sector energy consumption. Therefore, any effort in reducing the energy required for DHW producing is significant. The focus of this study was on investigating the performance of the two SDHW systems of the two Sustainable Archetype Houses, located at Kortright Center in Vaughan, Ontario and developing the TRNSYS models of the two systems in order to investigate the benefits of such systems in other major Canadian cities. The two houses are equipped with a comprehensive energy monitoring system to monitor the thermal performance of the twin houses and to investigate the effectiveness and efficiency of the mechanical systems used. The DHW system of House A consists of a flat plate solar collector in conjunction with a back-up mini gas boiler and a DWHR

unit, whereas the system of House B consists of an evacuated tube solar collector in conjunction with an electric water heater and a DWHR unit. The daily hot water draw schedule of 225 litres was also implemented in both houses. The hot water draw profile used in this study is the 5-second-water-draw profile based on the IEA Annex 42 schedule by the International Energy Agency and several other researches on the daily hot water consumption of Canadian households. It should be stated that about 180 litres of the daily hot water draw is used for simultaneous hot water draw events and this is when the DWHRs are capable of heat recovering. Investigating the performance of different components of the two SDHW systems were performed in two testing periods, one in summer and one in winter.

The effects of various factors on the performance and effectiveness of the DWHRs were investigated. It was shown that the cold side fresh inlet and inlet drain water temperatures do not change the effectiveness of the units, however colder fresh inlet water and warmer drain water would increase the heat recovery rate of the units. It was also concluded from the experimental data the most important factors, affecting the effectiveness of the DWHRs are the drain water flow rate and coil / drain water flow rate ratio; lower drain flow rates and smaller values for coil / drain flow rate ratio would lead to higher effectiveness of the units. The experimental results also showed that DWHRs can have an effectiveness of 50% and 55% for shower events with drain water flow rate of 7.2 l/min and sink usages with drain water flow rate of 4.5 l/min. By extrapolating the heat recovery values by the DWHRs during the two testing periods to a whole year performance of the units, it was concluded that DWHRs are capable of an annual heat recovery of 788.5 kWh. With the overall efficiency of 79% for the electric backup tank in House-B, the addition of the DWHR system with similar installation configuration and water draw conditions would result in annual cost savings and GHG emissions reduction of \$107 and 126.2 kg, respectively. Similarly, with the overall efficiency of 56% for the gas boiler in House-A, the addition of the DWHR system would result in annual cost savings and GHG emissions reduction of \$35 and 144 kg, respectively. With the DWHR unit's purchase and installation cost of \$600, the payback period for using this unit with similar electric backup tanks and gas boilers would be 5.6 and 17 years, respectively. This clearly shows that DWHRs are more advantageous in energy cost savings and have the shortest payback period, when used in a DHW system that utilizes and electric tank as the heating source. The NTU vs. drain flow rate relation was also derived for both DWHRs which were later used as input for the parameters of the developed

TRNSYS model of the DWHRs. It should also be mentioned that the two DWHRs piping set up is in a way that they preheat the water going to hot water taps which is not the best configuration. DWHRs are more beneficial, when they preheat all water going to both cold and hot water taps. From extrapolation the heat generation values by the two solar thermal collectors during the two testing periods, it was also concluded that the flat plate and evacuated tube solar collectors can generate 2038 kWh and 1383 kWh of heat, annually. This clearly shows that unlike general belief that evacuated tube solar thermal collectors have a better performance, compared to the flat plate collectors, the flat plate solar thermal collector in House-A has 32% more thermal energy output more than the evacuated tube collector. The efficiency versus reduced temperature difference of the two solar collectors was compared with manufacturer's data. It was also shown that for both collectors and during both testing periods, the efficiency decreases with the increase of reduced temperature difference, which is due to decrease in the ambient temperatures or lower solar irradiance on the collector surface which by itself is the result of low sun radiation availability or collectors' surface being covered by snow. Although the flat plate solar collector efficiencies from experimental data showed better correlation with the manufacturer's data, but the experimental efficiencies were shown to be always lower, compared to the manufacturer data. This is mainly due to the fact that the manufacturer's curve is obtained under controlled operating conditions, and the collector's inlet and outlet temperature are measured exactly at the inlet and outlet point of the collectors; whereas in the case of the two collectors in the Archetype houses, the two temperatures are measured at the inlet and outlet of the DHW tanks and temperature drops certainly occurs due to thermal losses from the solar loops' piping systems. It was also shown that the evacuated tube collector had a disappointing performance in the winter testing period, with the efficiency of 21%, compared to the 39.5% efficiency of the flat plate collector. The main reasons for this was due to three damaged tubes due to the damages to their vacuum seals and surface of the collector's tubes being covered by snow/ice for longer periods due to the geometry of the collector and high thermal insulation of the tubes. Both collectors have higher efficiencies during summer, with 52.8% and 34.5% efficiency for the flat plate and evacuated tube solar collector, respectively.

The electric backup tank and gas boiler showed to have an average efficiency of 79% and 56%, respectively. The efficiency of the electric tank can be increased by installing a one way valve on

the outlet port of the tank. The low efficiency of the gas boiler is due to the high capacity of it. This boiler is mainly intended for space heating purposes.

The two systems were modeled in TRNSYS and were validated with the experimental results. The models were then used to simulate the performance and obtain the benefits from these systems in reducing annual energy demand, cost and GHG emissions in five major Canadian cities. The simulated results for the base case models (without DWHRs and solar thermal collectors) of the two houses showed that the energy consumption by the gas boiler and electric backup tank would be 5468 kWh and 4452 kWh, respectively. This shows that the addition of the DWHR and the flat plate solar thermal collector would result in 1777 kWh of annual energy saving. Similarly, the addition of the DWHR and the evacuated tube collector would result in an annual energy saving of 1738 kWh.

The simulated results of the two systems for Canadian major cities showed that the city of Edmonton has the highest annual energy consumption by the gas boiler and the electric backup tank with 3763.4 kWh and 2852.9 kWh, respectively. The highest annual fuel cost for DHW production, with SDHW system of House-A was \$202.9 for Montreal. The highest savings in costs by the flat plate solar collector and DWHR unit with this system occur in Montreal too. The highest savings in annual GHG emissions by the flat plate solar collector and DWHR of House-A SDHW system were for the city of Edmonton. The highest annual fuel cost for DHW production, with SDHW system of House-B was concluded to be \$368.0 for Edmonton. The highest savings in costs by the evacuated tube solar collector and DWHR unit occur in Toronto and Edmonton, respectively. The highest savings in annual GHG emissions, by using House-B SDHW system, and by the evacuated tube solar collector and DWHR were also found to be for the city of Edmonton.

8.2. Recommendations

Following recommendations are made for improving the performance of the SDHW systems and future researches:

- The water supply to the houses has constant pressure changes. It is strongly recommended that the supply water pressure be kept constant by adding a separate boosting pump on the main supply line of the two houses.

- It is also beneficial to obtain the pressure drops of the supply water when passed through the wrapping coils of the DWHR systems. This can be done by installing two pressure gauges on the DWHRs cold side inlet and outlet.
- The piping configurations of the two DWHRs are not the most advantageous configuration. DWHRs can be more beneficial when they are configured in a way that they preheat all incoming water supply of the house, going to both cold and hot water taps. It would be interesting to see how much savings can be achieved, if the piping configurations of the two DWHRs are changed.
- The electric tank in House-B was shown to have the average efficiency of 79%. There are thermal energy losses from the outlet port and expansion tank of the electric tank due to lack of a one way valve. It is strongly recommended that this valve be installed and the differences in electricity consumptions be investigated.
- It is also recommended that the inclination angle of the evacuated tube solar thermal collector be increased and the thermal energy output during colder months be investigated. This has two advantages: 1- more heat can be absorbed by the collector during periods with smaller solar incidence angles and 2- there would be a lesser chance of snow and ice getting stuck in between the tubes.
- It is also recommended that two sets of temperature sensors be installed on the inlet and outlet points of both solar thermal collectors. With these sensors in place, the thermal losses from the solar piping loops can be obtained.
- The gas boiler in House-A was shown to have a low average efficiency. This is due to the fact that the boiler has a high capacity and is mainly intended for space heating purposes. It is recommended that the boiler be simultaneously used for space heating and water heating and the overall performance of the boiler be then investigated.

Appendix A: Sensor address, list, type and location

There are almost 300 sensors are installed in this monitoring system.. Figures A.1 and Figure A.2 show the DAQ infrastructure in House-A and House-B. Table A.1 and Table A.2 show sensor address, type and location.

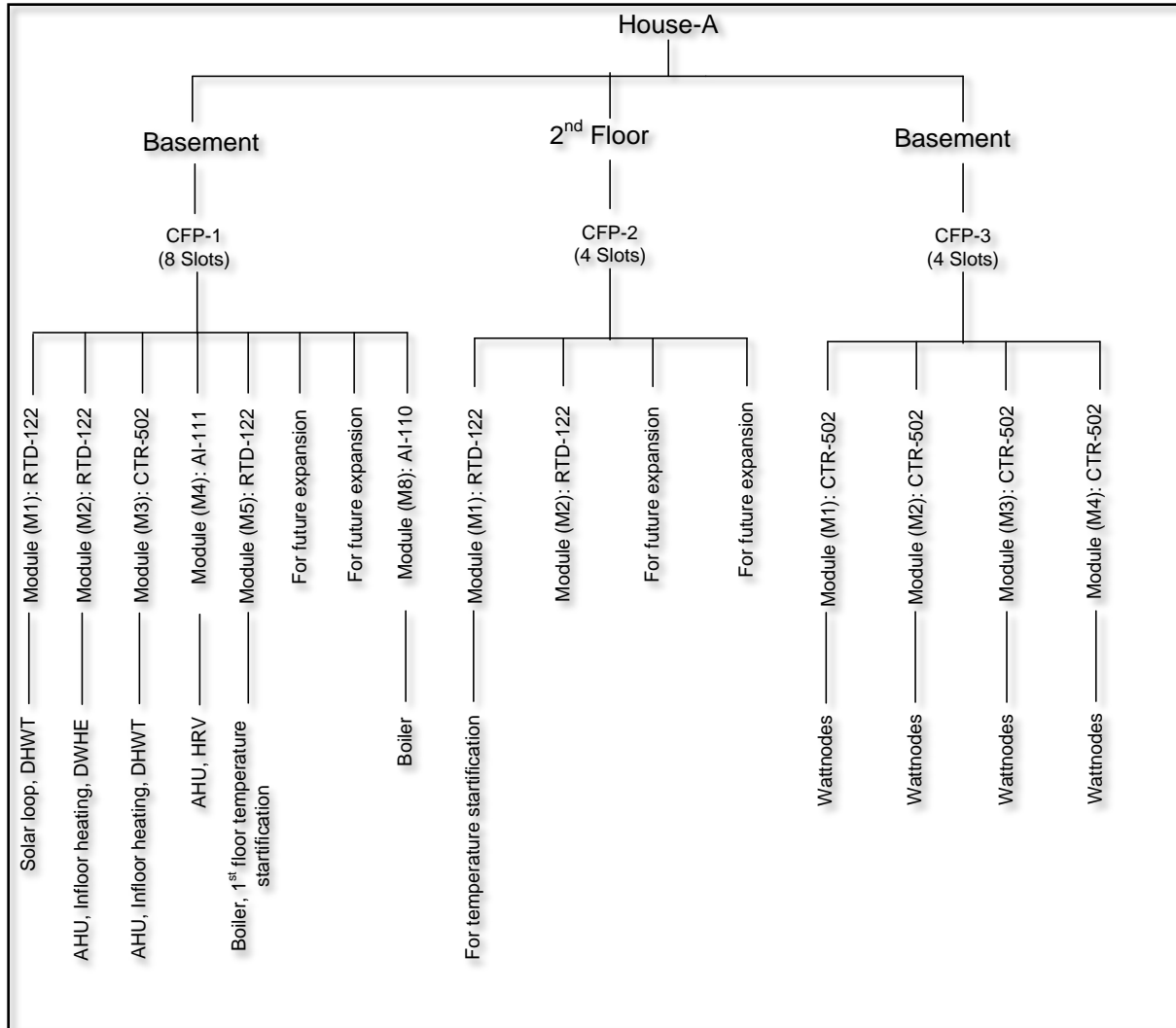


Figure A. 1: DAQ infrastructure in House-A

Table A.1: Nomenclature of Sensors, Channels, Modules and Compact field point of DAQ systems in House-A

Module: RTD-122 (Output signal: RTD)				
Address of sensors	Sensors	Sensors type	Location	Status
A-CFP1-M1-CH1	T1	Pt. 100	Un-tempered water	Installed
A-CFP1-M1-CH2	T4	Pt. 100	Tempered water line	Installed
A-CFP1-M1-CH3	T5	Pt. 500	Solar collector supply	Installed
A-CFP1-M1-CH4	T6	Pt. 500	Solar collector return	Installed
A-CFP1-M1-CH5	T19	Pt. 100	Recirculation of DHWT	Not installed
A-CFP1-M1-CH6	T7	Pt. 500	DHWT return from boiler	Installed
A-CFP1-M1-CH7	T8	Pt. 500	DHWT supply to Boiler	Installed
A-CFP1-M1-CH8	T3	Pt. 100	City water to DHWT	Installed

Module: RTD-122 (Output signal: RTD)				
Address of sensors	Sensors	Sensors type	Location	Status
A-CFP1-M2-CH1	T12	Pt. 100	Infloor heating supply	Installed
A-CFP1-M2-CH2	T14	Pt. 100	Infloor heating return	Installed
A-CFP1-M2-CH3	T11	Pt. 100	Boiler return from A-AHU	Installed
A-CFP1-M2-CH4	T18	Pt. 100	Boiler supply to A-AHU	Installed
A-CFP1-M2-CH5	T13	Pt. 100 (SM)	Drain water to GWHE	Installed
A-CFP1-M2-CH6	T17	Pt. 100 (SM)	Drain water from GWHE	Installed
A-CFP1-M2-CH7	T15	Pt. 500	City water to GWHE	Installed
A-CFP1-M2-CH8	T16	Pt. 500	Water from DGWHE	Installed

Module: CTR-502 (Output signal: Pulse)				
Address of sensors	Sensors	Sensors type	Location	Status
A-CFP1-M3-CH1	FL11	Flow rate	From GWHE to Tempering Valve	Installed
A-CFP1-M3-CH2	FL10	Flow rate	Tempered water	Installed
A-CFP1-M3-CH3	FL6	Flow rate	Recirculation water to DHWT	Installed
A-CFP1-M3-CH4	FL1	Flow rate	Solar collector return	Installed
A-CFP1-M3-CH5	FL2	Flow rate	City Water Line of House-A	Installed
A-CFP1-M3-CH6	FL3	Flow rate	From GWHE to DHWT	Installed
A-CFP1-M3-CH7	FL8	Flow rate	Boiler to infloor heating	Installed
A-CFP1-M3-CH8	FL9	Flow rate	Boiler to A-AHU	Installed

Module: AI-111 (Output signal: mA)				
Address of sensors	Sensors	Sensors type	Location	Status
A-CFP1-M4-CH1	RH8	Relative Humidity	Fresh air from Outdoor to HRV	Installed
A-CFP1-M4-CH2	AT8	Air Temp.		
A-CFP1-M4-CH3	RH9	Relative Humidity	Exhaust air from HRV to outdoor	Installed
A-CFP1-M4-CH4	AT9	Air Temp.		
A-CFP1-M4-CH5	RH10	Relative Humidity	Return air from zone to HRV	Installed
A-CFP1-M4-CH6	AT10	Air Temp.		

A-CFP1-M4-CH7	RH11	Relative Humidity	Supply air from HRV to zone	Installed
A-CFP1-M4-CH8	AT11	Air Temp.		
A-CFP1-M4-CH9	RH12	Relative Humidity	Main return air from zone to AHU	Installed
A-CFP1-M4-CH10	AT12	Air Temp.		
A-CFP1-M4-CH11	RH7	Relative Humidity	Main supply air AHU to zone	Installed
A-CFP1-M4-CH12	AT7	Air Temp.		
A-CFP1-M4-CH13	AF8	Air Flow station	Fresh air from Outdoor to HRV	Installed
A-CFP1-M4-CH14	AF9	Air Flow station	Exhaust air from HRV to outdoor	Installed
A-CFP1-M4-CH15	AV1	Air Velocity Meter	Main supply air AHU to zone	Installed
A-CFP1-M4-CH16	AV2	Air Velocity Meter	Main return air from zone to AHU	Installed

Module: RTD-122 (Output signal: RTD)

Address of sensors	Sensors	Sensors type	Location	Status
A-CFP1-M5-CH1	T9	Pt. 500	Boiler Loop Supply (Hot side)	Installed
A-CFP1-M5-CH2	T10	Pt. 500	Boiler Loop Return (Cold side)	Installed
A-CFP1-M5-CH3	T20	Pt. 100 (SM)	Flue gas from Boiler	Installed

Module: DO-410 (Digital control)

Address	Sensors	Sensors type	Location	Status
A-CFP1-M7-CH1	C1	Solenoid valve	Simulated water draw profile	GS
A-CFP1-M7-CH2	C2	Solenoid valve	Simulated water draw profile	GS
A-CFP1-M7-CH3	C3	Solenoid valve	Simulated water draw profile	GS
A-CFP1-M7-CH4	H1	Solenoid valve	Simulated water draw profile	GS
A-CFP1-M7-CH5	H2	Solenoid valve	Simulated water draw profile	GS
A-CFP1-M7-CH6	H3	Solenoid valve	Simulated water draw profile	GS
A-CFP1-M7-CH7				
A-CFP1-M7-CH8				

Module: AI-110 (Output signal: mA or mV)

Address of sensors	Sensors	Sensors type	Location	Status
A-CFP1-M8-CH1	NG1	Gas meter	Boiler	Installed
A-CFP1-M8-CH2	FL4	Flow rate (Proteus)	DHWT of Boiler loop	Installed
A-CFP1-M8-CH3	FL5	Flow rate (Proteus)	Boiler loop	Installed
A-CFP1-M8-CH4				
A-CFP1-M8-CH5				
A-CFP1-M8-CH6				
A-CFP1-M8-CH7				

A-CFP1-M8-CH8				
---------------	--	--	--	--

Module: RTD-122 (Output signal: RTD)

Address of sensors	Sensors	Sensors type	Location	Status
A-CFP2-M1-CH1	***	Pt. 100 (SM)	2 nd floor room temperature at 2' height	Installed
A-CFP2-M1-CH2	***	Pt. 100 (SM)	2 nd floor room temperature at 4' height	Installed
A-CFP2-M1-CH3	***	Pt. 100 (SM)	2 nd floor room temperature at 6' height	Installed
A-CFP2-M1-CH4	***	Pt. 100 (SM)	2 nd floor room temperature at 8' height	Installed
A-CFP2-M1-CH5				
A-CFP2-M1-CH6				
A-CFP2-M1-CH7				
A-CFP2-M1-CH8				

Module: CTR-502 (Output signal: Pulse), Sensors type: Watt-node

Address of sensors	Sensors	Location and CT size	Status
A-CFP3-M1-CH1	4-P3-2	HRV fan: 5 Amps	GS
A-CFP3-M1-CH2	2-P3-2	AHU hot water circulation pump: 5 Amps	GS
A-CFP3-M1-CH3	3-P-1	Two stage ASHP: 30 Amps	GS
A-CFP3-M1-CH4	4-P3-1	Boiler: 5 Amps	GS
A-CFP3-M1-CH5	2-P3-3	Boiler primary loop circulation pump: 5 Amps	GS
A-CFP3-M1-CH6	2-P3-1	DHW storage tank circulation pump: 5 Amps	GS
A-CFP3-M1-CH7	1-PV-3	Panel board receptacles, data logging: 15 Amps Data receptacles 1 st floor, broom closet: 15 Amps Data receptacles 2 nd floor, east bedroom closet: 15 Amps Data receptacles, attic, east wall: 15 Amps EXIT sign: 15 Amps and emergency lights: 15 Amps	GS
A-CFP3-M1-CH8	5-P3-1	Infloor heating circulation pump: 5 Amps	GS

Module: CTR-502 (Output signal: Pulse), Sensors type: Watt-node

Address of sensors	Sensors	Location and CT size	Status
A-CFP3-M2-CH1	5-P3-2	Solar collector glycol loop: 5 Amps	GS
A-CFP3-M2-CH2	7-P3-3	BRAC Grey water unit: 15 Amps	GS
A-CFP3-M2-CH3	1-PV-1	Grid to house: 100 Amps	GS
A-CFP3-M2-CH4	8-P-1	Lights: 60 Amps	GS

		Lighting panel feed, Lighting panel contactor, Foyer, washroom, Kitchen, Dining area, Living room, Living room (future bed room), 2 nd floor hall, Master bed room, 2 nd floor bed, bath, closet, Attic, and basement.	
A-CFP3-M2-CH5	9-P3-2	Receptacles: 60 Amps GP indoor, Adaptable bedroom, 3 rd floor, Bedroom 2& 3, Master bedroom, 2 nd floor bathroom, 2 nd floor hallway, Living room, Foyer, 1 st floor bathroom, and smoke detector.	GS
A-CFP3-M2-CH6	5-P3-3	DHW load circulator: 5 Amps	GS
A-CFP3-M2-CH7			
A-CFP3-M2-CH8	6-P3-3	Infloor radiant heating pump: 5 Amps	GS

Module: CTR-502 (Output signal: Pulse), Sensors type: Watt-node

Address of sensors	Sensors	Location and CT size	Status
A-CFP3-M3-CH1	6-P-1	Sewerage pump: 15 Amps	GS
A-CFP3-M3-CH2	7-P3-1	Water softener: 15 Amps	GS
A-CFP3-M3-CH3	7-P3-2		GS
A-CFP3-M3-CH4	11-P-1	Kitchen receptacles: 20 Amps	GS
A-CFP3-M3-CH5	12-P1-1	Kitchen fan with light: 30 Amps Oven: 30 Amps Cook top: 30 Amps	GS
A-CFP3-M3-CH6	10-P3-3	Fridge: 15 Amps	GS
A-CFP3-M3-CH7	13-P3-1	Dishwasher: 15 Amps	GS
A-CFP3-M3-CH8	13-P3-2	Garage and outdoor receptacles: 15 Amps	GS

Module: CTR-502 (Output signal: Pulse), Sensors type: Watt-node

Address of sensors	Sensors	Location and CT size	Status
A-CFP3-M4-CH1	13-P3-3	Garage lights: 15 Amps and exterior lights: 15 Amps	GS
A-CFP3-M4-CH2	10-P3-2	Washing machine: 15 Amps	GS
A-CFP3-M4-CH3	14-P-1	Dryer: 30 Amps	GS
A-CFP3-M4-CH4	10-P3-1	AHU fan and heap filter fan: 15 Amps	GS
A-CFP3-M4-CH5	FL11	GWHE to the Tempering Valve	
A-CFP3-M4-CH6			
A-CFP3-M4-CH7			
A-CFP3-M4-CH8			

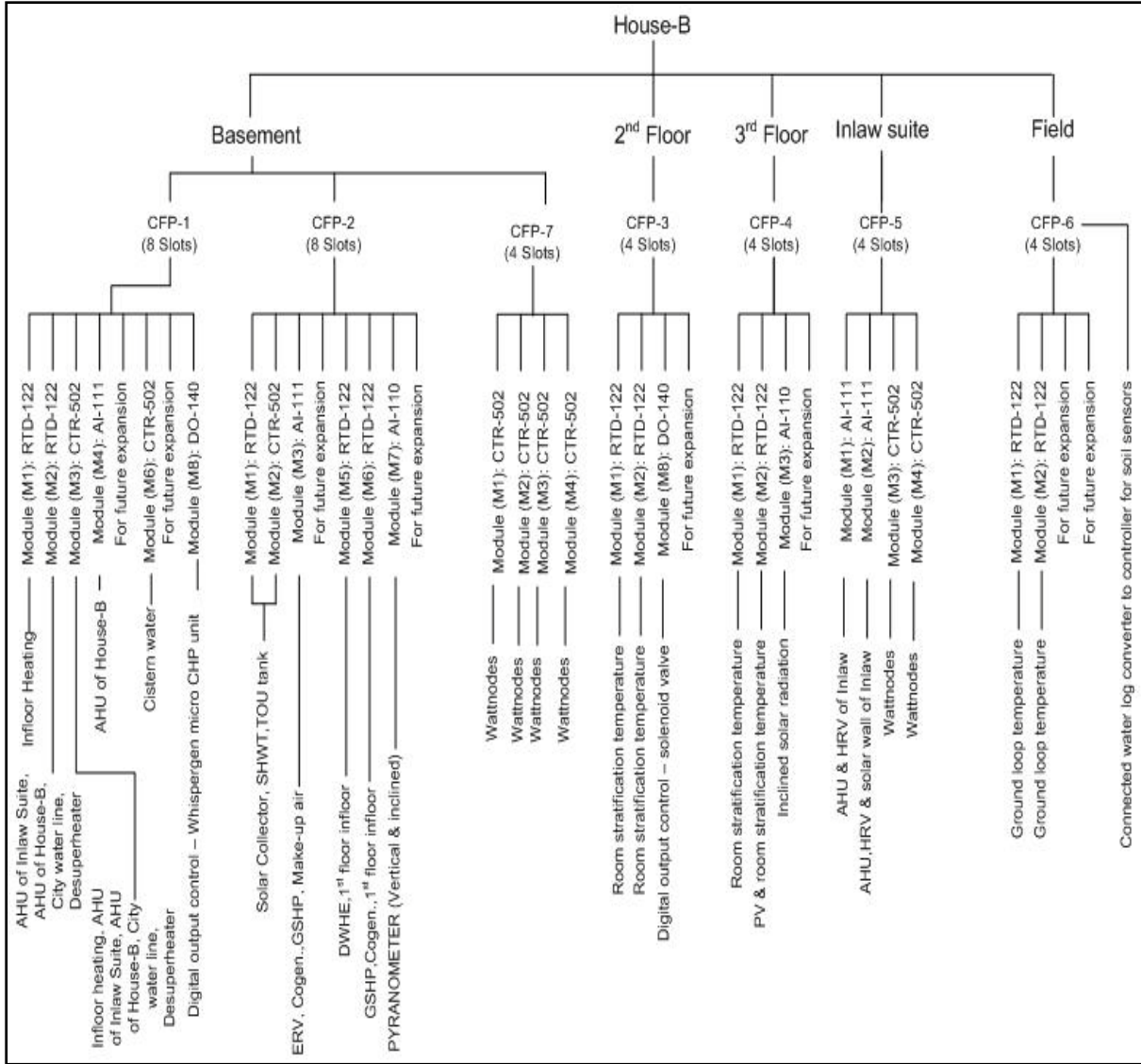


Figure A. 2: DAQ infrastructure in House-B

Table A.2: Nomenclature of Sensors, Channels, Modules and Compact field point of DAQ systems in House-B

Module: RTD-122 (Output signal: RTD)				
Address	Sensors	Sensors type	Location	Status
B-CFP1-M1-CH1	T12	Pt. 500	Radiant basement supply	Getting signal (GS)
B-CFP1-M1-CH2	T11	Pt. 500	Radiant basement return	GS
B-CFP1-M1-CH3	T10	Pt. 500	Radiant 3 rd floor supply	GS
B-CFP1-M1-CH4	T9	Pt. 500	Radiant 3 rd floor return	GS
B-CFP1-M1-CH5	T8	Pt. 500	Radiant 2 nd floor supply	GS
B-CFP1-M1-CH6	T7	Pt. 500	Radiant 2 nd return	GS
B-CFP1-M1-CH7	T6	Pt. 500	Radiant 1 st supply	GS
B-CFP1-M1-CH8	T5	Pt. 500	Radiant 1 st return	GS

Module: RTD-122 (Output signal: RTD)				
Address	Sensors	Sensors type	Location	Status
B-CFP1-M2-CH1	T4	Pt. 500	Buffer tank to Inlaw AHU supply	GS
B-CFP1-M2-CH2	T3	Pt. 500	Buffer tank to Inlaw AHU return	GS
B-CFP1-M2-CH3	T13	Pt. 500	Buffer tank to B-AHU supply	GS
B-CFP1-M2-CH4	T14	Pt. 500	Buffer tank to B-AHU return	GS
B-CFP1-M2-CH5	T18	Pt. 500	Desuperheater return	GS
B-CFP1-M2-CH6	T19	Pt. 500	Desuperheater supply	GS
B-CFP1-M2-CH7	T27	Pt. 100	City water	GS
B-CFP1-M2-CH8				

Module: CTR-502 (Output signal: Pulse)				
Address	Sensors	Sensors type	Location	Status
B-CFP1-M3-CH1	FL15	Flow rate	Radiant Basement	GS
B-CFP1-M3-CH2	FL14	Flow rate	Radiant 3 rd floor	GS
B-CFP1-M3-CH3	FL13	Flow rate	Radiant 2 nd floor	GS
B-CFP1-M3-CH4	FL12	Flow rate	Radiant 1 st floor	GS
B-CFP1-M3-CH5	FL9	Flow rate	Buffer tank to Inlaw AHU	GS
B-CFP1-M3-CH6	FL8	Flow rate	Buffer tank to B-AHU	GS
B-CFP1-M3-CH7	FL5	Flow rate	Desuperheater	GS
B-CFP1-M3-CH8	FL4	Flow rate	City water	GS

Module: AI-111 (Output signal: mA)				
Address	Sensors	Sensors type	Location	Status
B-CFP1-M4-CH1	RH13	RH	Supply air duct to 1 st floor of B-AHU	GS
B-CFP1-M4-CH2	AT13	Air Temp.		
B-CFP1-M4-CH3	RH14	RH	Supply air duct to 2 nd floor of B-AHU	GS
B-CFP1-M4-CH4	AT14	Air Temp.		
B-CFP1-M4-CH5	RH15	RH	Supply air duct to 3 rd floor of B-AHU	GS

B-CFP1-M4-CH6	AT15	Air Temp.		
B-CFP1-M4-CH7	RH11	RH	Return air duct of 1 st floor of B-AHU	GS
B-CFP1-M4-CH8	AT11	Air Temp.		
B-CFP1-M4-CH9	RH9	RH	Return air duct of 2 nd & 3 rd floor of B-AHU	GS
B-CFP1-M4-CH10	AT9	Air Temp.		
B-CFP1-M4-CH11	AF13	Air Flow	Supply air duct to 1 st floor of B-AHU	GS
B-CFP1-M4-CH12	AF12	Air Flow	Supply air duct to 2 nd floor of B-AHU	GS
B-CFP1-M4-CH13	AF11	Air Flow	Supply air duct to 3 rd floor of B-AHU	GS
B-CFP1-M4-CH14	AF7	Air Flow	Return air duct of 1 st floor of B-AHU	GS
B-CFP1-M4-CH15	AF5	Air Flow	Return air duct of 2 nd & 3 rd floor of B-AHU	GS
B-CFP1-M4-CH16				

Module: RTD 122 (Output signal: RTD)

Address	Sensors	Sensors type	Location	Status
B-CFP1-M5-CH1		Pt.100	Stratified Air Temperature 4’’ (Basement)	Installed
B-CFP1-M5-CH2		Pt.100	Stratified Air Temperature 48’’ (Basement)	Installed
B-CFP1-M5-CH3		Pt.100	Stratified Air Temperature 67’’ (Basement)	Installed
B-CFP1-M5-CH4		Pt.100	Stratified Air Temperature Ceiling (Basement)	Installed
B-CFP1-M5-CH5				
B-CFP1-M5-CH6				
B-CFP1-M5-CH7				
B-CFP1-M5-CH8				

Module: CTR-502 (Output signal: Pulse)

Address	Sensors	Sensors type	Location	Status
B-CFP1-M6-CH1	FL25	Flow rate	Cistern water	GS
B-CFP1-M6-CH2				
B-CFP1-M6-CH3				
B-CFP1-M6-CH4				
B-CFP1-M6-CH5				
B-CFP1-M6-CH6				
B-CFP1-M6-CH7				
B-CFP1-M6-CH8				

Module: RTD 122 (Output signal: RTD)

Address	Sensors	Sensors type	Location	Status
---------	---------	--------------	----------	--------

B-CFP1-M7-CH1		Pt.100	Stratified Air Temperature 4'' (First Floor)	Installed
B-CFP1-M7-CH2		Pt.100	Stratified Air Temperature 48'' (First Floor)	Installed
B-CFP1-M7-CH3		Pt.100	Stratified Air Temperature 67'' (First Floor)	Installed
B-CFP1-M7-CH4		Pt.100	Stratified Air Temperature Ceiling (First Floor)	Installed
B-CFP1-M7-CH5				
B-CFP1-M7-CH6				
B-CFP1-M7-CH7				
B-CFP1-M7-CH8				

Module: DO-410 (Digital control)

Address	Sensors	Sensors type	Location	Status
B-CFP1-M8-CH1		Pt. 100	Whispergen micro CHP unit	GS
B-CFP1-M8-CH2		Pt. 100	Whispergen micro CHP unit	GS
B-CFP1-M8-CH3		Pt. 100	Whispergen micro CHP unit	GS
B-CFP1-M8-CH4				
B-CFP1-M8-CH5				
B-CFP1-M8-CH6				
B-CFP1-M8-CH7				
B-CFP1-M8-CH8				

Module: RTD-122 (Output signal: RTD)

Address	Sensors	Sensors type	Location	Status
B-CFP2-M1-CH1	T24	Pt. 500	Solar collector supply	GS
B-CFP2-M1-CH2	T25	Pt. 500	Solar collector return	GS
B-CFP2-M1-CH3	T23	Pt. 100	Solar pre-heat tank supply to TOU tank	GS
B-CFP2-M1-CH4	T1	Pt. 100	Cold water to solar pre-heat tank	GS
B-CFP2-M1-CH5	T40	Pt. 100	Recirculation water to solar pre-heat tank	GS
B-CFP2-M1-CH6	T22	Pt. 100	Tempered water from TOU tank	GS
B-CFP2-M1-CH7	T2	Pt. 100	Un-tempered water from TOU tank	GS
B-CFP2-M1-CH8	T33	*Pt. 100 (SM)	Flue gas from CHP unit	GS

*Pt. 100 (SM) Surface mounted temperature sensor

Module: CTR-502 (Output signal: Pulse)

Address	Sensors	Sensors type	Location	Status
B-CFP2-M2-CH1	FL1	Flow rate	Solar collector supply	GS

B-CFP2-M2-CH2	FL2	Flow rate	Cold water to Solar pre-heat tank	GS
B-CFP2-M2-CH3	FL40	Flow rate	Recirculation water to Solar pre-heat tank	Damaged
B-CFP2-M2-CH4	FL3	Flow rate	Tempered water from TOU tank	GS
B-CFP2-M2-CH5	FL10	Flow rate	Un-tempered water from TOU tank	GS
B-CFP2-M2-CH6	FL19	Flow rate	Omega CHP unit	
B-CFP2-M2-CH7	FL11	Flow rate	GWHE to Tempering Valve	
B-CFP2-M2-CH8				

Module: AI-111 (Output signal: mA)

Address	Sensors	Sensors type	Location	Status
B-CFP2-M3-CH1	RH18	RH	Supply air from ERV to AHU	GS
B-CFP2-M3-CH2	AT18	Air Temp.		
B-CFP2-M3-CH3	RH19	RH	Return air from zone to ERV	GS
B-CFP2-M3-CH4	AT19	Air Temp.		
B-CFP2-M3-CH5	RH20	RH	Fresh air from outdoor to ERV	GS
B-CFP2-M3-CH6	AT20	Air Temp.		
B-CFP2-M3-CH7	RH21	RH	Exhaust air from ERV to outdoor	GS
B-CFP2-M3-CH8	AT21	Air Temp.		
B-CFP2-M3-CH9	AF16	Air Flow	Supply air from ERV to B-AHU	GS
B-CFP2-M3-CH10	AF15	Air Flow	Return air from zone to ERV	GS
B-CFP2-M3-CH11				
B-CFP2-M3-CH12	FL18	Flow rate (SPARLING)	CHP unit (NRCan)	GS
B-CFP2-M3-CH13	RH25	RH	Outdoor air RH (South side)	Not installed
B-CFP2-M3-CH14	AT25	Air Temp.	Outdoor air temperature (South side)	Not installed
B-CFP2-M3-CH15	RH24	RH	Outdoor air RH (North side)	GS
B-CFP2-M3-CH16	AT24	Air Temp.	Outdoor air temperature (North side)	GS

Module: RTD-122 (Output signal: RTD)

Address	Sensors	Sensors type	Location	Status
B-CFP2-M5-CH1	T30	Pt. 500	Pre-heat water to GWHE	GS
B-CFP2-M5-CH2	T26	Pt. 500	Warm water from GWHE	GS
B-CFP2-M5-CH3	T28	Pt. 100 (SM)	Drain water to GWHE	GS
B-CFP2-M5-CH4	T29	Pt. 100 (SM)	Drain water from GWHE	GS
B-CFP2-M5-CH5	T _{B1_3b_TOP}	Pt. 100 (SM)	1 st floor infloor top (North end)	Not installed

B-CFP2-M5-CH6	T _{B1_3b_BOT}	Pt. 100 (SM)	1 st floor infloor bottom (North end)	installed
B-CFP2-M5-CH7	T _{B1_2b_TOP}	Pt. 100 (SM)	1 st floor infloor top (Middle)	Damaged
B-CFP2-M5-CH8	T _{B1_2b_BOT}	Pt. 100 (SM)	1 st floor infloor bottom (Middle)	installed

Module: RTD-122 (Output signal: RTD)

Address	Sensors	Sensors type	Location	Status
B-CFP2-M6-CH1	NRCan1	Pt. 100	Solar tank CHP control	GS
B-CFP2-M6-CH2	NRCan2	Pt. 100	Buffer tank CHP control	GS
B-CFP2-M6-CH3	T16	Pt. 500	Supply from GSHP to Buffer tank	GS
B-CFP2-M6-CH4	T17	Pt. 500	Return to GSHP from Buffer tank	GS
B-CFP2-M6-CH5	T32	Pt. 500	Supply from CHP to Buffer tank	GS
B-CFP2-M6-CH6	T31	Pt. 500	Return to CHP from Buffer tank	GS
B-CFP2-M6-CH7	T _{B1_1b_TOP}	Pt. 100 (SM)	1 st infloor top (South end)	Damaged
B-CFP2-M6-CH8	T _{B1_1b_BOT}	Pt. 100 (SM)	1 st floor infloor bottom (South end)	GS

Module: AI-110 (Output signal: mA or mV)

Address	Sensors	Sensors type	Location	Status
B-CFP2-M7-CH1	PY_V	Pyranometer	Vertical position	GS
B-CFP2-M7-CH2	PY_I	Pyranometer	25° position	GS
B-CFP2-M7-CH3	NG2	Gas meter (SIERRA)	CHP unit	GS
B-CFP2-M7-CH4	FL16	Flow rate (Proteus)	GSHP ground loop	GS
B-CFP2-M7-CH5				
B-CFP2-M7-CH6	FL19	Water flow rate (Omega)	CHP unit (NRCan)	GS
B-CFP2-M7-CH7	FL6	Water flow rate (Proteus)	GSHP to Buffer tank	GS
B-CFP2-M7-CH8	FL17	Water flow rate (Proteus)	CHP unit	GS

Module: RTD-122 (Output signal: RTD)

Address	Sensors	Sensors type	Location	Status
B-CFP2-M8-CH1		Pt. 100 (SM)	Ground loop supply temperature (After pump)	GS
B-CFP2-M8-CH2		Pt. 100 (SM)	Ground loop return temperature (Before)	GS
B-CFP2-M8-CH3	T20	Pt. 500	Supply to ground loop (Before Pump)	GS
B-CFP2-M8-CH4	T21	Pt. 500	Return from ground loop (After pump)	GS
B-CFP2-M8-CH5				
B-CFP2-M8-CH6				
B-CFP2-M8-CH7				
B-CFP2-M8-CH8				

Module: RTD-122 (Output signal: RTD)				
Address	Sensors	Sensors type	Location	Status
B-CFP3-M1-CH1				
B-CFP3-M1-CH2				
B-CFP3-M1-CH3	T _{B2_2b_TOP}	Pt. 100 (SM)	2 nd floor infloor top (Middle)	Damaged
B-CFP3-M1-CH4				
B-CFP3-M1-CH5	T _{B2_3b_TOP}	Pt. 100 (SM)	2 nd floor infloor top (North end)	Damaged
B-CFP3-M1-CH6				

Module: RTD-122 (Output signal: RTD)				
Address	Sensors	Sensors type	Location	Status
B-CFP3-M2-CH1	***	Pt.100	Stratified Air Temperature 4'' (2 nd Floor)	Installed
B-CFP3-M2-CH2	***	Pt.100	Stratified Air Temperature 67'' (2 nd Floor)	Installed
B-CFP3-M2-CH3	***	Pt.100	Stratified Air Temperature 48'' (2 nd Floor)	Installed
B-CFP3-M2-CH4	***	Pt.100	Stratified Air Temperature Ceiling (2 nd Floor)	Installed
B-CFP3-M2-CH5	T _{B2_1b_TOP}	Pt. 100 (SM)	2 nd floor infloor top (South end)	installed
B-CFP3-M2-CH6	T _{B2_1b_BOT}	Pt. 100 (SM)	2 nd floor infloor bottom (South end)	installed
B-CFP3-M2-CH7	T _{B2_2b_BOT}	Pt. 100 (SM)	2 nd floor infloor bottom (Middle)	installed
B-CFP3-M2-CH8	T _{B2_3b_BOT}	Pt. 100 (SM)	2 nd floor infloor bottom (North end)	installed

*** Stratified stand placed on first floor as of January 26, 2011/ On Second Floor as of February 18,2011

Module: DO-410 (Digital control)				
Address	Sensors	Sensors type	Location	Status
B-CFP3-M3-CH1	C1	Solenoid valve	Simulated water draw profile	GS
B-CFP3-M3-CH2	C2	Solenoid valve	Simulated water draw profile	GS
B-CFP3-M3-CH3	C3	Solenoid valve	Simulated water draw profile	GS
B-CFP3-M3-CH4	H1	Solenoid valve	Simulated water draw profile	GS
B-CFP3-M3-CH5	H2	Solenoid valve	Simulated water draw profile	GS
B-CFP3-M3-CH6	H3	Solenoid valve	Simulated water draw profile	GS
B-CFP3-M3-CH7				
B-CFP3-M3-CH8				

Module: RTD-122 (Output signal: RTD)

Address	Sensors	Sensors type	Location	Status
B-CFP4-M1-CH1	T _{B3_1b_TOP}	Pt. 100 (SM)	3 rd floor infloor top (South end)	Not installed
B-CFP4-M1-CH2	T _{B3_1b_BOT}	Pt. 100 (SM)	3 rd floor infloor bottom (South end)	Not installed
B-CFP4-M1-CH3				
B-CFP4-M1-CH4				
B-CFP4-M1-CH5				
B-CFP4-M1-CH6				

Module: RTD-122 (Output signal: RTD)

Address	Sensors	Sensors type	Location	Status
B-CFP4-M2-CH1	T _{B3_2b_TOP}	Pt. 100 (SM)	3 rd floor infloor top (Middle)	installed
B-CFP4-M2-CH2	T _{B3_2b_BOT}	Pt. 100 (SM)	3 rd floor infloor bottom (Middle)	installed
B-CFP4-M2-CH3	T40	Pt. 100 (SM)	PV array temperature	GS
B-CFP4-M2-CH4	T41	Pt. 100 (SM)	Outlet air temperature under PV array	GS
B-CFP4-M2-CH5	T42	Pt. 100 (SM)	Inlet air temperature under PV array	GS
B-CFP4-M2-CH6	T _{B3_3b_TOP}	Pt. 100 (SM)	3 rd floor infloor top (North end)	installed
B-CFP4-M2-CH7	T _{B3_3b_BOT}	Pt. 100 (SM)	3 rd floor infloor bottom (North end)	installed
B-CFP4-M2-CH8				

Module: RTD-122 (Output signal: RTD)

Address	Sensors	Sensors type	Location	Status
B-CFP4-M3-CH1		Pt.100	Stratified Air Temperature 4'' (3 rd Floor)	Installed
B-CFP4-M3-CH2		Pt.100	Stratified Air Temperature 48'' (3 rd Floor)	Installed
B-CFP4-M3-CH3		Pt.100	Stratified Air Temperature 67'' (3 rd Floor)	Installed
B-CFP4-M3-CH4		Pt.100	Stratified Air Temperature Ceiling (3 rd Floor)	Installed
B-CFP4-M3-CH5				
B-CFP4-M3-CH6				
B-CFP4-M3-CH7				
B-CFP4-M3-CH8				

Appendix B: Experimental Uncertainty Analysis

The uncertainty analysis was performed on the mechanical system/equipment that are analyzed in the Chapter 5.

B1. Uncertainty of Sensors and Calibrators

A total of two error sources were considered in the uncertainty analysis. The first one was the accuracy value of sensors (Table B.1) and the second one was the accuracy value of calibrators (Table B.2). It should be mentioned that random error has been neglected in this analysis. For this purpose, the Square Root Sum of Squares (SRSS) method was followed which combines all errors or accuracy by squaring them, adding the squares together and taking the square root of the sum of those squares (ASHRAE Guideline 2, 2005).

Overall accuracy of sensors = $\sqrt{A_c^2 + A_s^2}$

where A_c = Calibrator accuracy, and A_s = Sensor accuracy.

The overall accuracy of sensors from Equation (B-1) was used in the propagation of errors calculation to determine the accuracy of mechanical system / equipment.

Table B.3: Manufacturer supplied sensors and accuracy

Sensor name	Sensor type	Manufacturer	Model number	Sensor accuracy
Turbine type flow rate	Measure liquid/water flow rate	Omega/Clark Solution	CFT110	±3.0%
Metering flow switch	Measure liquid/water flow rate	Proteus Industries Inc.	800 Series	±0.5%
Pyranometer	Measure global solar radiation	LI-COR, Inc.	LI-200SZ	±5.0%
Wattnode	Measure electrical energy	Continental Control Systems	WNB-3Y-208-P	±1.0%
RTD sensor (Pt.-100, directly immersed)	Measure Temperature	Omega	PRTF-10-2-100-1/4-6-E	±0.1%
RTD sensor (Pt.-100, surface mount)	Measure Temperature	Omega	RTD-2-F3105-36-T-B	±0.12%
RTD sensor (Pt.-500, directly immersed)	Measure Temperature	Kamstrup	65-00-0DO-310	N/A
Gas mass flow meter	Measure gas flow rate	SIERRA Instruments	826-NX-OV1-PV1-V1-T	±1.5%

- Flat plate solar thermal collector: the uncertainty analysis method was applied to Equation (5-12). The Overall accuracy of efficiency was found to be: $\pm 6.5\%$
- Evacuated tube solar thermal collector: the uncertainty analysis method was applied to Equation (5-20). The Overall accuracy of efficiency was found to be: $\pm 6.5\%$
- Drain Water Heat Recovery systems: the uncertainty analysis method was applied to Equation (5-15). The Overall accuracy of efficiency was found to be: $\pm 0.7\%$
- Electrical energy: This result was obtained from wattnodes and current transformer (CT) accuracy. Overall accuracy of electrical energy was concluded to be: $\pm 1.0\%$

References

- Aguilar, A., White, D., & Ryan, D. (2005). *Domestic Hot Water Heating and Water Heater Energy Consumption in Canada*. CBEEDAC 2005–RP-02.
- ASHRAE. (1999). *Building Energy Monitoring*. Atlanta: Communications and Publications.
- ASHRAE Guideline 2. (2005). *Engineering Analysis of Experimental Data*. Atlanta, USA: ASHRAE.
- Barua, R. (2010). *Assessment and Energy Benchmarking for Two Archetype Sustainable Houses Through Comprehensive Long Term Monitoring*. Toronto: Ryerson University.
- Bernier, M., Delisle, V., Picard, D., & Kummert, M. (2004). On the combined effect of wastewater heat recovery and solar domestic hot water heating. *Canadian Solar Buildings Conference*. Montreal, QC.
- Biaou, A., & Bernier, M. (2005). Domestic Hot Water Heating in Zero Net Energy Homes. *9th International IBPSA Conference*, (pp. pp.63-70). Montreal, Canada.
- California Energy Commission. (2006). Appliance Efficiency Regulations. *CEC-400-2006-002-Rev2*.
- Canada Gazette. (2004). Energy Efficiency Act: Regulations Amending the Energy Efficiency Regulations. *Vol. 138, No.19*.
- CMHC. (1996). *The EQUilibrium™ Sustainable Housing Demonstration Initiative*. Retrieved April 2010, from Canada Mortgage and Housing Corporation: http://www.cmhc-schl.gc.ca/en/co/maho/yohoyohe/heho/eqho/eqho_002.cfm
- Collins, M. (2009). *Effectiveness Testing of PowerPipe™ Drain Water Heat Recovery Systems*. Solar Thermal Research Laboratory. Waterloo: University of Waterloo.
- Dembo, A., Fung, A., Ringo NG, K., & Pyrka, A. (2010). The Archetype Sustainable House: Investigating its Potentials to Achieving the Net-Zero Energy Status Based on the Results of a Detailed Energy Audit. *International High Performance Buildings Conference*. Purdue, Indiana.

DOE. (2011b). Retrieved April 2011, from www.energysavers.gov.

DOE. (2001). *Heat Recovery from Wastewater Using Gravity-Film Heat Exchanger*. Retrieved February 2011, from www.gfxtechnology.com: <http://gfxtechnology.com/Femp.pdf>

Druck, H., Heidemann, W., & Müller-Steinhagen, H. (2004). Comparison Test of Thermal Solar Systems for Domestic Hot Water Preparation and Space Heating. *EuroSun2004*. Freiburg, Germany.

Environment Canada. (2011). *Fuel Combustion*. Retrieved November 2011, from www.ec.gc.ca.

Environment Canada. (2000). *National Climate Data and information Archive*. Retrieved November 2011, from www.climate.weatheroffice.gc.ca.

ES Renewables Ltd. (2011). Retrieved April 2011, from <http://esrenewables.tech.officelive.com/SolarWaterHeating.aspx>

Eslami-nejad, P., & Bernier, M. (2009). Impact of Grey Water Heat Recovery on the Electrical Demand of Domestic Hot Water Heaters. *11th International IBPSA Conference*, (pp. 681-687). Glasgow, Scotland.

European Commission Directorate General for Energy and Transport. (2004). *Basic European and International Standards on Solar Thermal Glazed Collectors & Solar Domestic Hot Water Systems*. Athens, Greece: Exergias S.A.

Feng, J., Megerian, S., & Potkonjak, M. (2003). Model-Based Calibration for Sensor Networks. *IEEE Xplore*, 737-742.

Gill, G., & Fung, A. (2011). Energy and Environmental Analysis of Residential Hot Water Systems; A Study for Ontario, Canada. *ASHRAE Transactions*, Vol. 117, Part 2, 506-520.

Hendron, R., & Burch, J. (2007). Development of Standardized Domestic Hot Water Event Schedules for Residential Buildings. *Energy Sustainability*. Long Beach, CA: National Renewable Energy Laboratory.

Hewitt, N., & Henderson, P. (2001). *Drainwater Heat Recovery System - An Energy Conservation Project*. Coleraine, Northern Ireland.

- Jordan, U., & Vajen, K. (2001). *Realistic Domestic Hot Water Profiles in Different Time Scales*. Marburg: Universitat Marburg.
- Kalb, C., & Seader, J. (1974). Fully developed viscous flow heat transfer in curved circular tubes with uniform wall temperature. *AlchE Journal* , 20(2), 340-346.
- Kim, Y., & Seo, T. (2007). Thermal Performances Comparisons of the Glass Evacuated Tube Solar Collectors With Shapes of Absorber Tube. *Renewable Energy* (32), 772-795.
- Knight, I., Kreutzer, N., Manning, M., Swinton, M., & Ribberink, H. (2007). *European and Canadian non-HVAC Electric and DHW Load Profiles for Use in Simulating the Performance of Residential Cogeneration Systems*. International Energy Agency (IEA Annex 42).
- Kravchenko, V. (1966). Empirical Equation Derived for Temperature Dependence of Density of Heavy Water. *Springer New York* , 212.
- Laughton, C. (2010). *Solar Domestic Water Heating*. Washington, DC: Earthscan.
- London Economics LLD. (2011, March). *Independent Power Producers Society of Alberta*. Retrieved November 2011, from www.ippsa.com.
- M. Tanaka, G. G. (2001). Recommended table for the density of water between 0oC and 40oC based on recent experimental reports. *Metrologia*, Volume 38 , 301-309.
- Merrigan, T., & Parker, D. (1990, August). Electrical Use, Efficiency, and Peak Demand of Electric Resistance, Heat Pump, Desuperheater, and Solar Hot Water Systems. American Council for an Energy Efficient Economy, Asilomar Conference Center, Pacific Grove, CA.
- NAHB Research Center. (2002). *Domestic Hot Water System Modeling For the Design of Energy Efficient Systems*. Upper Marlboro, MD.
- NIST. (2009, July 02). *National Institute of Standards and Technology*. Retrieved July 02, 2009, from www.nist.gov: <http://ts.nist.gov/MeasurementServices/Calibrations/flow.cfm#18020C>
- NRCan. (2007). (Natural Resources Canada, National Energy Use Database, 1990 to 2007) Retrieved 2010, from <http://www.nrcan.gc.ca>: <http://www.nrcan.gc.ca>

- NRCan. (2009, May). Retrieved April 2010, from <http://www.nrcan.gc.ca>
- NRCan. (2009, September). *Energy Efficiency Trends in Canada: 1990 to 2007*. Retrieved March 2011, from Natural Resources Canada:
<http://oee.nrcan.gc.ca/publications/statistics/trends09/pdf/trends.pdf>
- Parker, D. (2003). Research highlights from a large scale residential monitoring study in a hot climate. *Energy and Buildings* 35 , 863-876.
- Pengra, D., & Dillman, L. (2009). *Notes on Data Analysis and Experimental Uncertainty*. Ohio Wesleyan University.
- Perlman, M., & Mills, B. (1985). Development of Residential Hot Water Use Patterns. *ASHRAE Transactions* , 657-679.
- Picard, D., Bernier, M., & Charneux, R. (2007). Domestic Hot Water Production in a Net Zero Energy Triplex in Montreal. *2nd Canadian Solar Buildings Conference*, (pp. pp.1-8). Calgary.
- Proskiw, G. (1995). *Design and Analysis of a Residential Grey-Water Heat Recovery System*. Prepared for Natural Resources Canada and Centra Gas Manitoba, Winnipeg, Manitoba.
- Proskiw, G. (1998). *Technology Profile: Residential Grey-Water Heat Recovery Systems*. Prepared for Natural Resources Canada and Manitoba Hydro Electrical Board, Winnipeg, Manitoba.
- Solar Energy Laboratory of University of Wisconsin. (2005). TRNSYS 16 Volume 9 - Weather Data. Wisconsin, Madison, U.S.A.
- SQL Server. (2008). *Microsoft Corporation*. Retrieved April 03, 2010, from [www.microsoft.com: http://msdn.microsoft.com/en-us/library/ms143432.aspx](http://msdn.microsoft.com/en-us/library/ms143432.aspx)
- SRCC Document. (1994). *Methodology for Determining the Thermal Performance Rating for Solar Collectors*. Florida: Solar Rating & Certification Corporation (SRCC).
- Statistics Canada. (2011). *Energy Statistics Handbook, 2nd Quarter 2011*. Statistics Canada.

Stevenson, D. (1983). *Residential Hot Water Use Patterns (Volume I)*. Report for the Canadian Electrical Association Research and Development, Montreal, QC.

Tanaka, M., Girard, G., Davis, R., Peuto, A., & Bignell, N. (2001). Recommended table for the density of water between 0oC and 40oC based on recent experimental reports. *Metrologia*, *Volume 38* , 301-309.

Taylor, D., & Crossman, G. (1996). *Virginia Power Water Heater Testing and Optimization Project*. Final Report for Virginia Power, Old Dominion University, Norfolk, Virginia.

The California Public Utilities Commission (CPUC). (2009). *California Solar Initiative Program Handbook*. California: California Solar Initiative.

The Engineering ToolBox. (2005). Retrieved December 2008, from Propylene Glycol based Heat-Transfer Fluids: http://www.engineeringtoolbox.com/propylene-glycol-d_363.html

The U.S. Department of Energy (DOE). (2001). Energy Conservation Program for Consumer Products: Energy Conservation Standards for Water Heaters: Final Rule. *Federal Register, Rules and Regulations* , Vol. 66 (11), pp. 4474 - 4497.

The U.S. Department of Energy (DOE). (2000). *Technical Support Document: Energy Efficiency Standards for Consumer Products: Residential Water Heaters, Including: Regulatory Impact Analysis*”,. Retrieved April 2011, from <http://www1.eere.energy.gov>

Trinkl, C., Zörner, W., Alt, C., & Stadler, C. (2005). Performance of Vacuum Tube and Flat Plate Collectors Concerning Domestic Hot Water Preparation and Room Heating. *2nd European Solar Thermal Energy Conference*. Freiburg.

Van Decker, G. (2008, February). *Analysis of Drain Water Heat Recovery Applications in Northern Minnesota Based on Demographic Characteristics, Supply Water Temperature, and Two Studies by Natural Resources Canada*. Retrieved December 2010, from Renewability: http://www.renewability.com/uploads/documents/en/analysis_dwahr_minnesota.pdf

Viessmann Ltd. (2010b). *Vitosol Solar Heating Systems*. Retrieved May 4, 2011, from www.viessmann.com.

Viessmann Ltd. (2010). *Vitotech technical guide*. Retrieved April 12, 2011, from www.viessmann.com.

Vitotech technical guide. (2010). *Viessmann Limited*. Retrieved April 8, 2010, from www.viessmann.com: <http://www.scribd.com/doc/19338747/Viessmann-Vitosol-Thermal-Solar-Collectors-System-Design-Guidelines>

Walker, A., Mahjouri, F., & Stiteler, R. (2004). Evacuated-Tube Heat-Pipe Solar Collectors Applied to the Recirculation Loop in a Federal Building. *Solar 2004 Conference*. Portlan, Oregon USA.

Weiss, W., & Rommel, M. (2008). *Process Heat Collectors; State of the Art within Task 33*. Gleisdorf, Austria: AEE INTEC.

Wiehagen, J., & Sikora, J. (2003). *Performance Comparison of Residential Hot Water Systems*. Upper Marlboro, Maryland: NAHB Research Centre.

Wong, L., Mui, K., & Guan, Y. (2010). Shower Water Heat Recovery in high-rise residential buildings of Hong Kong. *Applied Energy* , 87, 703-709.

Zaloum, C., Lafrance, M., & Gusdorf, J. (2007). *Drain Water Heat Recovery Characterization and Modeling*. Ottawa: Sustainable Buildings and Communities, Natural Resources Canada.

Zambolin, E., & Del Col, D. (2010). Experimental Analysis of Thermal Performance of Flat Plate and Evacuated Tube Solar Collectors in Stationary Standard and Daily Conditions. *Journal of Solar Energy* , 84, 1382-1396.

Zhang, D., Barua, R., & Fung, A. (2011). TRCA-BILD Archetype Sustainable House - Overview of Monitoring System and Preliminary Results for Mechanical Systems. *ASHRAE Transactions* , Vol. 117, Part 2, 597-612.